


Tailored Collaboration

Altering Environmental Conditions to Enhance Non-Mechanical Dewatering of Residuals

Web Report #4338

 Subject Area: Water Quality



Altering Environmental Conditions to Enhance Non-Mechanical Dewatering of Residuals



About the Water Research Foundation

The Water Research Foundation is a member-supported, international, 501(c)3 nonprofit organization that sponsors research that enables water utilities, public health agencies, and other professionals to provide safe and affordable drinking water to consumers.

The Foundation's mission is to advance the science of water to improve the quality of life. To achieve this mission, the Foundation sponsors studies on all aspects of drinking water, including resources, treatment, and distribution. Nearly 1,000 water utilities, consulting firms, and manufacturers in North America and abroad contribute subscription payments to support the Foundation's work. Additional funding comes from collaborative partnerships with other national and international organizations and the U.S. federal government, allowing for resources to be leveraged, expertise to be shared, and broad-based knowledge to be developed and disseminated.

From its headquarters in Denver, Colorado, the Foundation's staff directs and supports the efforts of more than 800 volunteers who serve on the Board of Trustees and various committees. These volunteers represent many facets of the water industry, and contribute their expertise to select and monitor research studies that benefit the entire drinking water community.

Research results are disseminated through a number of channels, including reports, the Website, Webcasts, workshops, and periodicals.

The Foundation serves as a cooperative program providing subscribers the opportunity to pool their resources and build upon each others' expertise. By applying Foundation research findings, subscribers can save substantial costs and stay on the leading edge of drinking water science and technology. Since its inception, the Foundation has supplied the water community with more than \$460 million in applied research value.

More information about the Foundation and how to become a subscriber is available at www.WaterRF.org.

Altering Environmental Conditions to Enhance Non-Mechanical Dewatering of Residuals

Prepared by:

David A. Cornwell and Damon K. Roth

Environmental Engineering & Technology, Inc., 712 Gum Rock Court, Newport News, VA 23606

Jointly sponsored by:

Water Research Foundation

6666 West Quincy Avenue, Denver, CO 80235

City of Cleveland Division of Water

1201 Lakeside Avenue, Cleveland, OH 44114-1132

City of Raleigh Public Utilities

PO Box 590, Raleigh, NC 27602

and

Aqua America, Inc.

762 West Lancaster Avenue, Bryn Mawr, PA 19010-3402

Published by:



DISCLAIMER

This study was jointly funded by the Water Research Foundation (the Foundation) and City of Cleveland Division of Water, City of Raleigh Public Utilities, and Aqua America, Inc. (the co-funding utilities). The Foundation and the co-funding utilities assume no responsibility for the content of the research study reported in this publication or for the opinions or statements of fact expressed in the report. The mention of trade names for commercial products does not represent or imply the approval or endorsement of the Foundation or the co-funding utilities. This report is presented solely for informational purposes.

Copyright © 2013
by Water Research Foundation

ALL RIGHTS RESERVED.
No part of this publication may be copied, reproduced
or otherwise utilized without permission.

Printed in the U.S.A.



Printed on recycled paper

CONTENTS

LIST OF TABLES	vii
LIST OF FIGURES	ix
FOREWORD	xiii
ACKNOWLEDGMENTS	xv
EXECUTIVE SUMMARY	xvii
CHAPTER 1: INTRODUCTION	1
Background.....	1
Research Concept.....	2
Research Plan.....	5
CHAPTER 2: METHODS AND MATERIALS	7
Materials	7
Controlled Environment Testing.....	9
Field Testing – Cleveland	12
Field Testing – Raleigh.....	13
Methods.....	15
Total Solids Analysis	15
Air Velocity Measurement.....	15
Temperature and Humidity Measurement	16
CHAPTER 3: RESULTS AND DISCUSSION.....	17
Controlled-Environment Experiments	17
Ventilation Test 1.....	17
Ventilation Test 2.....	19
Ventilation Test 3.....	23
Ventilation Test 4.....	26
Ventilation Test 5.....	28
Drying Previously Dewatered Cake.....	28
Summary of Controlled Environment Testing.....	31
Cleveland Pilot Studies	35
Shakedown Test Results	36
Cleveland Test 1 – October 27, 2011.....	38
Cleveland Test 2 – December 14, 2011	40
Cleveland Test 3 – January 12, 2012	41
Cleveland Test 4 – January 31, 2012	43
Cleveland Test 5 – March 7, 2012	45
Cleveland Test 6 – April 11, 2012	46
Cleveland Test 7 – May 23, 2012	48

Cleveland Test 8 – June 26, 2012	49
Summary of Cleveland Field Pilot Studies	51
Raleigh Pilot Studies	57
Raleigh Test 1 – January 30, 2012	58
Raleigh Test 2 – March 7, 2012	60
Raleigh Test 3 – April 10, 2012	62
Raleigh Test 4 – May 9, 2012	63
Raleigh Test 5 – June 8, 2012	64
Raleigh Test 6 – July 31, 2012	66
Raleigh Test 7 – August 27, 2012	67
Raleigh Test 8 – September 19, 2012	68
Summary of Raleigh Field Pilot Studies	71
CHAPTER 4: CASE STUDIES	74
Costing	74
Drying Beds	74
Enclosing Structure	74
Ventilation Fans	76
Example Installation Costs	77
Cleveland Case Study	80
Raleigh Case Study	84
Aqua Case Study	89
Mentor On-the-Lake WTP	89
Shenango WTP	92
CHAPTER 5: SUMMARY	99
Controlled-Environment Testing	99
Cleveland Field Testing and Case Study	100
Raleigh Field Testing and Case Study	102
Aqua Case Study	103
Areas for Future Research	104
REFERENCES	106
ABBREVIATIONS	107

TABLES

1.1	Variables affecting evaporation	4
2.1	Summary of sand media used for sand column tests	7
3.1	Summary of ventilation tests conducted during this period.....	18
3.2	Solids concentration data from Ventilation Test 1	19
3.3	Solids concentration data from Ventilation Test 2	21
3.4	Solids concentration data from Ventilation Test 3	25
3.5	Solids concentration data from Ventilation Test 4	27
3.6	Solids concentration data from Ventilation Test 5	28
3.7	Summary of controlled-environment test results on Harwood’s Mill sludge.....	34
3.8	Cleveland Test 1 parameters	39
3.9	Cleveland Test 2 parameters	40
3.10	Cleveland Test 3 parameters	42
3.11	Cleveland Test 4 parameters	44
3.12	Cleveland Test 5 parameters	45
3.13	Cleveland Test 6 parameters	47
3.14	Cleveland Test 7 parameters	48
3.15	Cleveland Test 8 parameters	50
3.16	Summary of effective evaporation rates and Q_{eff} calculated from Cleveland test results.....	52
3.17	Comparison of calculated effective evaporation rates from West Bed and historical evaporation rates	53
3.18	Evaporation rate and ambient weather conditions used for regression analysis.....	54
3.19	Summary of loading dates and initial solids concentrations for Raleigh tests	58

3.20	Summary of Raleigh Test 6 Drying Performance.....	66
4.1	Capital costs for generic six-bed enhanced non-mechanical dewatering installation.....	79
4.2	Comparison of capital costs for dewatering options at Morgan WTP.....	84
4.3	Comparison of present value costs (20 years, 6% interest) for residuals management options at Morgan WTP.....	84
4.4	Sliding cost scale for transport of residuals from E.M. Johnson WTP.....	84
4.5	Residual solids removal costs at E.M. Johnson WTP for FY2010.....	85
4.6	Comparison of residual solids removal costs at 21.8 and 50.0 percent solids concentration.....	86
4.7	Comparison of required annual yield based on loading depth for E.M. Johnson WTP.....	88
4.8	Capital costs for converting existing sand drying beds to enhanced non-mechanical dewatering beds at E.M. Johnson WTP.....	89
4.9	Average solids production at Shenango WTP (2001 through 2008) and disposal cost.....	92
4.10	Calculated effective evaporation rates for Shenango, PA.....	93
4.11	Potential cost savings from increasing dewatered cake solids concentration from 15 percent to 20 percent at Shenango WTP.....	94
4.12	Potential cost savings from increasing dewatered cake solids concentration from 15 percent to 50 percent at Shenango WTP.....	95
4.13	Capital costs for converting existing residuals clarifier to enhanced non-mechanical dewatering beds at Shenango WTP.....	97
4.14	Comparison of required annual yield based on loading depth for Shenango WTP.....	97

FIGURES

2.1	Calculated change in percent solids over time using different sand media	7
2.2	Controlled-environment test bed section	9
2.3	Sludge application point in pilot-scale bed	10
2.4	Experimental apparatus setup with one pilot-scale bed	10
2.5	Ventilation register configuration in pilot-scale bed	11
2.6	Field pilot test set up at Morgan WTP in Cleveland, Ohio.....	12
2.7	Field pilot test set up at E.M. Johnson WTP in Raleigh, North Carolina.....	13
2.8	Test frame for Raleigh cake drying tests	14
2.9	Control frame for Raleigh cake drying tests	14
2.10	Solids sampling locations for controlled-environment testing	15
2.11	Air velocity measurement apparatus.....	16
3.1	Distribution of air velocity, in fpm, over the sludge surface for Test 3.....	17
3.2	Distribution of air velocity, in m/s, over the surface of Bed 2 during Test 4	20
3.3	Distribution of air velocity, in m/s, over the surface of Bed 3 during Test 4	20
3.4	Sludge cracking observed in Bed 2 at the end of Ventilation Test 3.....	22
3.5	Sludge cracking observed in Bed 3 at the end of Ventilation Test 3.....	22
3.6	Distribution of air velocity, in m/s, over the surface of Bed 2 during Ventilation Test 3.....	23
3.7	Distribution of air velocity, in m/s, over the surface of Bed 3 during Ventilation Test 3 – Configuration 1	24
3.8	Distribution of air velocity, in m/s, over the surface of Bed 3 during Ventilation Test 3 – Configuration 2	24
3.9	Distribution of cake solids concentrations, in percent solids, in Bed 2 on drying day 15	25

3.10	Distribution of cake solids concentrations, in percent solids, in Bed 3 on drying day 14	25
3.11	Distribution of air velocity, in m/s, over the surface of Bed 2 during Ventilation Test 4.....	26
3.12	Distribution of air velocity, in m/s, over the surface of Bed 3 during Ventilation Test 4.....	27
3.13	Pile 1 on Drying Day 1	29
3.14	Pile 2 (left) and Pile 3 (right) on Drying Day 1	29
3.15	Drying performance over time during drying of previously dewatered cake.....	30
3.16	Change in solids concentration and equivalent depth over time for Ventilation Test 4, Bed 2	32
3.17	Total equivalent evaporation and effective evaporation rates for Ventilation Test 4, Bed 2	33
3.18	Effective evaporation rate based on fan configuration	35
3.19	Drying performance over time during initial shakedown testing at Morgan WTP	37
3.20	Drying performance over time during initial shakedown testing at Morgan WTP	38
3.21	Drying performance over time during Cleveland Test 1 (10/27/2011)	39
3.22	Drying performance over time during Cleveland Test 2 (12/14/2011)	41
3.23	Drying performance over time during Cleveland Test 3 (1/12/2012)	42
3.24	Comparison of West Bed after 13 days of dewatering during Cleveland Test 1 (left photo) to West Bed after six days of dewatering during Cleveland Test 3 (right photo)	43
3.25	Drying performance over time during Cleveland Test 4 (1/31/2012)	44
3.26	Drying performance over time during Cleveland Test 5 (3/07/2012)	46
3.27	Drying performance over time during Cleveland Test 6 (4/11/2012)	47
3.28	Drying performance over time during Cleveland Test 7 (5/23/2012)	49

3.29	Drying performance over time during Cleveland Test 8 (6/26/2012)	50
3.30	Comparison of effective evaporation rate from enhanced non-mechanical dewatering to the historical evaporation rates	53
3.31	Relationship between net evaporation and average bed velocity for different temperature and solar radiation values	56
3.32	Relationship between net evaporation and Q_{eff} for different temperature values	57
3.33	Drying performance over time during Raleigh Test 1 (1/30/2012)	59
3.34	Air flow distribution across test bed at termination of Raleigh Test 1	60
3.35	Air flow distribution across test bed at initiation of Raleigh Test 2	60
3.36	Drying performance over time during Raleigh Test 2 (3/7/2012)	61
3.37	Dried cake in the test bed at the termination of Raleigh Test 1	62
3.38	Drying performance over time during Raleigh Test 3 (4/10/2012)	63
3.39	Drying performance over time during Raleigh Test 4 (5/9/2012)	64
3.40	Drying performance over time during Raleigh Test 5 (5/9/2012)	65
3.41	Air flow distribution across test bed following Raleigh Test 5	65
3.42	Drying performance over time, by depth, during Raleigh Test 7	68
3.43	Windrow configuration for Raleigh Test 8	69
3.44	Air flow distribution over windrow for Raleigh Test 8	70
3.45	Drying performance over time during Raleigh Test 8	70
3.46	Example of desiccation cracking during drying of thickened sludge	71
3.47	Example of the structure of mechanically-dewatered cake during drying	72
4.1	Sketch of traditional greenhouse structure, individual installation	75
4.2	Sketch of traditional greenhouse structure, multiple installation	75
4.3	Sketch of a hoop house structure	76

4.4	Sketch of a stretched-fabric structure	76
4.5	Plan view of generic six-bed enhanced non-mechanical dewatering installation.....	77
4.6	Section view along lateral bed axis of generic six-bed enhanced non-mechanical dewatering installation	78
4.7	Section view along longitudinal bed axis of generic six-bed enhanced non-mechanical dewatering installation	78
4.8	Annual cost savings from drying mechanically-dewatered residuals from 20 percent solids concentration to 50 percent solids concentration.....	80
4.9	Comparison of total drying bed area required for traditional and enhanced non-mechanical dewatering beds for Morgan WTP.....	81
4.10	Potential layout for enhanced non-mechanical dewatering beds at Morgan WTP.....	82
4.11	Sketch of potential enhanced non-mechanical dewatering bed layout at E.M. Johnson WTP	87
4.12	Extension arm fabricated by Mentor On-the-Lake WTP mechanics to till over sludge lagoon residuals	90
4.13	Residuals being tilled in the Mentor On-the-Lake WTP Sludge Lagoons	91
4.14	Aerial view of Shenango WTP site.....	96
5.1	Effective evaporation rate as a function of applied air flow	100
5.2	Relationship between net evaporation and applied volumetric flow rate for different temperature values	101
5.3	Relationship between net evaporation and average bed centerline velocity for different temperature and solar radiation values.....	102
5.4	Comparison of total drying bed area required for traditional and enhanced non-mechanical dewatering beds for Morgan WTP.....	105

FOREWORD

The Water Research Foundation (Foundation) is a nonprofit corporation dedicated to the development and implementation of scientifically sound research designed to help drinking water utilities respond to regulatory requirements and address high-priority concerns. The Foundation's research agenda is developed through a process of consultation with Foundation subscribers and other drinking water professionals. The Foundation's Board of Trustees and other professional volunteers help prioritize and select research projects for funding based upon current and future industry needs, applicability, and past work. The Foundation sponsors research projects through the Focus Area, Emerging Opportunities, and Tailored Collaboration programs, as well as various joint research efforts with organizations such as the U.S. Environmental Protection Agency and the U.S. Bureau of Reclamation.

This publication is a result of a research project fully funded or funded in part by Foundation subscribers. The Foundation's subscription program provides a cost-effective and collaborative method for funding research in the public interest. The research investment that underpins this report will intrinsically increase in value as the findings are applied in communities throughout the world. Foundation research projects are managed closely from their inception to the final report by the staff and a large cadre of volunteers who willingly contribute their time and expertise. The Foundation provides planning, management, and technical oversight and awards contracts to other institutions such as water utilities, universities, and engineering firms to conduct the research.

A broad spectrum of water supply issues is addressed by the Foundation's research agenda, including resources, treatment and operations, distribution and storage, water quality and analysis, toxicology, economics, and management. The ultimate purpose of the coordinated effort is to assist water suppliers to provide a reliable supply of safe and affordable drinking water to consumers. The true benefits of the Foundation's research are realized when the results are implemented at the utility level. The Foundation's staff and Board of Trustees are pleased to offer this publication as a contribution toward that end.

Denise L. Kruger
Chair, Board of Trustees
Water Research Foundation

Robert C. Renner, P.E.
Executive Director
Water Research Foundation

ACKNOWLEDGMENTS

Environmental Engineering & Technology, Inc. (EE&T) wants to thank all of the utilities that participated in this project. Appreciation is extended to Larry Ploscik, Cleveland Division of Water (CWD), who oversaw and conducted the field testing in Cleveland, OH, and Nick Pizzi of EE&T who assisted Larry for many of the tests. We thank Bryan Hamilton, City of Raleigh, for overseeing field testing in Raleigh, NC, and also Amber Greune, North Carolina State University, who assisted with field testing in Raleigh.

The Project Advisory Committee (PAC) was Carel Vandermeijden, Greater Cincinnati Water Works; Sanjay Reddy, Black & Veatch, Walnut Creek, CA; and Terry Rolan, Water Advice Network, Maxton, NC.

We appreciate the assistance of the WaterRF project manager, Mary Smith.

EXECUTIVE SUMMARY

OBJECTIVES

The purpose of this work was to (1) investigate methods of enhancing drying during non-mechanical dewatering by controlling environmental conditions and (2) determine whether it was economically beneficial to do so. By enhancing drying it will be possible to increase turnover of drying beds compared to traditional non-mechanical dewatering methods, which in turn will reduce the total footprint required for the process. Enhancing drying will also reduce the final volume and mass of residuals, which, in turn, will reduce transport and disposal costs.

BACKGROUND

Non-mechanical dewatering processes rely on percolation and evaporation to remove water from water treatment plant residuals. Previous research has focused on optimizing the removal of water via drainage in non-mechanical dewatering processes. While this stage is where the majority of water removed from the residuals is removed, the evaporation stage is where the majority of time to dewater residuals occurs. This evaporation stage is highly dependent on ambient conditions, and limited research has investigated how to optimize evaporative drying of residuals.

Evaporation is a physical state change from water to air, and as such it is controlled by several factors including latent heat of evaporation, partial pressure, temperature, and overall pressure. From a practical standpoint, the four key variables that affect evaporation are temperature, wind, exposed surface, and humidity. Of these four, the easiest variable to control is air velocity (wind), which can be induced through forced-air ventilation.

APPROACH

This work was conducted in two phases. First, controlled-environment pilot-scale tests were conducted in EE&T's laboratory using residuals from the Harwood's Mill Water Treatment Plant operated by Newport News Water Works (Newport News, VA). Following these investigations, field pilot-scale tests were conducted at the Morgan Water Treatment Plant (WTP) operated by Cleveland Division of Water (Cleveland, OH) and the E.M. Johnson Water Treatment Plant operated by City of Raleigh (Raleigh, NC). Testing in Cleveland focused on dewatering of thickened residuals, while the Raleigh testing focused on drying of residuals that had been previously dewatered using the plant's belt filter presses.

Following testing, case studies were developed for Cleveland Division of Water and City of Raleigh demonstrating the economics of using an enhanced non-mechanical dewatering process at their facilities. Case studies were also developed for Aqua America using data provided from facilities they operate in Ohio and Pennsylvania.

RESULTS/CONCLUSIONS

Controlled-environment testing indicated the importance of both volumetric air flow rates and air velocities in drying water treatment plant residuals. It was demonstrated that evaporation correlated strongly with overall volumetric air flow rate, which is implicit in the vapor-balance calculations that predict evaporation rates; increasing the amount of air flowing over the bed increases the amount of air into which moisture can evaporate.

Pilot testing in Cleveland indicated that evaporation from non-mechanical dewatering can be improved with the enhanced non-mechanical dewatering process. Effective evaporation rates achieved in the pilot test units were significantly higher than historical evaporation rates for the Cleveland area with an observed 300 percent to 800 percent improvement in evaporation, depending on the season. Correlations were developed linking effective evaporation rates to air flow/velocity, ambient temperature, and ambient solar radiation.

Data from the field testing was used to model area requirements for enhanced non-mechanical dewatering beds at Morgan WTP. These model results were compared to previous modeling efforts used to size traditional non-mechanical dewatering beds for the same facility. It was demonstrated that the enhanced non-mechanical dewatering process would be able to reduce the area required for dewatering by more than two-thirds compared to traditional non-mechanical dewatering beds. A layout was developed for the enhanced non-mechanical dewatering beds at Morgan WTP, and the cost for those facilities was compared to costs for traditional non-mechanical dewatering beds, centrifuge dewater, and sewer disposal that had been developed for a previous study. The 20-year present value cost for the enhanced non-mechanical dewatering beds was 15 percent less than the next least expensive option (traditional non-mechanical dewatering beds) and approximately 60 percent less expensive than the current residuals management process (sewer disposal) at Morgan WTP. This case study clearly shows that the enhanced non-mechanical dewatering process can be cost-effective and relatively low-footprint for large water treatment plants.

Raleigh field testing investigated the drying of residuals that had been previously dewatered by the belt filter presses. It became apparent over the course of testing that drying of mechanically-dewatered residuals is fundamentally different than drying of thickened residuals. During the drying of thickened residuals, the cake remains physically connected so that moisture from the center and bottom of the cake layer can move the surface of the cake via capillary action. Because evaporation can only happen at the air: liquid interface, this capillary action serves to create more uniform drying across the depth of the cake layer. Mechanically dewatered residuals, at least those produced by the belt filter presses at E.M. Johnson WTP, are not part of a cohesive whole but instead consist of small agglomerations of dewatered cake, interspersed with void spaces. When piled into a drying bed or windrow, the cake on the surface of the layer dries rapidly, but the center and bottom of the cake layer dries very little.

Case studies were conducted at two Aqua America facilities. The study conducted at the Mentor On-the-Lake WTP indicated that tilling of residuals in traditional non-mechanical dewatering processes can significantly improve drying. Tilling roughly doubled the final solids concentration in conventional sludge lagoons, which reduced overall residuals management costs at that facility by more than 33 percent. The study at the Shenango WTP indicated that enhanced non-mechanical dewatering of mechanically-dewatered sludge can be economically favorable.

APPLICATIONS/RECOMMENDATIONS

Utilities and water industry professionals can make use of this study to evaluate enhanced non-mechanical dewatering at: (a) existing water treatment plants with high costs for residuals disposal and, (b) new or existing water treatment plants looking to add a residuals dewatering process. This research has demonstrated that enhanced non-mechanical dewatering can be economically favorable for both large and small water treatment plants, and may be the only non-mechanical dewatering process with a small enough footprint to be usable at large water treatment plants.

RESEARCH PARTNERS

This project was a Tailored Collaboration between Aqua Pennsylvania, the City of Raleigh, Cleveland Division of Water, and the Water Research Foundation.

CHAPTER 1

INTRODUCTION

BACKGROUND

One of the backbones of conventional water treatment systems is the removal of particles present in raw water through sedimentation and filtration processes. These processes produce residual waste solids, both from the raw water particles removed by the process and from chemical precipitates produced as part of the treatment step. These residuals must be removed from the treatment plant and disposed of, either in a landfill, monofill, or through a beneficial reuse process.

Transport and disposal costs for water treatment plant residuals are generally based on the mass of residuals that are handled. However, the vast majority of a given mass of residuals is comprised of water. Residuals moved from a conventional sedimentation basin using alum or ferric coagulant generally consist of more than 99 percent water. It is advantageous to reduce the mass of residuals that must be handled by removing water from the solid residuals. Additional water may be removed through a gravity thickening process, which may produce a thickened sludge ranging from two to five percent solids. It is important to note the distinction between sludge and residuals. Sludge, as it is referred to here, is a component of residuals that is primarily composed of coagulant solids. Although some utilities transport and dispose of thickened sludge at this stage, further cost savings can be achieved by dewatering the thickened sludge to further remove water and reduce the mass of residuals prior to disposal.

Several dewatering technologies exist. Mechanical dewatering processes use pressure or centrifugal force to separate the solids from free water in the thickened sludge. Non-mechanical dewatering processes rely on percolation and evaporation to remove water. Compared to mechanical dewatering processes, non-mechanical dewatering requires limited energy inputs and can be very effective and inexpensive when properly sized and designed. However, despite the simplicity of this method, more complicated and energy intensive mechanical dewatering technologies are often implemented by water treatment plants due to the relatively large footprint required for non-mechanical dewatering.

The large footprint associated with non-mechanical dewatering is related to the inconsistent dewatering rate of these processes. Non-mechanical dewatering relies on two distinct processes for water removal: an initial drainage phase, during which free water percolates through the thickened sludge and the bottom of the non-mechanical dewatering bed, and an evaporation phase. While previous research has described methods of designing non-mechanical dewatering systems for water treatment plant residuals (Vandermeijden and Cornwell, 1998), this research primarily focused on optimizing the drainage phase, during which the majority of water is removed from the residuals. However, because the drainage phase alone is not capable of producing solids that are dry enough to handle and transport with conventional equipment, the evaporative phase is still needed to further dewater the solids. This evaporative phase traditionally has relied on ambient weather conditions, and as a result is highly dependent on unreliable, seasonally-affected factors. During periods when the weather is not conducive to evaporative drying, it is necessary to stockpile and store the residuals until conditions improve and the required drying can be achieved. However, by enclosing the beds and controlling airflow

across the beds, it should be possible to modify environmental conditions to enhance the evaporative drying phase of non-mechanical dewatering.

Research on enhancing sludge drying has primarily focused municipal sewage and industrial wastewater sludges (Seginer and Bux 2006, Mathioudakis et al. 2009, Slim et al. 2008, Zhao et al. 2010). Although the concepts are relatively similar, sludge drying can vary depending on the characteristics of the sludge being dried (Ruiz and Wisniewski 2008, Vaxelaire et al. 2000). Given that water treatment plant sludges are highly inert and contain significantly fewer organics and volatiles than municipal sewage sludges, additional research was necessary to investigate methods of enhancing the drying of water treatment plant residuals during non-mechanical dewatering.

RESEARCH CONCEPT

The focus of this work was to investigate methods of enhancing drying during non-mechanical dewatering by controlling environmental conditions, and to determine whether it was economically beneficial to do so. By enhancing drying it will be possible to increase turnover of drying beds compared to traditional non-mechanical dewatering methods, which in turn will reduce the total footprint required for the process.

Evaporation is a physical state change from water to air. As such it is controlled by the latent heat of evaporation, partial pressure, temperature and overall pressure. From a practical standpoint, there are four key variables that can affect the evaporation rate:

Temperature – The higher the temperature, the higher the rate of evaporation. A temperature increases, or an increase in light intensity causes the water molecules to gain more energy, move faster, and evaporate at a higher rate. From a thermodynamic standpoint, higher energy = higher evaporation.

Wind – When there is wind, the water vapor is removed as it forms, decreasing the vapor partial pressure. So higher wind equals lower partial pressure which means more driving force for higher evaporation.

Exposed Surface – Evaporation is a function of the surface between the two phases, so an increase the exposed surface can increase evaporation.

Humidity – The amount of water vapor in the air. The higher the humidity, the higher the partial pressure, and the slower the evaporation. Humidity and wind are related in the sense that the lower the humidity in the wind the higher the evaporation.

One simple way of measuring evaporation in a drying bed setting would be a vapor balance which accounts for humidity and wind, as calculated by Equation 1.1:

$$E = \frac{518,400(\omega_{out} - \omega_{in})Q_v}{\rho} \quad (1.1)$$

where E	=	average evaporation rate (inches/month)
ρ	=	density of air (lb/ft ³)
Q_v	=	volumetric air flow rate (ft ³ /min/ft ²)
ω	=	moisture content (lb/ft ³)

The change in humidity, ($\omega_{out} - \omega_{in}$), represents the increase in moisture in the air that is removed from the sludge and increasing Q_v or decreasing ω_{in} would raise E , all else being equal. Therefore, one way to increase E is to provide dry wind over the sludge or through the sludge and another is to increase ventilation.

This, of course, only accounts for two of the key four variables. The two other key variables are related to temperature and surface area exposure. Temperature is the temperature of the water in the sludge on a micro-scale, which is not practical to measure. Factors that affect the surface water temperature that can be measured are solar radiation (R_A) and air temperature (T_A). An increase in radiation on the sludge surface or an increase in air temperature that in turn increases the water droplet temperature would both increase the evaporation rate.

Increasing the surface between the sludge (water) and the air increases the air/water interface and increases evaporation. The plain surface area of the sludge – that is the bed area -- has been established by the optimal loading rate. So the water/air interface is initially about the same as the bed area. As the sludge dries, it tends to crack. The exposed surface area is increased by the cracking that takes place but this is not controlled by the operator and is a natural phenomenon. The use of a tilling device, commonly called a mole, can be used to force an increase in the exposed surface.

Therefore, the following variables affect evaporation of water from the sludge, and at least in theory, are variable and can be modified to improve drying:

R_A	-	Solar radiation (W/m ²)
ω_{in}	-	Air humidity, (lb/ft ³)
T_A	-	Air temperature, (°C)
Q_v	-	Ventilation air rate, (ft ³ /min/ft ²)
TIL	-	Use of sludge tiling

Seginer and Bux (2005) studied evaporation in a greenhouse with forced ventilation for the drying of biosolids in Germany. They defined the evaporation rate as shown in Equation 1.2:

$$E = f(e, s, c) \quad (1.2)$$

where e	=	outdoor environment factors
s	=	state of the sludge
c	=	control variables

They studied biosolids evaporation rates inside a controlled greenhouse structure where they could vary ventilation. They evaluated the impacts of ventilation, radiation and temperature over different seasons and the use of a mole. They used a linear regression to determine which variables most affected evaporation. A modified version of their results is shown in Table 1.1

(variables have been changed to use the nomenclature above, and SS = dry sludge solids concentration).

Table 1.1
Variables affecting evaporation

	Linear regression R^2	Regression residual error mm/h
R_A (Solar Radiation)	0.575	0.100
R_A, Q_V (“”, Ventilation Air Rate)	0.740	0.078
R_A, Q_V, T_A (“”, “”, Air Temperature)	0.808	0.067
R_A, Q_V, T_A, SS (“”, “”, “”, Dry Sludge Solids Concentration)	0.838	0.062

Source: Modified from Seginer and Bux (2005).

They found that the determination coefficient, R^2 , increased as variables were added. They concluded that R_A , Q_V , and T_A significantly affect the evaporation rate and that the changing sludge solids concentration had only a minor affect. That is, as the sludge dried, the evaporation rate did not change very much. Interestingly, the use of tilling had little affect although they did conclude that they did not have enough data to evaluate this variable. Note that they did not alter or look for a relationship with influent ω_A .

Control of environmental conditions is accomplished primarily by two methods: enclosing the drying beds in a greenhouse-type structure, and by controlling airflow over the beds using fans. There are several advantages to enclosing the beds. Enclosing the beds allows controlled air ventilation across the beds by eliminating the influence from natural winds. It can also allow for increased air temperatures above the beds, and prevents the reintroduction of water into the drying residuals from precipitation.

Controlled air ventilation is also advantageous for increasing drying. Two mechanisms are responsible for evaporation: diffusion (heat and mass transfer by molecular motion) and advection (heat and mass transfer by the movement of air over the water surface) (Sartori 2005). At the surface of drying residuals the air velocity is extremely low and a very thin layer of water vapor enters the air through diffusion. In the absence of air flow causing advection, this will develop into a thin boundary layer of saturated air that can inhibit further drying. Air flow, either due to natural wind flow or forced air ventilation, can prevent the formation of the saturated boundary layer by increasing the advective transport of water from the residuals' surface (Allen et al. 1998).

Enhancing drying has the potential for additional benefits beyond the dewatering of thickened water treatment plant residuals. Due to physical limitations, most mechanical dewatering technologies are unable to produce dewatered cake from coagulant (alum and ferric) solids in excess of 20 to 30 percent solids without bulking agents such as lime. Therefore, more than 70 percent of the mass of cake from a mechanical dewatering process is water, which increases transport and disposal costs. Because evaporative drying does not feature the same constraints as mechanical dewatering processes, non-mechanical dewatering processes are capable of producing solids concentrations in excess of 50 percent, further decreasing transport and disposal costs. As part of this work, enhanced drying of previously dewatered cake from a mechanical dewatering process was investigated.

RESEARCH PLAN

This work was conducted in two phases. First, controlled-environment pilot-scale tests were conducted in EE&T's laboratory using residuals from the Harwood's Mill Water Treatment Plant operated by Newport News Water Works (Newport News, VA). Following these investigations, field pilot-scale tests were conducted at the Morgan Water Treatment Plant operated by Cleveland Division of Water (Cleveland, OH) and the E.M. Johnson Water Treatment Plant operated by City of Raleigh (Raleigh, NC). Testing in Cleveland focused on dewatering of thickened residuals, while the Raleigh testing focused on drying of residuals that had been previously dewatered using the plant's belt filter presses.

Following testing, case studies were developed for Cleveland Division of Water and City of Raleigh demonstrating the economics of using an enhanced non-mechanical dewatering process at their facilities. Case studies were also developed for Aqua America using data provided from facilities they operate in Ohio and Pennsylvania.

CHAPTER 2 METHODS AND MATERIALS

MATERIALS

For controlled-environment testing at EE&T's Laboratory, thickened solids were collected from the nearby Harwood's Mill WTP operated by Newport News Waterworks (Newport News, VA). Harwood's Mill produces alum sludge in the range of 1.0 to 2.0 percent solids concentration, which is thickened without the addition of polymer and is relatively high in organic content.

Prior to evaluating the drying phase of dewatering, it was necessary to optimize the drainage phase of the dewatering process. Laboratory time-to-filter (TTF) tests were conducted on the Harwood's Mill sludge to optimize free water release during the drainage phase of dewatering, per the procedure described by Vandermeijden and Cornwell (1998). Initial testing indicated that a cationic polymer (Magnafloc LT 22s) optimized release of water from the Harwood's Mill sludge; however, the resultant flocs formed with that polymer were unstable and prone to break down under shearing forces. Instead, the anionic polymer (Magnafloc LT 27) was found to minimize TTF while forming flocs that remained flocculated after bed loading. Due to changes in sludge composition associated with seasonal variation in organic loading to the plant, TTF testing was repeated for each new load of sludge collected from Harwood's Mill to optimize polymer dose. Optimal polymer dose for this sludge was found to vary between 7 to 12 lb/dry-ton of residuals.

As part of optimizing construction of the sand beds, pilot dewatering column testing, as described in Vandermeijden and Cornwell (1998), was conducted to evaluate different filter sands. Table 2.1 summarizes the characteristics of the sands tested. Columns 1 and 4 consisted of commercially available filter sand, while Columns 2 and 3 were produced by selectively sieving the sand used in Column 4.

Thickened sludge from Harwood's Mill at a concentration of 1.54 percent solids concentration was loaded into the columns at a rate of 3 lb dry solids/ft². To simulate the rate at which sludge is actually loaded into full-scale drying beds, the sludge for each column was dived into six evenly sized aliquots, or "lifts", that were added to the columns every five minutes. With this process, it took 30 minutes to completely load each column. Polymer was added to each lift immediately prior to loading into the column at a dose of 2.25 lb/dry-ton. Because the mass of sludge added to each column was known, the change in depth of the sludge (and thus, the change in sludge volume) was used to determine the change in solids concentration as the sludge dried. Sands 2 and 3 were filter media sands whereas 1 and 4 were run of the mill gravel yard sands and consequently much cheaper material. The change in solids concentration over time is shown in Figure 2.1.

Table 2.1
Summary of sand media used for sand column tests

	Column 1	Column 2	Column 3	Column 4
Effective Size (mm)	0.52	1.1	0.85	0.7
Uniformity Coefficient	1.60	1.36	1.53	1.79

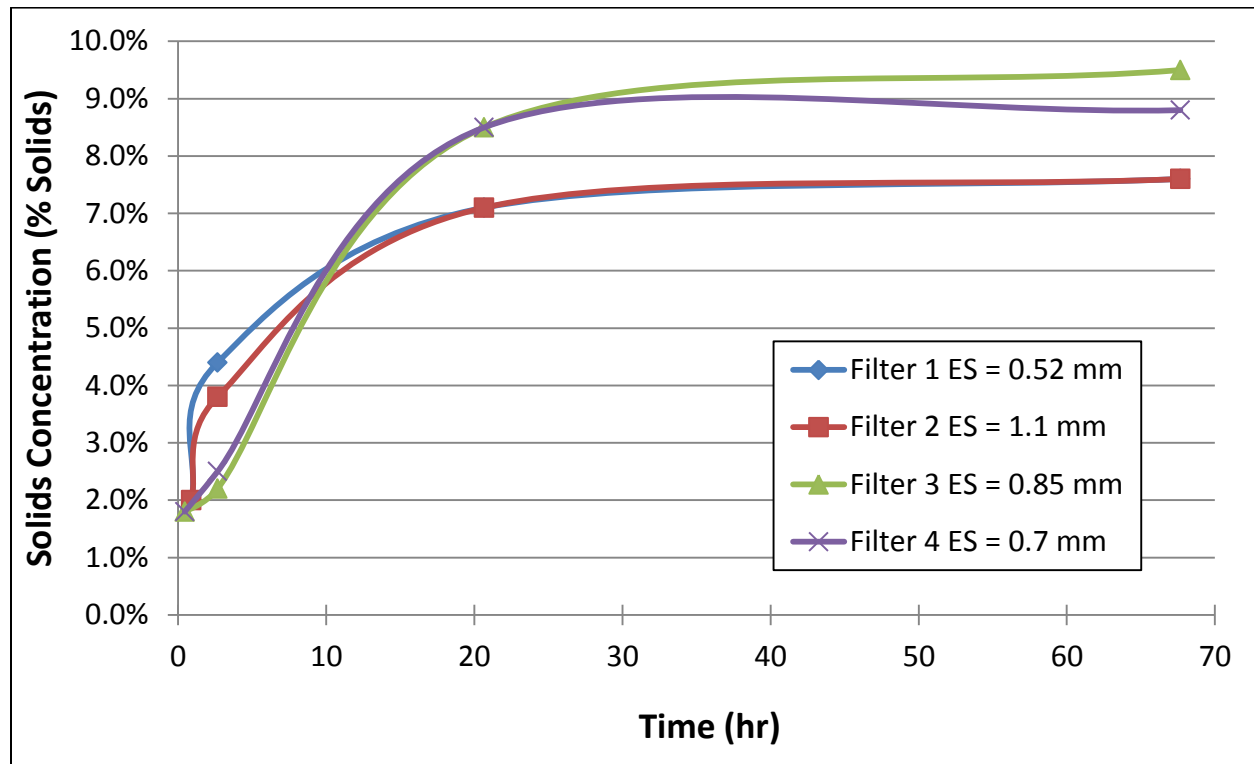


Figure 2.1 Calculated change in percent solids over time using different sand media

Based on the depth of solids in the columns, the two columns with the selectively sieved sand drained more quickly than the columns filled with sand with a smaller effective size. However, drainage from the columns filled with commercially available sand ultimately drained more water after a period of 20 minutes. Supernatant was present in each column immediately after loading, indicating that free water was separating from the solids more quickly than it could drain through the layers of residual solids and sand. After a period of one hour, the supernatant had drained through each column.

These results suggested that the composition of the sand in the dewatering beds ultimately had a very minor impact on the drainage of free water through the bed. Based on these findings, the sand used in Column 4 was subsequently used in all pilot-scale dewatering beds. This sand was relatively inexpensive and readily available.

Controlled Environment Testing

Three pilot-scale test beds were constructed for controlled-environment and field pilot tests. These 3-foot wide by 8-foot long beds were constructed using fiberglass-lined plywood. The beds were constructed with side wall depths of approximately three feet so that thickened sludge could be loaded at the target solids loading rate of 3 lb/ft²; however, because these relatively tall walls would interflow with airflow over the bed, it was necessary to construct the beds with removable end walls. Figure 2.2 shows the configuration of these beds.

Solids collected from Harwood's Mill were stored in a bulk 1,000 gallon storage tank to allow for controlled loading of the beds. For each test run, solids were transferred from the tank to the bed using a transfer pump, which was rate controlled using a downstream ball valve. A submersible pump located in the sludge holding tank was used to keep the feed solids well mixed during loading. Fresh polymer was activated in bulk solution, containing 0.1 to 0.2 percent active solution, and fed to the sludge line downstream of the flow control valve. As shown in Figure 2.3, as sludge was loaded into the bed it was fed to a bucket that served as a stilling chamber, which prevented the sludge from disturbing the sand and allowed for additional polymer mixing. Figure 2.4 shows the setup of one of the controlled-environment test beds.

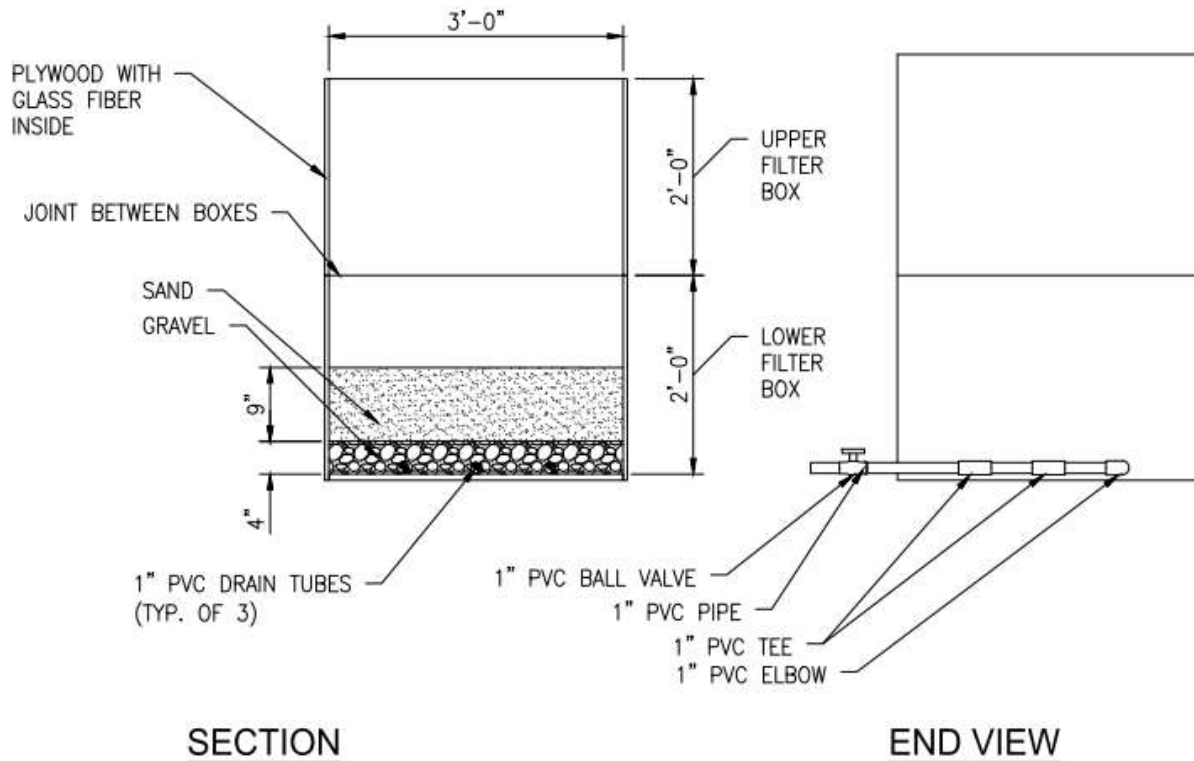


Figure 2.2 Controlled-environment test bed section



Figure 2.3 Sludge application point in pilot-scale bed



Figure 2.4 Experimental apparatus setup with one pilot-scale bed

Feed sludge flow was monitored using a Doppler flow meter. Flow control during the loading process was necessary to ensure even loading of the bed. If the bed was loaded too quickly, it was possible for the loaded sludge to blind the sand particles, keeping the bed from draining freely.

Various ventilation configurations were tested. Initial testing utilized a ventilation register, as shown in Figure 2.5. Subsequent tests used various configurations of 100 cfm, 300 cfm, and 500 cfm fans, as described in Chapter 3. Solids samples were collected from the beds on a regular basis for total solids testing to measure the progress of the sludge drying.

During the controlled-environment testing, the drying of previously dewatered cake was also evaluated. Cake was obtained from the E.M. Johnson WTP operated by the City of Raleigh, NC. Sludge produced at E.M. Johnson WTP, which uses ferric sulfate for coagulation, is currently dewatered using belt filter presses. The resultant residuals cake averages 20 to 22 percent solids concentration.

Because of the solid nature of the cake, it was not necessary to isolate the residuals in dewatering beds for drying. Instead, two volumes of cake (6-foot long by 1-foot wide by 8 inches high and 6-foot long by 1-foot high by 18 inches high) were arranged on a solid surface and subjected to forced air ventilation across their surface. A separate, one-cubic foot volume of cake was set aside to dry as a control. Solids samples were collected from the cake piles on a regular basis for total solids testing to measure the progress of the cake drying.

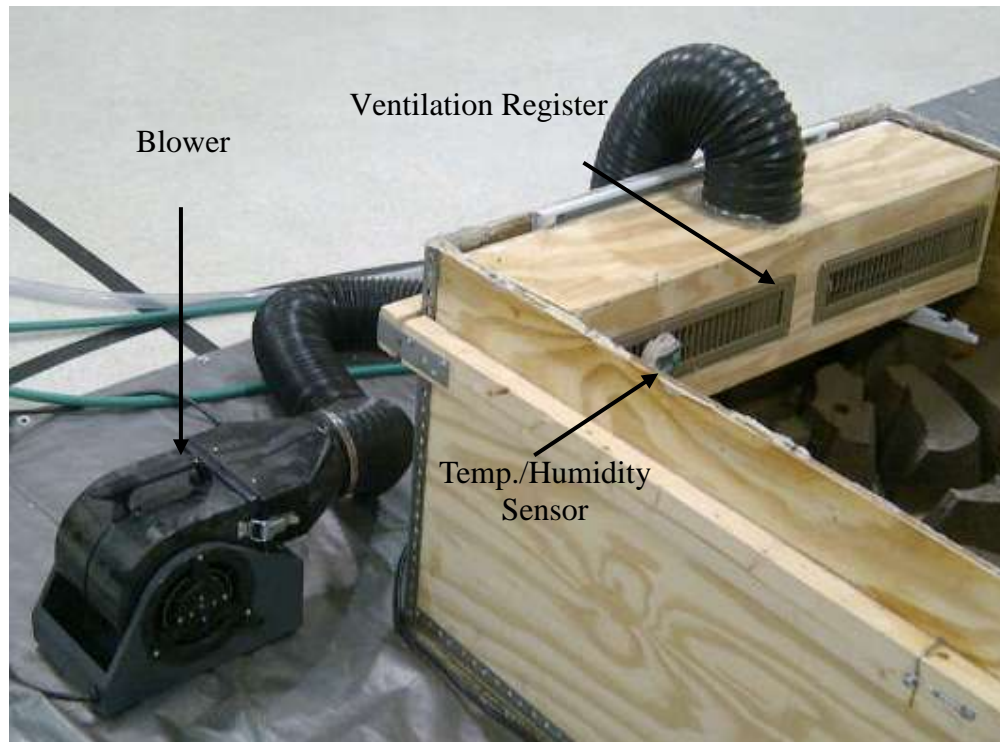


Figure 2.5 Ventilation register configuration in pilot-scale bed

Field Testing – Cleveland

Field testing in Cleveland was conducted at the Cleveland Division of Water (CWD) Morgan WTP. This plant is not currently designed for residuals treatment, and produces a thin sludge with a solids concentration of approximately 0.4 percent, which is stored on-site and discharged to the municipal sewer system. Prior to each test Morgan plant personnel worked to isolate a portion of the sludge storage tank to manually thicken the solids by allowing them to settle and manually decanting the supernatant. These thickened solids were then used for the dewatering bed testing.

The test set up was similar to that utilized for controlled-environment testing. As before, thickened solids were transferred to a day tank for feeding solids onto the bed. Two test beds were set up at Morgan WTP, each in located in an 8-foot by 8-foot corrugated polyethylene greenhouse structure, as shown in Figure 2.6. Because of the limited dimensions of the greenhouse structure, each 3-foot wide bed was shortened to a 6-foot length, providing 18 square feet of drying bed area. Based on the results from the controlled-environment testing, each bed was ventilated using a single, laminar-flow fan positioned centrally on the narrow end of the bed.



Figure 2.6 Field pilot test set up at Morgan WTP in Cleveland, Ohio

Initially, the polymer feed system for each bed was located inside the bed's greenhouse structure. However, as temperatures dropped during the winter months, the bulk solids storage tank had to be abandoned and the polymer feed system had to be reconfigured due to problems with freezing. The polymer feed equipment was relocated inside of an adjacent building, and solids were transferred directly from the plant's sludge storage tanks to the test beds. As with the controlled-environment testing, samples were collected from the beds on a regular basis for total solids testing to measure the progress of the cake drying.

Field Testing – Raleigh

Field testing in Raleigh was conducted at the E.M. Johnson WTP. A polycarbonate greenhouse structure, shown in Figure 2.7, was placed in an abandoned drying bed to house dewatered cake for further drying. Because the cake was not liquid, it was necessary to manually place pile solids for drying tests. Two frames (two-foot wide by 6-foot long by 1-foot high) were constructed from PVC and fine wire cloth to assist in measuring consistent volumes of cake for testing. One frame was located inside the greenhouse with ventilation, as shown in Figure 2.8. The second frame was located outside the greenhouse to serve as a control volume, as shown in Figure 2.9.



Figure 2.7 Field pilot test set up at E.M. Johnson WTP in Raleigh, North Carolina



Figure 2.8 Test frame for Raleigh cake drying tests



Figure 2.9 Control frame for Raleigh cake drying tests

As with the controlled-environment testing, samples were collected from the cake piles on a regular basis for total solids testing to measure the progress of the cake drying. As noted in Chapter 3, for some tests the E.M. Johnson WTP operators manually turned the cake over on a daily basis to evaluate the impact of tillage on drying.

METHODS

Total Solids Analysis

The primary analytical tool for monitoring the drying of residuals solids was a total solids analysis. Total solids for solids samples collected during controlled-environment testing were measured using a Kett FD 720 infrared moisture balance. For field testing at Cleveland, samples collected from the beds were analyzed at Morgan WTP's laboratory using EPA Method 1684. Total solids for solids samples collected during on-site testing at Raleigh were measured using a CEM Smart Turbo, Model 907940 moisture balance.

During controlled-environment testing, three solids samples were collected from each bed during each sampling event, as shown in Figure 2.10. Each sample consisted of a small core from the drained solids, which was then homogenized to normalize the solids concentration gradient over the depth of the sludge layer. For field testing the number of samples was reduced to two per sampling event, both due to the shorter length of the beds/piles and to minimize the additional labor placed on the plant staff assisting with the sampling.

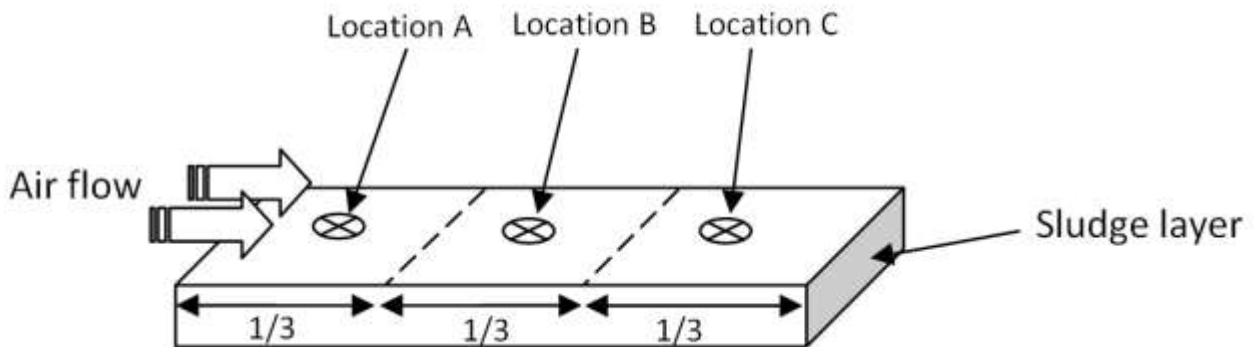


Figure 2.10 Solids sampling locations for controlled-environment testing

Air Velocity Measurement

Air velocity measurements were collected using an Extech1RK12 Anemometer. After each bed loading, air velocity measurements were collected approximately six inches above the solids surface using a 12-inch by 12-inch grid to pattern the air velocity distribution over the bed. As shown in Figure 2.11, because of interference issues the anemometer was suspended from above the bed to minimize turbulence.



Figure 2.11 Air velocity measurement apparatus

Temperature and Humidity Measurement

For the controlled-environment and field testing, each bed/pile was equipped with two Oakton RH/TempLog temperature and humidity data logger monitors. These monitors were located at the fan intake, to monitor the air being forced on to the beds, and at the far end of the bed, to monitor the exhaust air. Temperature and relative humidity measurements were recorded every half-hour.

CHAPTER 3 RESULTS AND DISCUSSION

CONTROLLED-ENVIRONMENT EXPERIMENTS

Controlled-environment testing using sludge from Harwood's Mill WTP was conducted over a period of five months, at EE&T's Newport News pilot facility. Testing was conducted inside, so ambient evaporation and influence from solar radiation was minimal. The primary variable evaluated during controlled-environment testing was the test bed ventilation rate, although the solids loading rate applied to each bed also varied due to variations in the Harwood's Mill WTP sludge that affected the loading procedure. The five ventilation tests conducted the controlled-environment testing are summarized in Table 3.1.

Ventilation Test 1

The initial ventilation test utilized only one test bed, which was loaded on March 18, 2011. The solids concentration of the alum sludge was measured to be 2.0 percent, and the calculated loading rate was 2.47 lb/ft². After three days, the bed had reached drained solids concentration of 8.70 percent, and ventilation across the bed was initiated using the blower and register shown previously in Figure 2.5.

Air velocity measurements, shown in Figure 3.1, indicated that there were several limitations to the ventilation configuration used for this test. Due to the presence of the register over the sludge, there was no air movement over the first foot of the bed, which was covered by the register. Even more problematic was the presence of a large dead zone at the far end of the bed. While the register was effective at inducing air flow over the surface of the cake in its immediate vicinity, the presence of the wall at the far end of the bed requires air to move up vertically to clear wall, which creates a dead zone over the last 1+ foot of the bed.

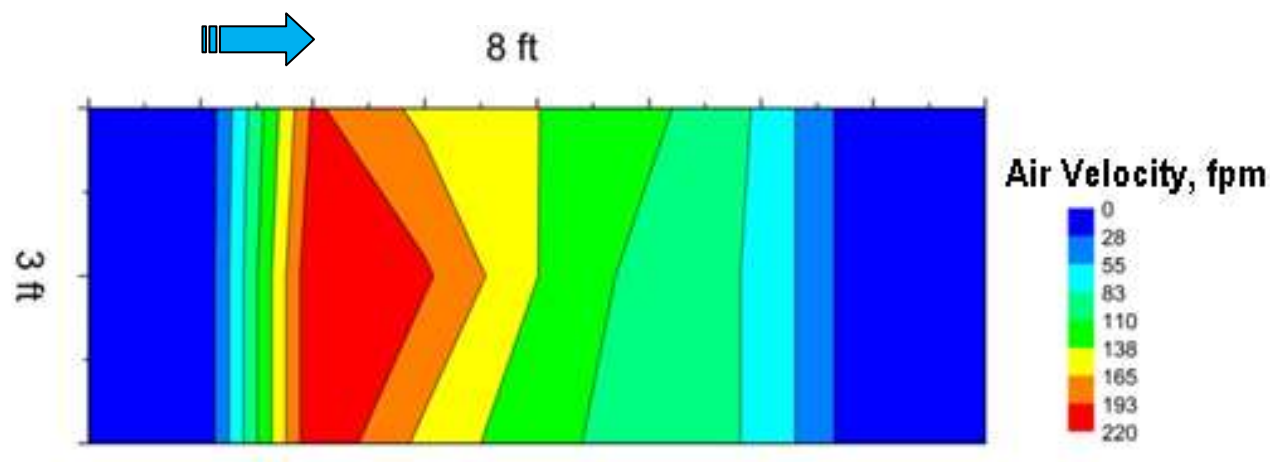


Figure 3.1 Distribution of air velocity, in fpm, over the sludge surface for Test 3

Table 3.1
Summary of ventilation tests conducted during this period

Test run	Loading date	End date	Initial TSS (% solids)	Solids loading rate (lb/ft ²)			Ventilation rate target (cfm)			Ventilation configuration (cfm)		
				Bed 1	Bed 2	Bed 3	Bed 1	Bed 2	Bed 3	Bed 1	Bed 2	Bed 3
1	3/18/2011	4/20/2011	2.0	2.47	N/A	N/A	250	N/A	N/A	Register at end of bed	N/A	N/A
2	5/11/2011	6/6/2011	1.8	2.28	2.21	2.54	0	300	300	Control	Three fans at side of bed	One fan at end of bed
3	6/7/2011	6/22/2011	1.5	N/A	2.86	3.04	N/A	600	600	N/A	Six fans at side of bed	Two fans at end of bed
4	6/24/2011	7/18/2011	1.5	N/A	4.00	3.63	N/A	600	300	N/A	Two fans at end of bed with wall cut out	Register at end of bed with wall cut out
5	8/23/2011	9/7/2011	1.4	N/A	3.19	3.18	N/A	800	800	N/A	One fan at end of bed with laminar-flow diffuser	Two fans at end of bed

The variations in air distribution over the bed shown in Figure 3.1 contributed significantly to variations in drying rates across the bed. Table 3.2 shows the solids concentrations measured from the three sample locations: S1 was located immediately in front of the ventilation register, S2 was located at the center of the bed, and S3 was located towards the far end of the bed. As expected, the rate at which the solids dried correlated closely with the air velocities shown in Figure 3.1.

Table 3.2
Solids concentration data from Ventilation Test 1

Drying days	S1 % solids	S2 % solids	S3 % solids
3	8.90	8.75	8.44
4	9.68	8.64	8.21
5	9.25	8.69	9.07
7	11.01	9.65	9.26
10	12.76	9.76	9.48
12	12.57	11.64	10.62
13	18.30	10.61	11.58
14	16.54	10.47	10.04
18	N/A	12.08	10.56
19	23.13	12.84	9.84
20	22.40	15.05	9.42
21	N/A	18.93	10.34
24	N/A	17.30	10.81
26	N/A	19.19	12.50
28	N/A	29.17	15.29
31	N/A	N/A	18.18
33	N/A	N/A	19.31

Ventilation Test 2

Given the results of Test 1, Ventilation Test 2 was configured to evaluate if overall sludge drying could be improved by better dispersing the ventilation across the bed surface. To that end, two different configurations were tried. Bed 2 was set up with three 100 cfm fans distributed along the length of the bed, as shown in Figure 3.2. Bed 3 was set up with one 300 cfm fan directed down the length of the bed, as Figure 3.3 shows. Bed 1 was tested without ventilation as a control.

The sludge obtained from Harwood's Mill WTP for Ventilation Test 2 was more difficult to dewater than the sludge used in Ventilation Test 1. TTF testing conducted prior to loading indicated an optimal polymer dose of 11 lb/dry-ton was required, and even at this high dose the sludge was not inclined to release water. For that reason, the beds had to be loaded more slowly, and the solids loading rate for Beds 1 and 2 (2.28 lb/ft² and 2.21 lb/ft², respectively) ended up approximately 15 percent lower than the solids loading rate for Bed 3 (2.54 lb/ft²).

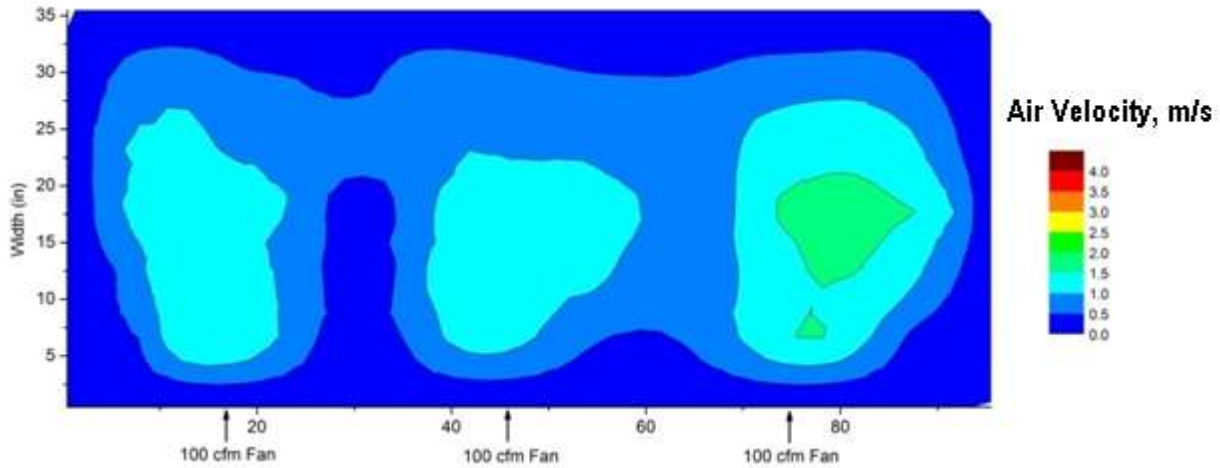


Figure 3.2 Distribution of air velocity, in m/s, over the surface of Bed 2 during Test 4

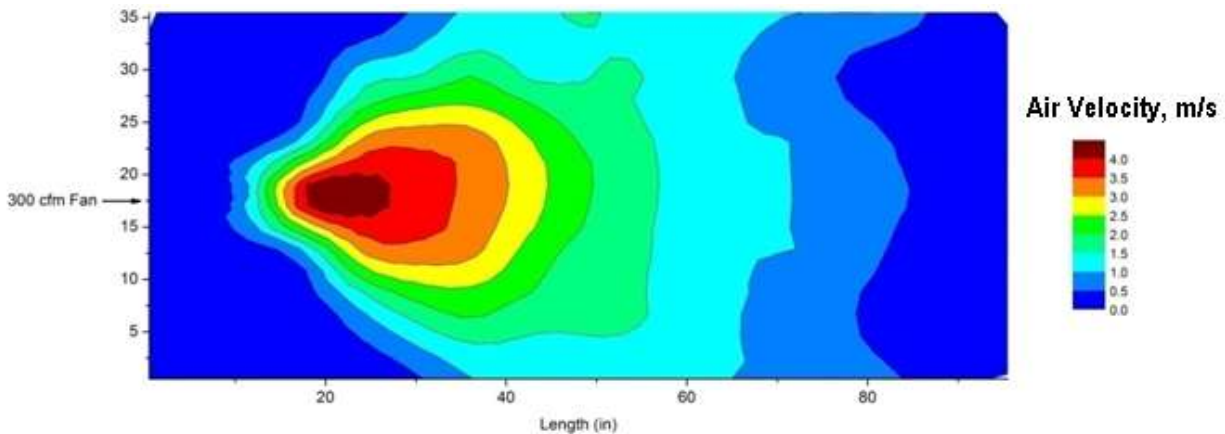


Figure 3.3 Distribution of air velocity, in m/s, over the surface of Bed 3 during Test 4

The difficulty in getting the sludge to release free water was also reflected in the low drained solids concentrations observed during Test 2. After 24 hours of draining, the solids concentration in each bed remained below six percent. This small change can significantly increase drying time; the amount of water to be removed to achieve a 20 percent cake increases by approximately 55 percent when going from 6 percent to 20 percent, as compared to going from 8 percent to 20 percent.

Table 3.3 presents the solids concentration measurements recorded during Ventilation Test 2. Sample locations were similar to those described for Ventilation Test 1. Drying performance varied significantly between the control bed and the ventilated beds; while the control bed never exceeded 13 percent solids after 61 days of drying, both of the ventilated beds had localized areas of drying in that exceed 20 percent solids after 22 days.

Table 3.3
Solids concentration data from Ventilation Test 2

Drying days	Bed 1 (control)			Drying days	Bed 2 (3-100 cfm fans)			Drying days	Bed 3 (1-300 cfm fan)		
	Solids concentration (%)				Solids concentration (%)				Solids concentration (%)		
	S1	S2	S3		S1	S2	S3		S1	S2	S3
1	6.26	4.97	5.68	1	5.93	5.24	6.22	1	5.21	6.19	5.34
2	6.03	5.80	5.64	4	7.74	7.04	7.18	4	7.68	7.58	8.31
5	6.59	6.19	6.83	6	8.50	7.80	8.32	6	7.71	8.17	9.69
7	7.64	7.03	7.3	8	11.02	11.05	11.12	8	8.30	9.95	15.08
9	7.18	6.86	7.43	11	8.91	9.46	9.56	11	8.42	14.17	12.30
12	7.89	7.65	7.89	13	9.53	9.91	10.25	13	8.52	13.58	10.98
14	7.31	7.35	6.59	15	12.35	15.99	10.25	15	11.08	16.52	15.26
16	7.99	7.76	8.66	20	11.34	15.69	18.40	20	11.62	16.68	18.23
21	8.06	8.10	9.15	22	26.43	18.64	17.21	22	16.01	27.19	21.11
23	8.78	9.42	9.18	22	16.28	16.31	18.56	22	15.40	21.69	13.03
27	8.77	9.95	9.00	25	19.23	14.90	21.84	25	15.61	25.05	11.23
29	9.18	9.36	8.84								
33	9.50	11.03	9.18								
36	10.29	10.27	10.42								
41	11.51	10.33	10.55								
43	11.23	11.05	9.96								
48	11.78	12.25	11.86								
51	12.50	12.74	12.49								
55	11.71	11.00	12.04								
58	N/A	11.81	N/A								
61	12.73	11.88	12.34								

Visual observation of the beds clearly indicated that drying was not achieved uniformly across the beds. Bed 2, shown in Figure 3.4 at the end of Ventilation Test 2, indicated hot spots of localized drying at the locations where the fans hit. This effect was more pronounced in Bed 3, shown in Figure 3.5. These results indicated that more uniform airflow across the beds was needed to increase the effectiveness of drying.



Figure 3.4 Sludge cracking observed in Bed 2 at the end of Ventilation Test 3 (3 fans @ 100 cfm each)



Figure 3.5 Sludge cracking observed in Bed 3 at the end of Ventilation Test 3 (1 fan @ 300 cfm)

Ventilation Test 3

Ventilation Test 3 attempted to improve the distribution of ventilation by: (a) increasing the number of fans ventilating each bed and, (b) increasing the overall ventilation rate applied to the beds. This was accomplished by maintaining the same configuration as in Test 2, but doubling the number of fans in each bed. Bed 1 was left undisturbed from Ventilation Test 2 to continue to allow for a control.

Figure 3.6 shows the distribution of air velocity across Bed 2, which now included a total of six 100 cfm fans blowing along the short axis of the bed. While the air flow distribution was increased over that observed in Test 2, the 100 cfm fans still had difficulty in exceeding air velocities of 2 m/s.

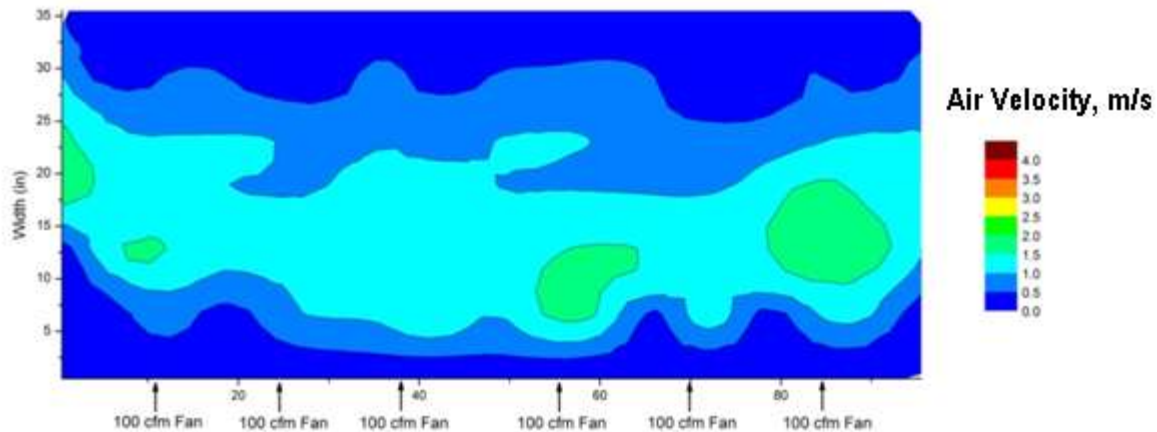


Figure 3.6 Distribution of air velocity, in m/s, over the surface of Bed 2 during Ventilation Test 3

As with Bed 2, the number of fans for Bed 3 was doubled so that two 300 cfm fans were directed along the long axis of the bed. The initial distribution of air flow across Bed 3 is shown in Figure 3.7. However, after the initial measurement of air flow across the bed, it was determined that changing the angle of the fans would more effectively cover the bed surface. Therefore, after seven days, the fan angles were changed to achieve the distribution of air velocity shown in Figure 3.8.

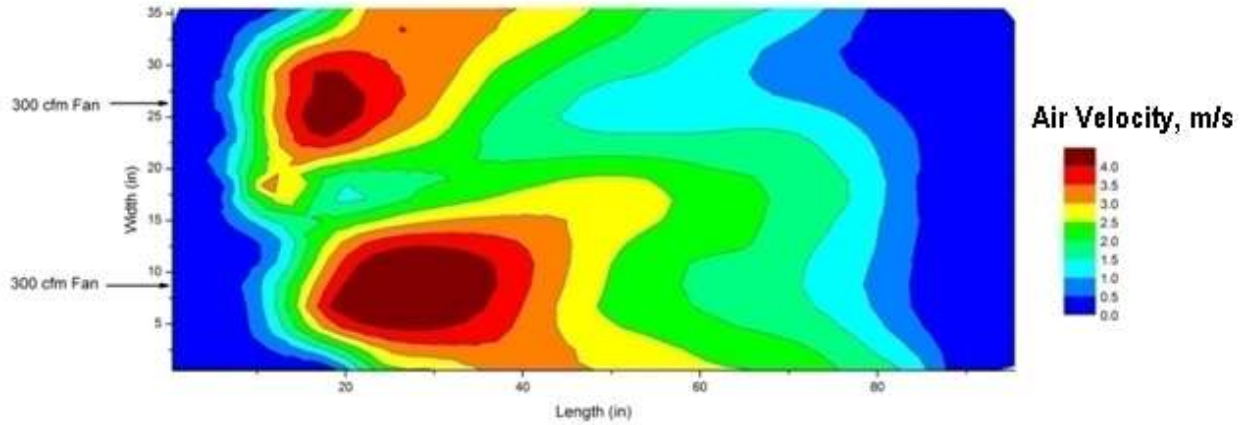


Figure 3.7 Distribution of air velocity, in m/s, over the surface of Bed 3 during Ventilation Test 3 – Configuration 1

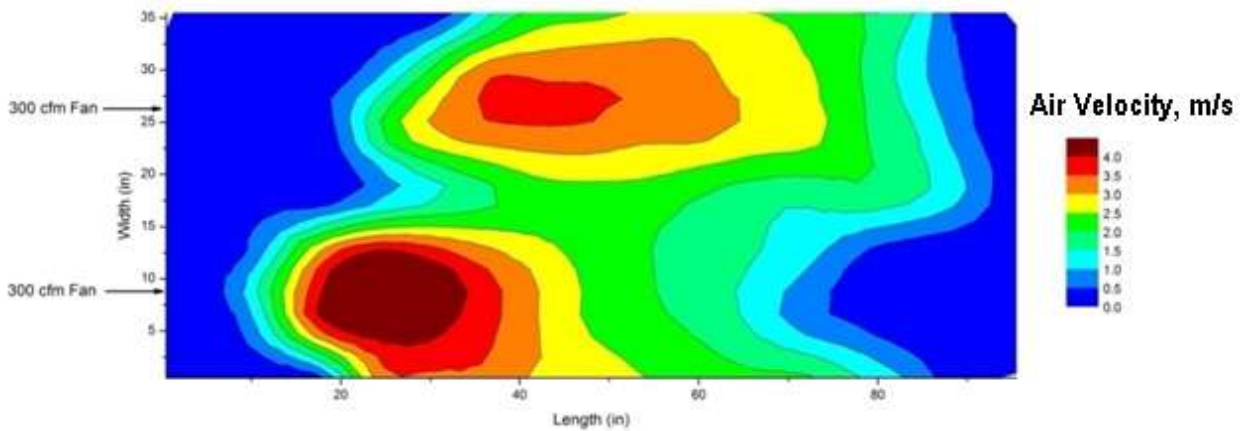


Figure 3.8 Distribution of air velocity, in m/s, over the surface of Bed 3 during Ventilation Test 3 – Configuration 2

Table 3.4 presents the solids concentration data measured over the course of Ventilation Test 3. As with Ventilation Test 2, drying in Bed 2 was more uniform than that observed in Bed 3, but portions of Bed 3 were drying much faster than Bed 2. On June 21st and 22nd, multiple samples were taken from both Bed 2 and Bed 3 to profile the final solids concentration at a higher resolution. The results of these samples are shown in Figures 3.9 and 3.10. As these figures show, there was a considerable area in the first third of Bed 3 that had a very high solids concentration, visually appearing to be in excess of 50 percent. The higher air flow rate improved drying in Bed 3 in locations where air velocities were highest.

Table 3.4
Solids concentration data from Ventilation Test 3

Drying days	Bed 2 (6-100 cfm fans)			Drying days	Bed 3 (2-300 cfm fans)		
	Solids concentration (%)				Solids concentration (%)		
	S1	S2	S3		S1	S2	S3
1	7.59	7.68	8.38	1	8.00	7.23	7.47
3	8.22	8.60	8.17	2	7.54	8.16	9.15
6	12.29	10.26	13.52	5	8.57	9.47	13.01
8	12.12	12.46	11.20	7	8.78	12.26	22.01
10	14.04	15.27	14.90	9	8.78	12.26	22.01
13	17.07	13.94	18.56	12	11.72	14.89	19.71
14	N/A	12.26	N/A	13	13.53	20.61	19.81

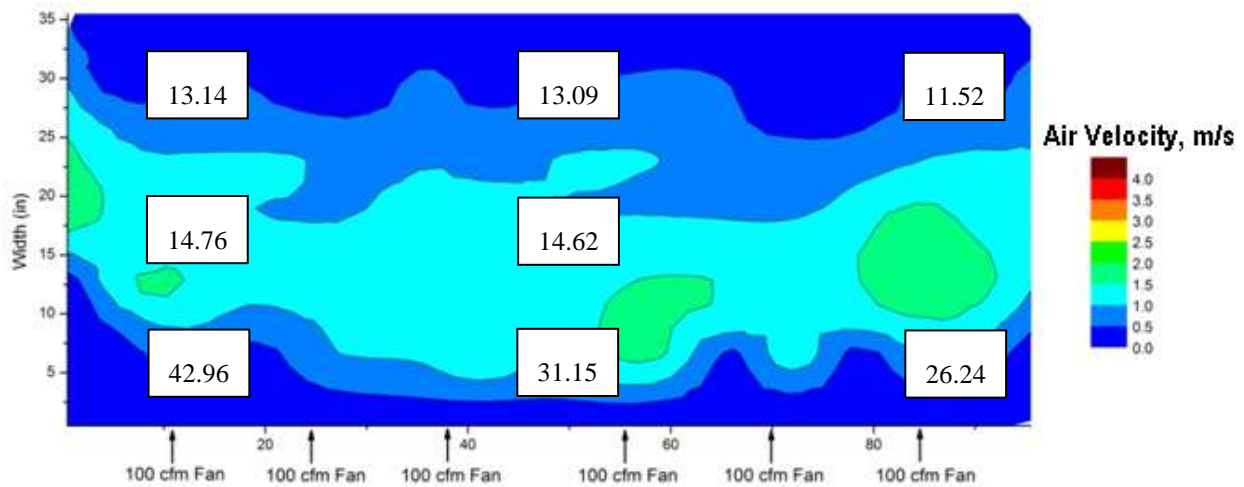


Figure 3.9 Distribution of cake solids concentrations, in percent solids, in Bed 2 on drying day 15

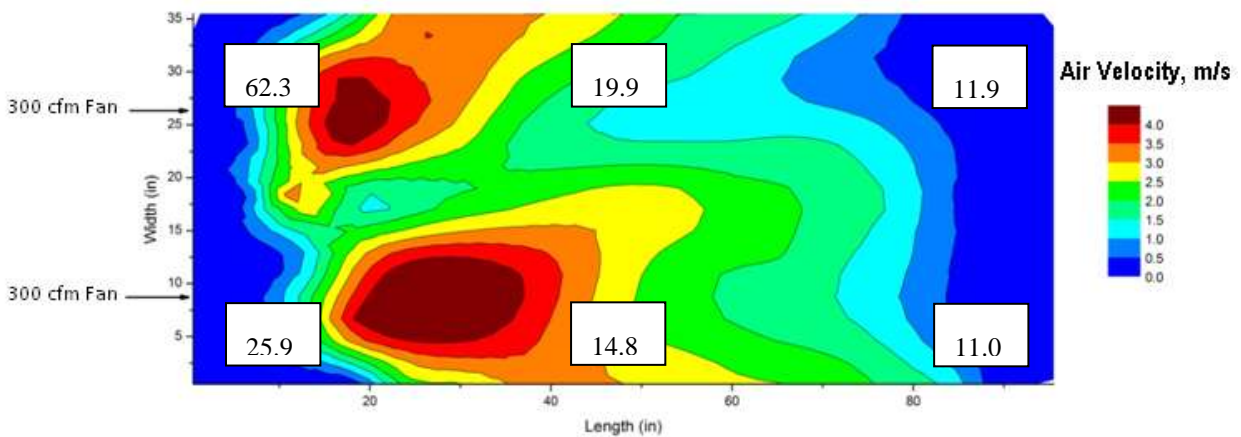


Figure 3.10 Distribution of cake solids concentrations, in percent solids, in Bed 3 on drying day 14

In both Test 2 and Test 3, Bed 3, which had the end fan configuration, outperformed Bed 2, which had the side fan configuration that more evenly disturbed the air flow over the sludge. Based on air velocity measurements, the end fan configuration produced higher localized air velocities, although the air flow is not as evenly distributed over the sludge as in the side fan configuration. Because the performance in Bed 2 was lower despite the uniform air flow, and because that configuration would be harder to construct full-scale, it was decided to concentrate testing on end fan configurations.

Ventilation Test 4

After the results from Ventilation Test 3 were analyzed, it was speculated that wall effects were preventing effective circulation of air above the sludge layer. A full-scale bed would not have an end wall at the ramp end of the bed. In order to minimize wall effects, outlet holes were cut into the bed above the sludge layer, and the ventilation register/fans were placed directly over the sludge with air directed parallel to the sludge's surface. Bed 2 was ventilated with two 300-cfm fans placed at the end of the bed, while Bed 3 was ventilated with one 300 cfm blower distributing to a register located in the end of the bed; this configuration provides a direct comparison of ventilating at 300 cfm vs. 600 cfm. Figures 3.11 and 3.12 show the air flow patterns resulting from these bed configurations. The solids concentration data measured over the course of Ventilation Test 4 is presented in Table 3.5.

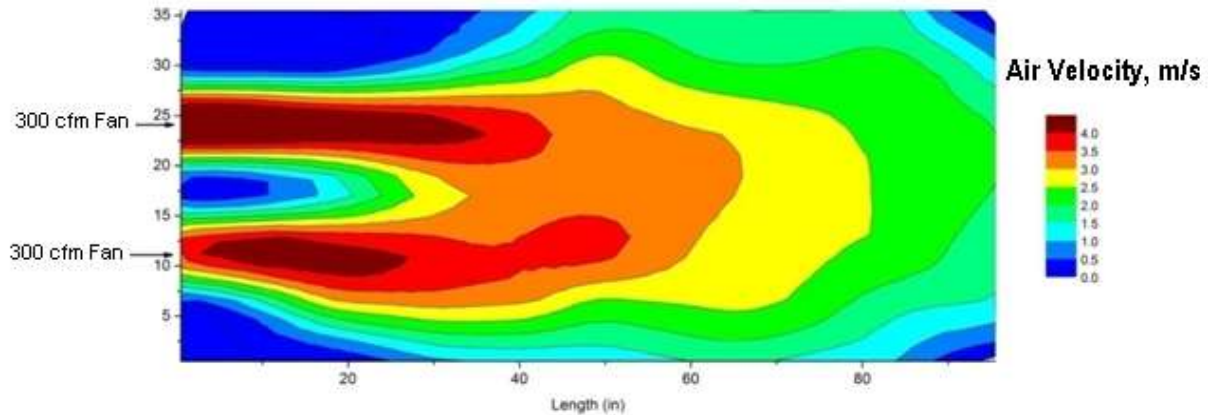


Figure 3.11 Distribution of air velocity, in m/s, over the surface of Bed 2 during Ventilation Test 4

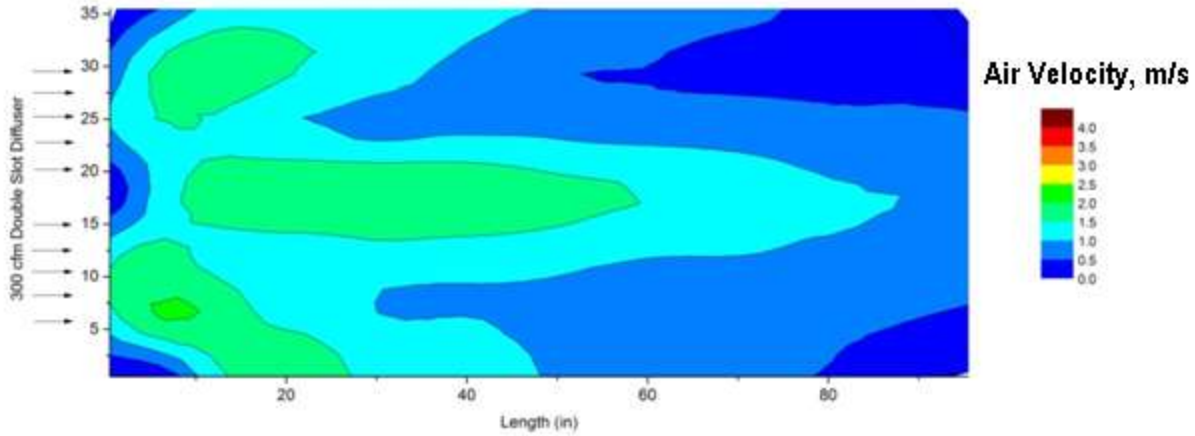


Figure 3.12 Distribution of air velocity, in m/s, over the surface of Bed 3 during Ventilation Test 4

Table 3.5
Solids concentration data from Ventilation Test 4

Drying days	Bed 2 (2-300 cfm fans)			Drying days	Bed 3 (1-300 cfm fan w/ register)		
	Solids concentration (%)				Solids concentration (%)		
	S1	S2	S3		S1	S2	S3
1	7.65	8.28	7.49	3	7.2	7.88	7.02
4	8.56	10.95	9.28	5	8.21	8.21	8.02
6	11.45	15.42	9.71	7	11.35	11.77	11.59
8	17.26	15.44	11.47	11	14.86	9.68	10/09
12	17.02	21.27	15.51	14	15.41	12.06	12.38
15	22.47	26.24	16.64	17	23.14	14.19	15.52
18	21.55	17.67	17.45	19	20.02	12.71	12.37
20	22.72	26.67	21.11	21	23.72	18.42	16.56
				24	22.12	16.47	16.91

A significant change in the test bed configuration for Test 4 was the reduction in wall effects by removing the end walls from the bed after loading. As Figures 3.11 and 3.12 show, this significantly increased the coverage of air flow across the bed. This configuration is also more representative of full-scale installations, where the proportion of bed area adjacent to the bed walls will be significantly reduced compared to pilot-scale testing.

By comparing the performance of Bed 2 to Bed 3, it is clear that the additional air flow across Bed 2 significantly increased performance. Although the coverage of Bed 3 is greatly improved compared to previous tests, the higher velocities achieved by the two 300 cfm fans in Bed 2 resulted in more rapid drying of the cake.

Ventilation Test 5

The approach for Ventilation Test 5 was slightly different than for the other ventilation tests. For this test, the total air flow rate was kept constant between the two beds; however, Bed 2 was ventilated with a single 800 cfm fan with a diffuser to maintain uniform flow, while Bed 3 was ventilated with two 400 cfm fans. The objective was to compare a high-velocity fan to the general fans that had been used. The flow rate of 800 cfm was used since that was the smallest high-velocity fan available. The high velocity fan was able to provide over 3.5 m/s velocity at the end of the bed, which is twice that provided by standard fans. The solids data collected during this test are shown in Table 3.6.

The primary goal for this test was to evaluate if the laminar-flow fans would be successful for field trials. The results from Bed 3 were promising, and showed that the single, laminar-flow fan was more successful in drying the bed than two smaller fans with the same cumulative air-flow rate. Based on these results, the laminar-flow fans were selected for all field-testing.

Table 3.6
Solids concentration data from Ventilation Test 5

Drying days	Bed 2 (1-800 cfm fan)			Drying days	Bed 3 (2-400 cfm fans)		
	Solids concentration				Solids concentration		
	(%)				(%)		
	S1	S2	S3		S1	S2	S3
1	6.59	6.51	6.855	1	7.03	6.87	6.72
3	10.51	11.64	11.97	5	15.04	11.89	8.955
6	17.67	17.44	13.62	8	20.93	13.93	12.24
9	28.82	18.21	16.11	14	33.46	22.69	19.39
15	42.25	59.91	29.46				

Drying Previously Dewatered Cake

As seen in Figure 3.10, enhanced non-mechanical dewatering (and non-mechanical dewatering in general) can potentially remove much more water from water treatment plant residuals than is possible using mechanical dewatering technologies. This introduces the possibility for additional cost savings for utilities that currently have mechanical dewatering processes; instead of transporting and disposing of residuals that are more than 75 percent water, it may be possible to use enhanced non-mechanical dewatering to remove more than half of the remaining water in the mechanically dewatered cake.

This was evaluated at EE&T's Newport News laboratory using a cake sample was collected from the E.M. Johnson WTP on August 4, 2011. The sample was kept covered until test piles could be configured on August 16, 2011. Three test piles were formed: Pile 1, measuring 12 inches by 12 inches by 12 inches, was kept as a control (Figure 3.13); Pile 2 was arranged 6-foot long by 1-foot wide by 8 inches high (Figure 3.14, left) and Pile 3 was arranged 6-foot long by 1-foot wide by 18 inches high (Figure 3.14, right). Both Piles 2 and 3 were set up with a 400 cfm fan blowing parallel to the top of the pile, along the long axis. The angle of repose of the dewatered cake was not conducive towards piling in a 1' wide pile that was 18

inches high, so two support boards were provided to keep the pile together. All of the piles lost cohesiveness as the cake continued to dewater.



Figure 3.13 Pile 1 on Drying Day 1 (12-inch x12-inch x12-inch)



Figure 3.14 Pile 2 (6-ft x1-ft x8-inch, left) and Pile 3 (6-ft x1-ft x18-inch, right) on Drying Day 1

The solids concentrations recorded from each bed are shown in Figure 3.15. Clearly, the shorter pile (Pile 2, 8 in. high) dried much more quickly than the control pile (12 in. high), or Pile 3 (18 in. high). However, it should be noted that the solids comprising Pile 2 were already at a higher solids concentration (28 percent) when the test began than either Pile 1 (22 percent) or Pile 3 (23 percent). Therefore, less water needed to be removed from Pile 2 to achieve a given solids concentration. Airflow was the same over Pile 2 and Pile 3, and no air was applied to Pile 1 (Control).

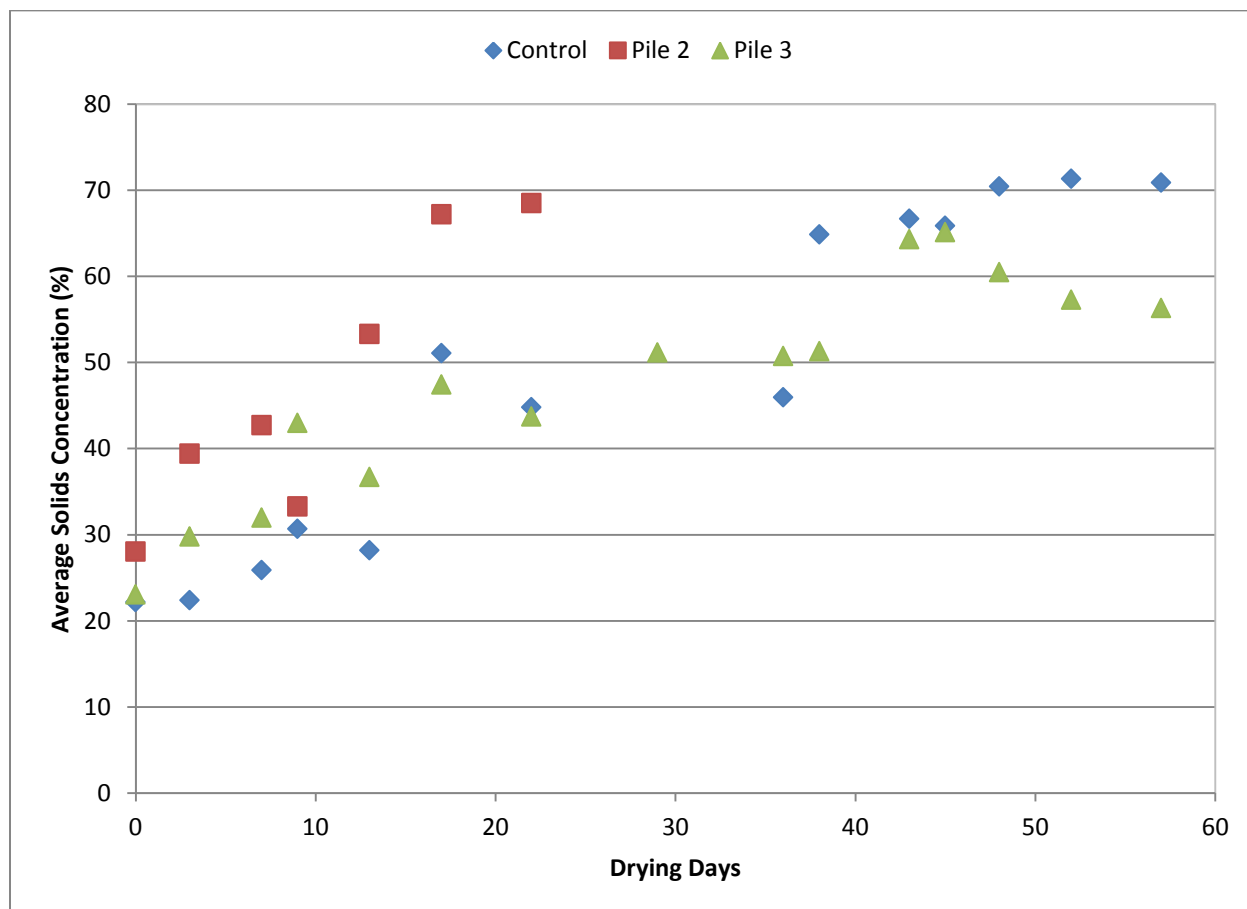


Figure 3.15 Drying performance over time during drying of previously dewatered cake

While temperature and humidity data were not recorded during this test, it is possible to use the mass of solids present in each pile to determine the overall water loss from each pile, which can then be converted to an effective evaporation rate. For the purposes of determining the mass of each pile, it was assumed the unit weight of the wet sludge was 70 lb/ft³.

As noted previously, the 8 inch deep pile contained significantly less water than the 18 inch deep pile; not only was the initial cake solids concentration higher (28 percent compared to 23 percent), but there was less overall cake mass to dry. For Pile 2, it took 13 days to dry the cake from 28 percent solids concentration to 53.32 percent solids concentration, which required the removal of approximately 70.8 pounds of water. Over the 6-foot by 1-foot pile, this is equivalent to an evaporation rate of 5.23 in./mo. Pile 3, on the other hand, took 29 days to dry from 23 percent solids concentration to 51 percent solids concentration. While the overall time

was higher, so was the overall mass of water evaporation; because the mass of cake was more than twice that of Pile 2, approximately 177 pounds of water needed to be evaporated to raise the cake solids concentration to over 50 percent solids. The equivalent evaporation rate over the period was 5.70 in./mo., which is similar to that for Pile 2. Pile 1, which was not ventilated, was much smaller and had a lower overall evaporation rate; after 13 days, the solids concentration had only increased from 22 percent solids concentration to 28 percent solids concentration, which is equivalent to 0.81 in./mo. of evaporation. However, later test data showed better evaporation from the control pile. After 38 days the solids concentration had increased to 64 percent solids concentration, which would be equivalent to 5.75 in./mo. of evaporation.

Summary of Controlled Environment Testing

Pilot-scale testing of non-mechanical dewatering can be complicated by small variances in between loadings. Because moisture content is inversely proportional to the solids concentration, small differences in the drained solids concentration can result in large differences in the amount of drying that is required. If a change in sludge composition reduces the drained solids concentration of the bed for a given run, the time required to reach a target solids concentration may change dramatically compared to other test runs, even if evaporation is the same.

Therefore, it is useful to look past the overall time required to reach a target solids concentration for a given test run, to instead investigate the effective evaporation rate of that test run. The effective evaporation rate can be calculated by comparing change in the equivalent depth of the residuals over time, which can be calculated using Equation 2.1.

$$D_E = \frac{SLR \times 12 \text{ in./ft}}{SS \times 62.4 \text{ lb/ft}^3} \quad (2.1)$$

where D_E = equivalent depth (in.)
 SLR = solids loading rate (lb/ft²)
 SS = solids concentration (%)

The equivalent depth of the residuals should not be confused with the physical depth of the sludge in the dewatering bed. During the drainage phase, the depth of the residuals will decrease linearly with the increase in the residuals solids concentration. However, as residuals dry (particularly once desiccation cracking is observed), this linear relationship between sludge depth and evaporation breaks down due to changes in residuals characteristics (Vandermeijden and Cornwell, 1998.) Therefore, the equivalent depth of the residuals is a conceptual tool that is equivalent to the depth of a mass of water that is equal to the mass of wet solids loaded in the bed.

This concept is illustrated in Figure 3.16, which presents the solids concentration, and the corresponding equivalent depth, of the residuals in Ventilation Test 4 - Bed 2, over time. As noted in Table 3.1, the initial solids concentration of the sludge loaded onto the bed was 1.5 percent and the solids loading rate for this bed was 4 lb/ft². The corresponding equivalent depth of the solids loaded onto the bed would be 51.2 inches; therefore, over 80 percent of the total equivalent depth was removed during the first 24 hours through drainage. However, even though the drainage mechanism removes the majority of the water from the residuals, the resulting

solids concentration of the residuals was only 7.81 percent solids, which is still too fluid to handle. After draining, it took an additional 14 days to remove an additional 6.33 inches of equivalent depth for the residuals to reach the target of 20+ percent solids.

The change in equivalent depth can be used to calculate the effective evaporation rate of the enhanced non-mechanical dewatering process. Figure 3.17 presents the total evaporation from Ventilation Test 4 – Bed 2. Note that the horizontal axes on Figures 3.16 and 3.17 are not the same; in Figure 3.16, the drying days are defined as the number of days from the bed loading, while in Figure 3.17 the days of evaporation are defined as the number of days from the time when the bed reached its drained solids concentration. In this test, the bed appeared to finish draining after Drying Day 1, which is the set as the origin in Figure 3.17.

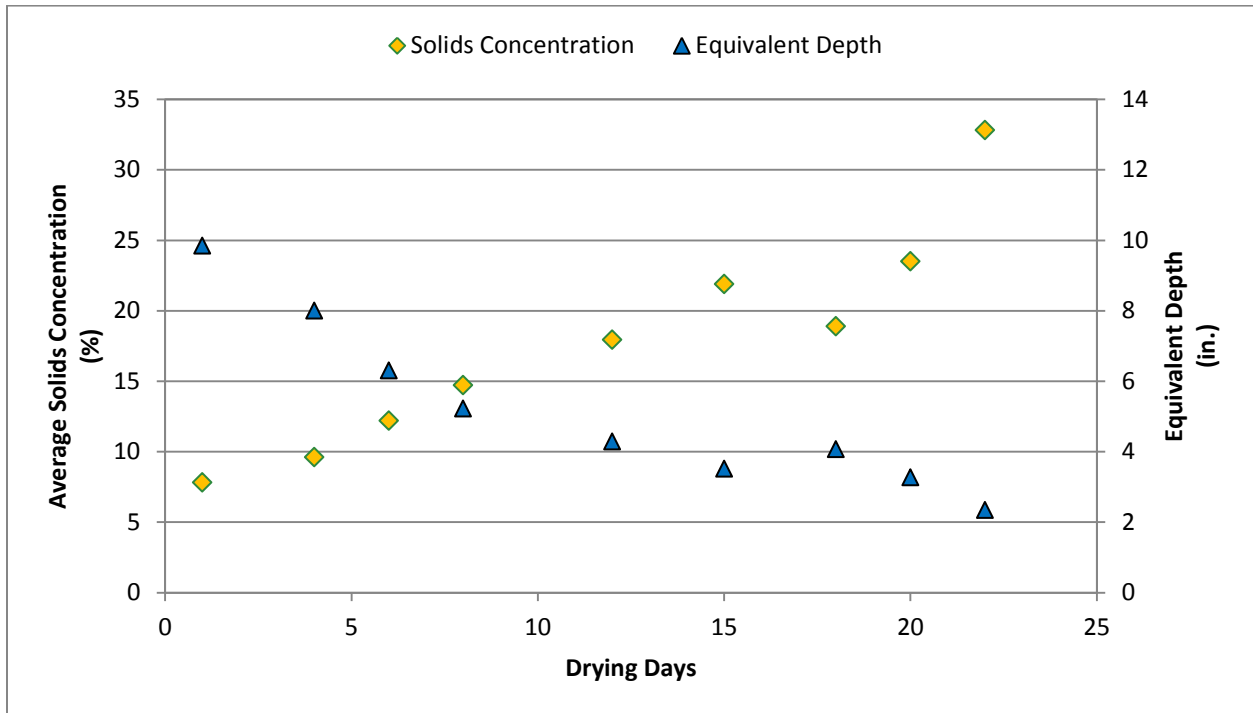


Figure 3.16 Change in solids concentration and equivalent depth over time for Ventilation Test 4, Bed 2

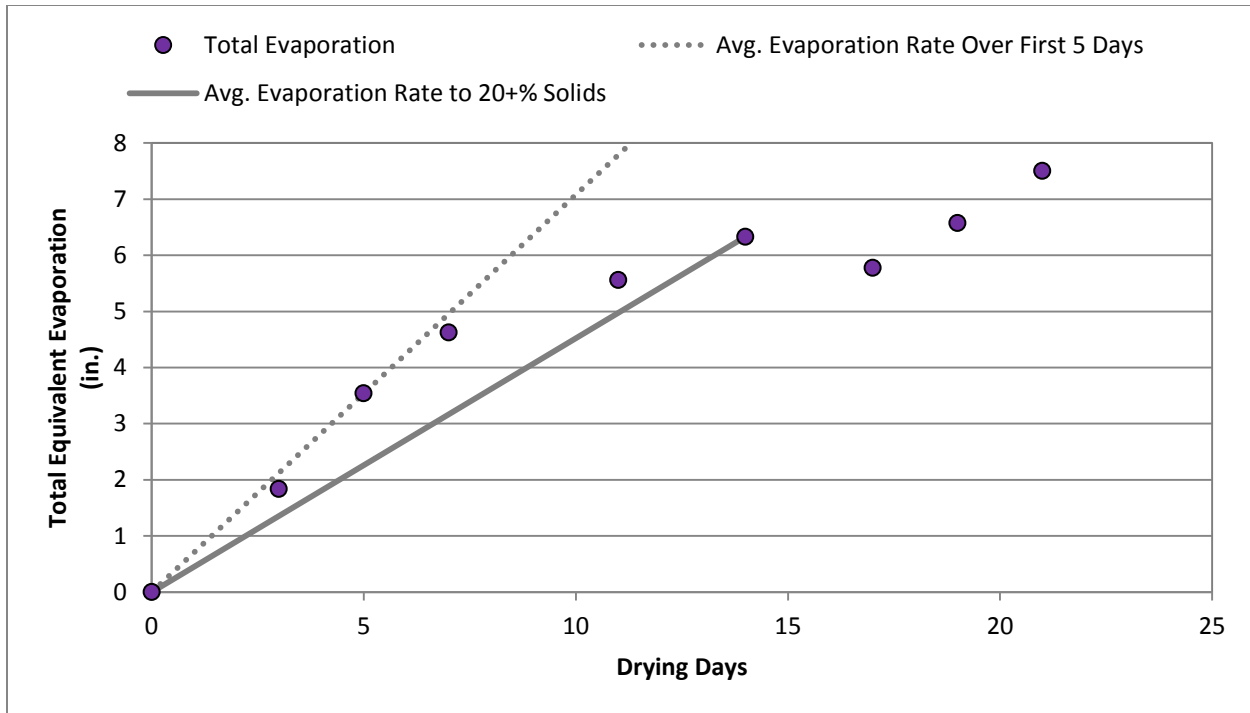


Figure 3.17 Total equivalent evaporation and effective evaporation rates for Ventilation Test 4, Bed 2

As Figure 3.17 shows, evaporation is not a linear process from the drying residuals. As the residuals dry, the exterior of the cake dries more rapidly than the interior. This forms a crust, which can impede transport of free water to the cake surface where evaporation occurs, which slows evaporation over time.

The effective evaporation rate of the process can be calculated using Equation 2.2.

$$E = \frac{D_{E,t} - D_{E,d}}{T_t - T_d} \times 30 \text{ days/mo} \quad (2.2)$$

where E = average evaporation rate (in./mo.)
 $D_{E,t}$ = equivalent depth at time t (in.)
 $D_{E,d}$ = equivalent depth of the drained solids (in.)
 T_t = number of drying days to time t (days)
 T_d = number of drying days to reach the drained solids concentration (days)

Graphically, the effective evaporation rate can be visualized as the slope of the line from the origin to the total evaporation. This can be seen in Figure 3.17, where the average evaporation rate after five days of evaporation (21.2 in./mo.) is compared to the average evaporation rate after 14 days of evaporation (13.6 in./mo.), at which point the solids had met the target solids concentration of 20 percent.

These calculations were performed for each of the controlled-environment tests on the Harwood's Mill sludge. Table 3.7 summarizes the results from each test.

Table 3.7
Summary of controlled-environment test results on Harwood's Mill sludge

Test	Bed 1			Bed 2			Bed 3		
	Days of evaporation to 20+ % solids	Ventilation rate (cfm)	Effective evaporation rate (in./mo.)	Days of evaporation to 20+ % solids	Ventilation rate (cfm)	Effective evaporation rate (in./mo.)	Days of evaporation to 20+ % solids	Ventilation rate (cfm)	Effective evaporation rate (in./mo.)
1	25	250	3.98	N/A	N/A	N/A	N/A	N/A	N/A
2	N/A	N/A	N/A	21	3 @ 100	7.25	21	1 @ 300	8.84
3	N/A	N/A	N/A	14	6 @ 100	9.31	13	2 @ 300	11.56
4	N/A	N/A	N/A	14	2 @ 300	13.57	18	1 @ 300	9.83
5	N/A	N/A	N/A	14	1 @ 800	16.75	14	2 @ 400	14.91

Four different fan configurations were evaluated for the controlled environment testing using Harwood's Mill sludge: fans on the side of the bed, blowing across the short axis; fans on the end of the bed, blowing along the long axis without a cut-out at the end; fans on the end of the bed, blowing along the long axis with a cut-out at the end (to eliminate dead space), and a laminar-flow fan on the end of the bed, blowing along the long axis. Figure 3.18 presents the effective evaporation rate for each configuration, as a function of applied air flow.

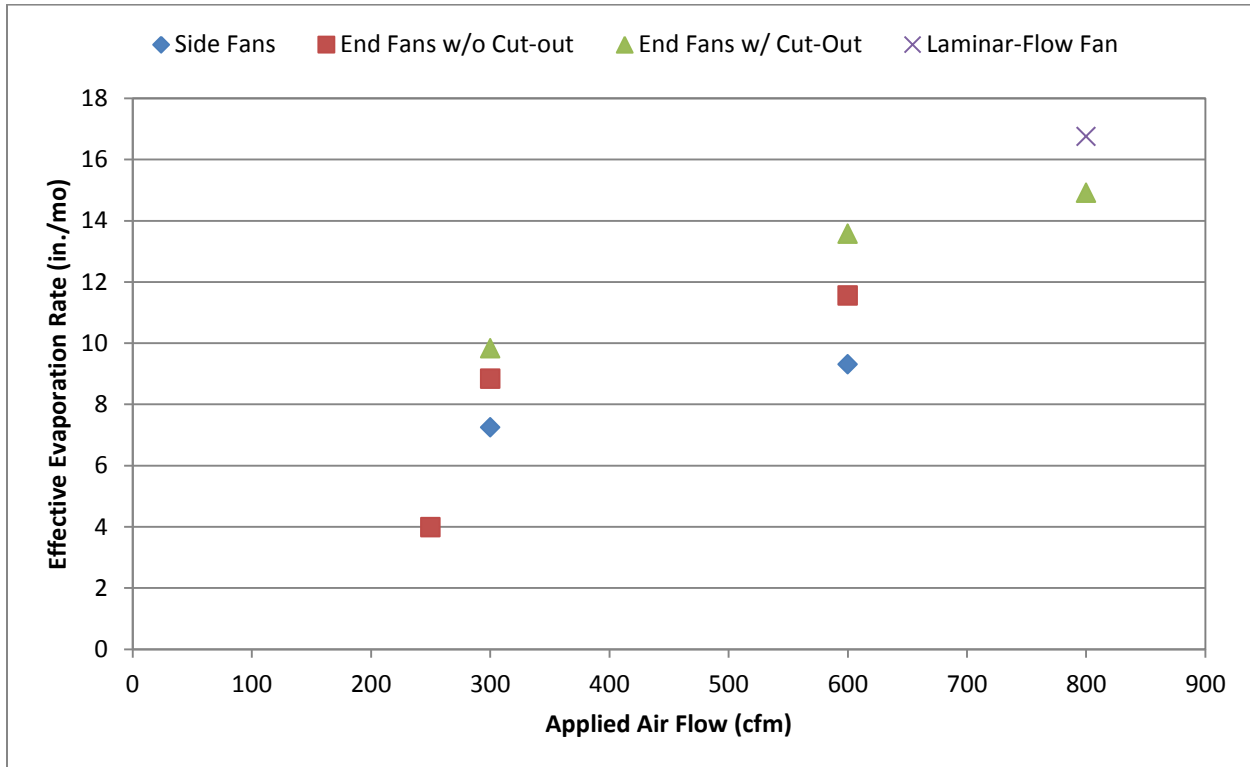


Figure 3.18 Effective evaporation rate based on fan configuration

Based on the data shown in Figure 3.18, the laminar-flow fan oriented along the long axis of the test bed appears to be the most effective configuration. As expected, effective evaporation rates were higher for the bed with the end cut out than for the beds with the ends present, due to the better distribution of air across the former. Because the smaller fans used for the side fan configuration could not produce as high of velocity as the larger fans, effective evaporation rate was lower for those beds. It was also visually evident that the laminar flow fan resulted in more uniform drying throughout the bed.

CLEVELAND PILOT STUDIES

Field pilot studies were initiated at the Morgan WTP in October 2011, and continued through June 2012. During that time eight (8) tests were conducted to assess the performance of the enhanced non-mechanical dewatering beds. The goal of this testing was to dewater thickened sludge, ranging from 1.2 to 1.6 percent solids concentration, to a dewatered cake concentration of 20+ percent solids concentration.

Morgan WTP staff conducted the bed loadings, with EE&T assistance, and took bi-weekly samples for analysis. Since the solids concentration was unknown at the time of sampling, the exact number of drying days to reach 20 percent solids concentration could not be measured. Rather, the sampling date of the first sample to reach approximately 20 percent or more was recorded as the “final concentration”, although the solids continued to dry until they were removed from the bed. Over time collection procedures were refined to more fully characterize the drying bed performance.

Shakedown Test Results

The initial loading of the pilot test beds at Morgan WTP took place on October 6, 2011. This loading was conducted primarily to test the equipment and loading protocols, so the testing was not fully controlled. For this reason, the West Bed was loaded at a rate of 1.5 lb/ft², while the East Bed was loaded at 2.0 lb/ft². The final drained solids concentration was not measured as part of this run because of its preliminary nature.

However, once the beds were loaded, the team decided to set up ventilation and collect some limited data as a preliminary measure of the beds’ performance in the field. The West Bed was configured with the laminar-flow fan blowing 800 cfm along the long axis of the bed, while the East Bed was held as a control bed and was not ventilated. Data collected from this initial test are presented in Figure 3.19.

Preliminary temperature and humidity data collected inside of West Greenhouse also provided insight on the mechanism of drying in the field. Unlike the controlled environment testing, which was conducted under relatively constant temperature conditions, the field units experienced significant diurnal temperature fluctuations. These fluctuations served to be enhance and impede dewatering. As Figure 3.20 shows, during the day the greenhouse temperatures exceeded the ambient temperature by more than 50 percent. Between the greater potential for holding moisture (as evidenced by the lower relative humidity) and the additional energy imparted to the residuals, the increased temperature in the greenhouse would serve to increase drying, even without ventilation. However, because the greenhouse structure lacks the capacity to retain this heat during the cool nights, the temperature drops below the dew point for the moist air inside the greenhouse and becomes saturated, during which time drying cannot occur. Because the ambient relative humidity remains below the saturation threshold, it could potential be drying the solids during hours when the greenhouse air is too moist for drying.

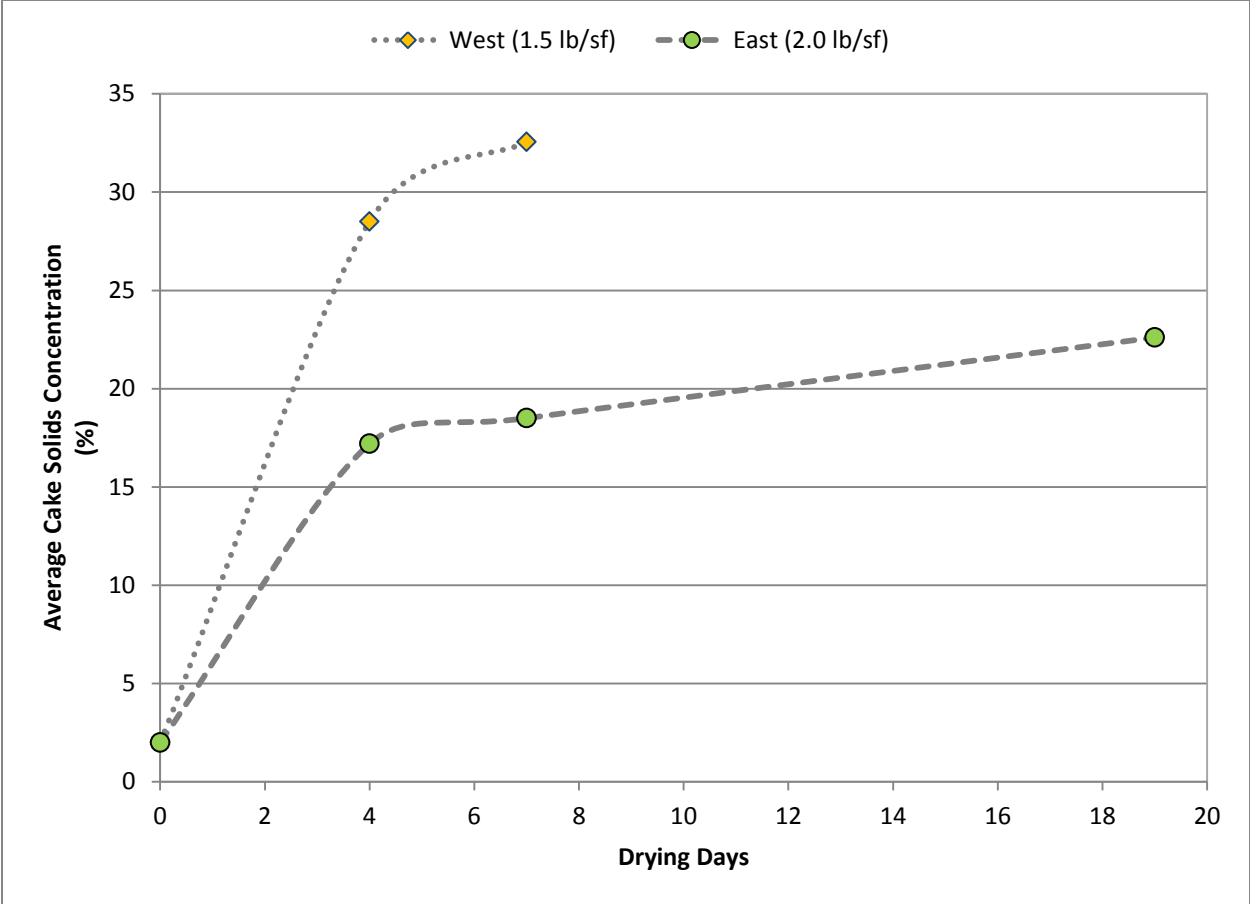


Figure 3.19 Drying performance over time during initial shakedown testing at Morgan WTP

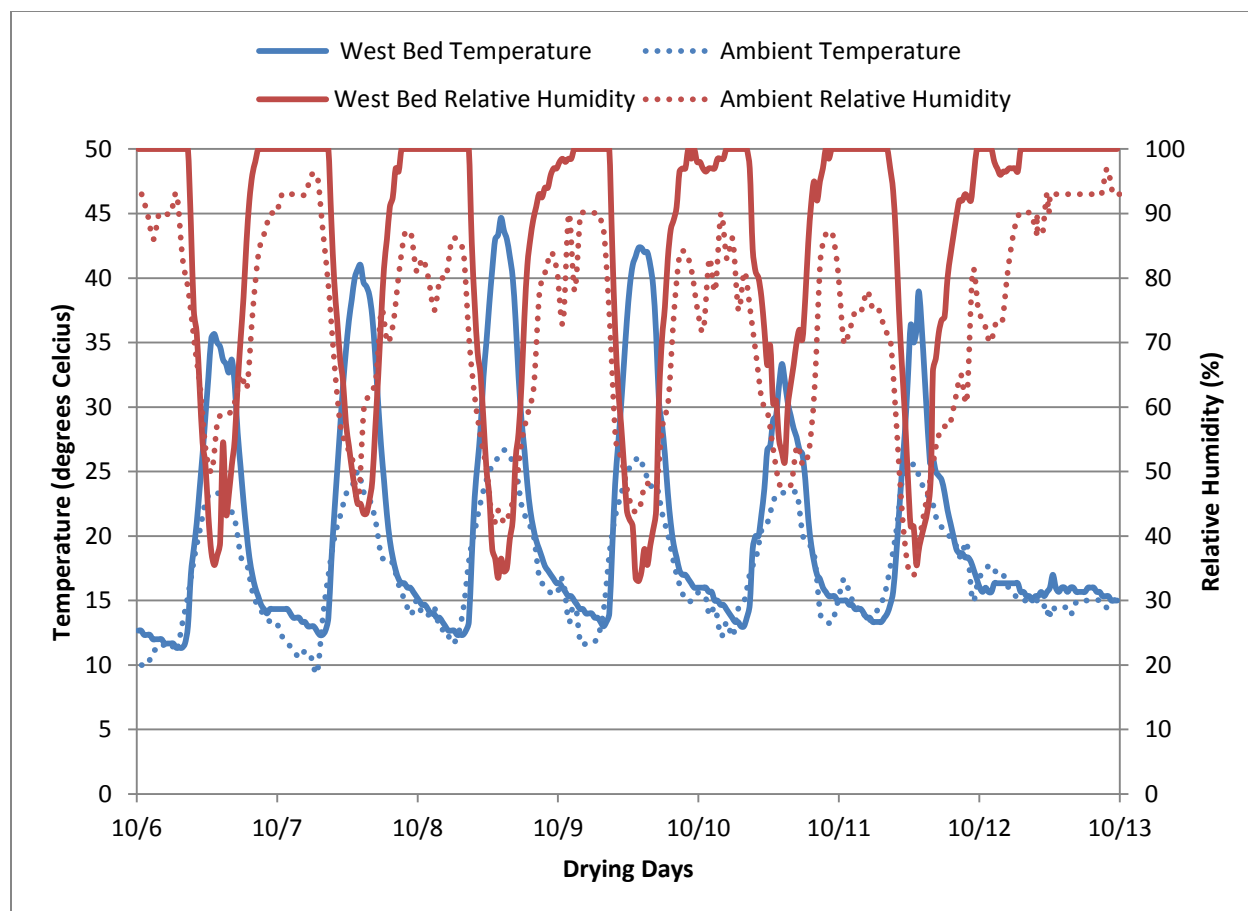


Figure 3.20 Drying performance over time during initial shakedown testing at Morgan WTP

Cleveland Test 1 – October 27, 2011

The first full test of the enhanced non-mechanical dewatering beds at Morgan WTP began on October 27, 2011. For this first test, the East Bed was set as a control, while the West Bed configured with the laminar-flow fan blowing 800 cfm along the long axis of the bed. Parameters for Cleveland Test 1 are summarized in Table 3.8, and Figure 3.21 shows the drying performance in each bed.

Test 1 results were very promising. The enhanced non-mechanical dewatering bed using forced air ventilation reached the target dewatered cake concentration in eight days, less than 20 percent of the time required for the control bed to achieve the equivalent concentration (although it should be noted that the control bed approached the target concentration after eight days as well, before its drying rate decreased significantly). Furthermore, the enhanced bed achieved a final dewatered solids concentration in excess of 50 percent, indicating that this process can dewater water treatment plant residuals to a higher concentration than mechanical dewatering processes can.

Table 3.8
Cleveland Test 1 parameters

	East bed	West bed
Loading date	10/27/2011	10/27/2011
Initial solids concentration (%)	1.3	1.3
Calculated solids loading rate (lb/ft ²)	2.98	2.98
Drained solids concentration (%)	8.1	7.27
Measured solids concentration at target (%)	19.6	20.1
Drying days to 20+ percent solids (days)	39	8
Measured average air velocity (fps)	0	16.9
Average ambient temp (°F)	44.3	44.5
Average solar radiation (W/m ²)	136.2	178.2

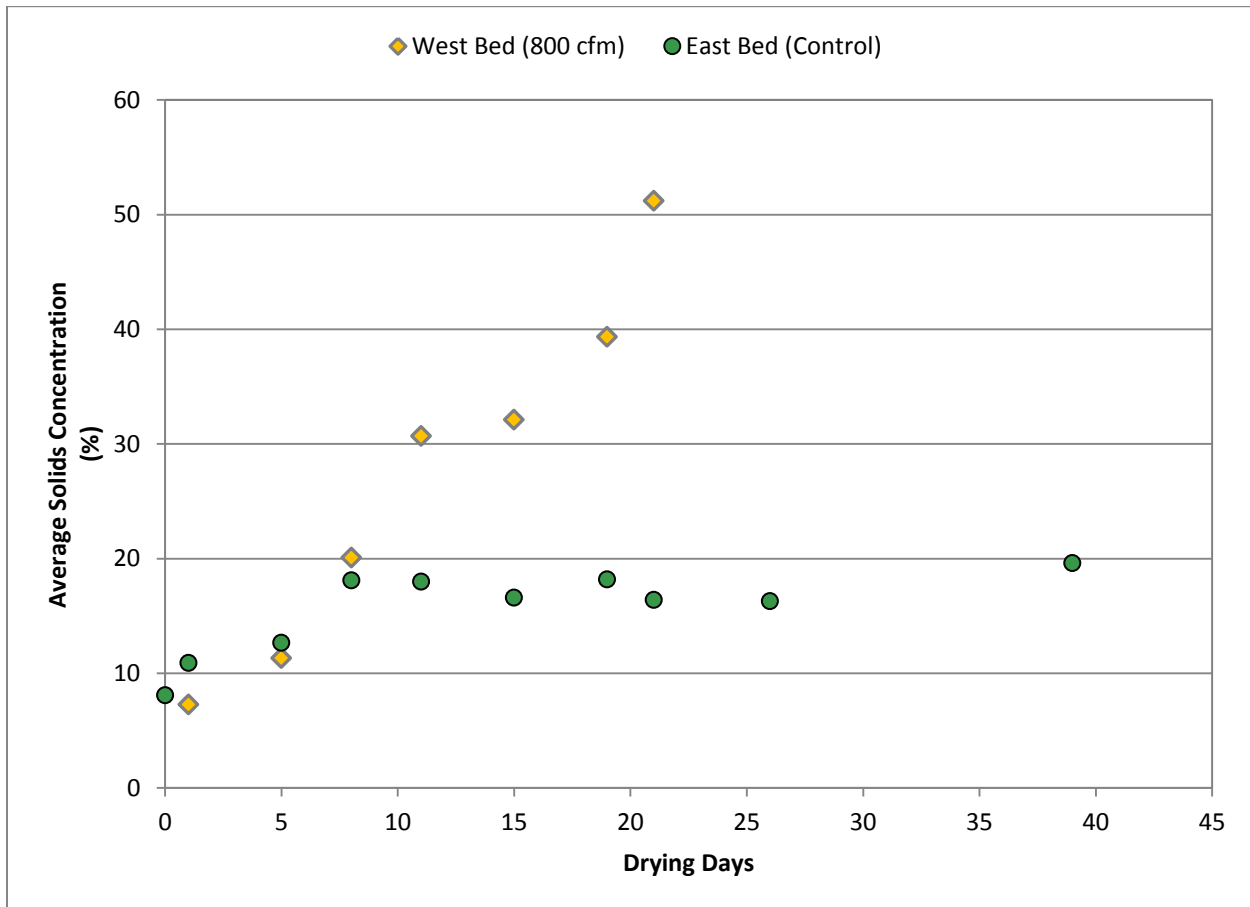


Figure 3.21 Drying performance over time during Cleveland Test 1 (10/27/2011)

Cleveland Test 2 – December 14, 2011

The second test of the enhanced non-mechanical dewatering beds at Morgan WTP began on December 14, 2011. As before, the East Bed was set as a control, while the West Bed configured with the laminar-flow fan blowing 800 cfm along the long axis of the bed. Parameters for Cleveland Test 2 are summarized in Table 3.9, and Figure 3.22 shows the drying performance in each bed.

Cleveland Test 2 was unusual in that the beds were able to attain a very high solids concentration (11.5 and 12.1 percent solids) after only one day of drying. While this level of performance is desirable, the other Cleveland tests were not able to achieve as high of a drained solids concentration so quickly. Because of the high drained solids concentration, it was only necessary to evaporate approximately two inches to bring the solids concentration in each bed to the 20 percent target. After eight days, the West Bed had reached average solids concentration of 18.5 percent, and the run was terminated to attempt another loading. The East Bed was allowed to continue to dry until it reached the target solids concentration of 20.0 percent, which it reached after 23 days of drying.

During the period that the West Bed was drying temperatures remained above freezing, so no freeze-thaw dewatering occurred during that time. After the West Bed had finished, there were isolated days when the temperatures were below 0°C while the East Bed was still drying. It is possible that some of the dewatering observed for the East Bed occurred via freeze-thaw rather than through evaporation, but the residuals removed from the East Bed at the end of the test did not have the “coffee ground” texture that is characteristic of freeze-thaw dewatering.

Table 3.9
Cleveland Test 2 parameters

	East bed	West bed
Loading date	12/14/2011	12/14/2011
Initial solids concentration (%)	1.3	1.3
Calculated solids loading rate (lb/ft ²)	2.98	2.98
Drained solids concentration (%)	12.1	11.5
Measured solids concentration at target (%)	20.0	18.5
Drying days to 20+ percent solids (days)	23	8
Measured average air velocity (fps)	0	11.2
Average ambient temp (°F)	36.3	40.1
Average solar radiation (W/m ²)	86.1	39.2

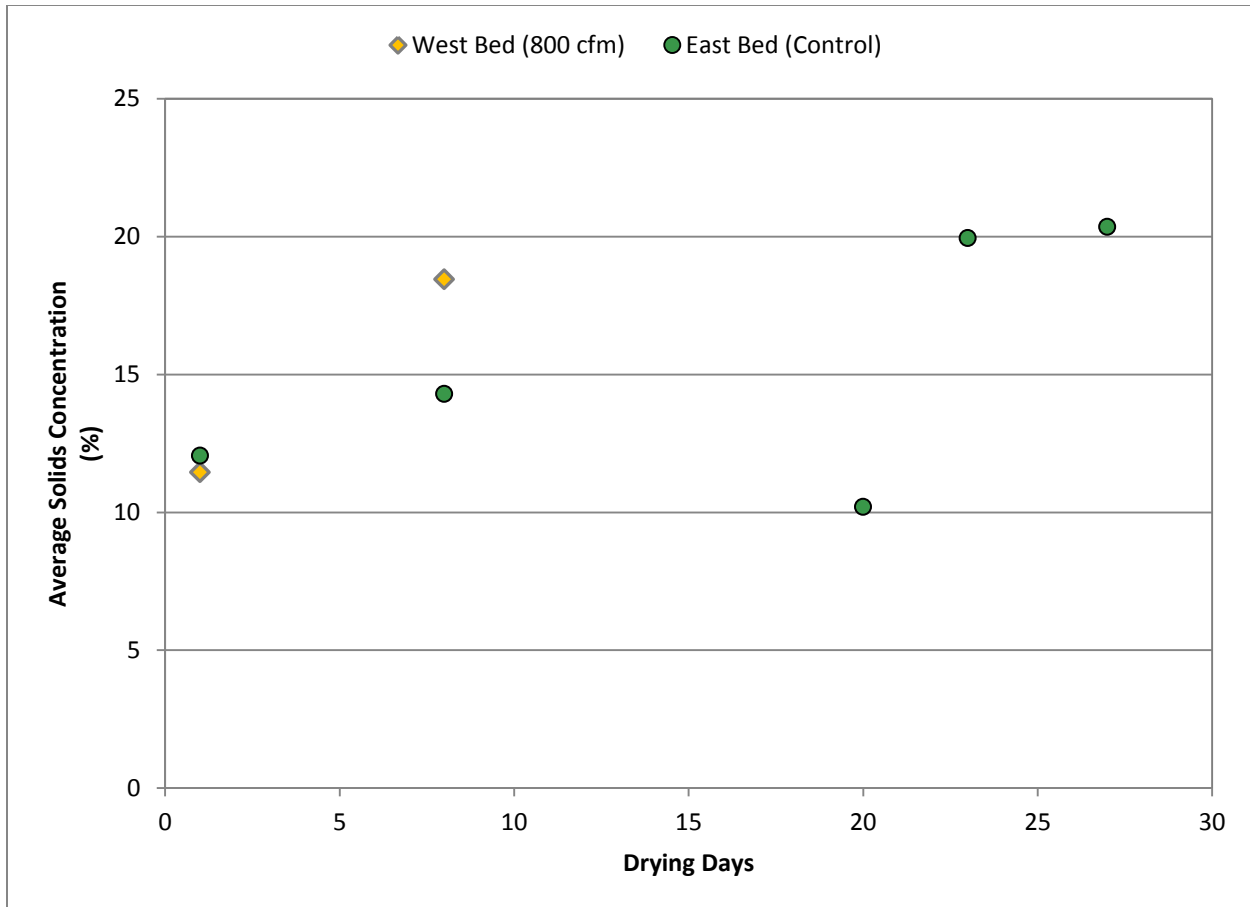


Figure 3.22 Drying performance over time during Cleveland Test 2 (12/14/2011)

Cleveland Test 3 – January 12, 2012

The third test at Morgan WTP was initiated on January 12, 2012. For this test, only the West Bed was loaded. The West Bed was configured with the laminar-flow fan blowing 800 cfm along the long axis of the bed, as with previous tests. Parameters for Cleveland Test 2 are summarized in Table 3.10, and Figure 3.23 shows the drying performance in each bed.

Immediately after loading the beds, the ambient temperature and internal bed temperature drop several degrees below freezing for an extended period. By January 16, temperatures increased and led to an extended period of above-freezing temperature. These factors induced freeze-thaw dewatering, which rapidly raised the solids concentration of the bed above the 20 percent solids target within five days of loading. Figure 3.24 compares the West Bed after 13 days of dewatering during Cleveland Test 1 to the West Bed after six days of dewatering during Cleveland Test 3. The fine texture of the dewatered residuals in the latter is a tell-tale sign of freeze-thaw dewatering, compared to the more cohesive cake observed during Cleveland Test 1.

Table 3.10
Cleveland Test 3 parameters

	East bed	West bed
Loading date	N/A	1/12/2012
Initial solids concentration (%)	N/A	1.2
Calculated solids loading rate (lb/ft ²)	N/A	2.31
Drained solids concentration (%)	N/A	6.65
Measured solids concentration at target (%)	N/A	23.1
Drying days to 20+ percent solids (days)	N/A	5
Measured average air velocity (fps)	N/A	14.4
Average ambient temp (°F)	N/A	26.7
Average solar radiation (W/m ²)	N/A	102.4

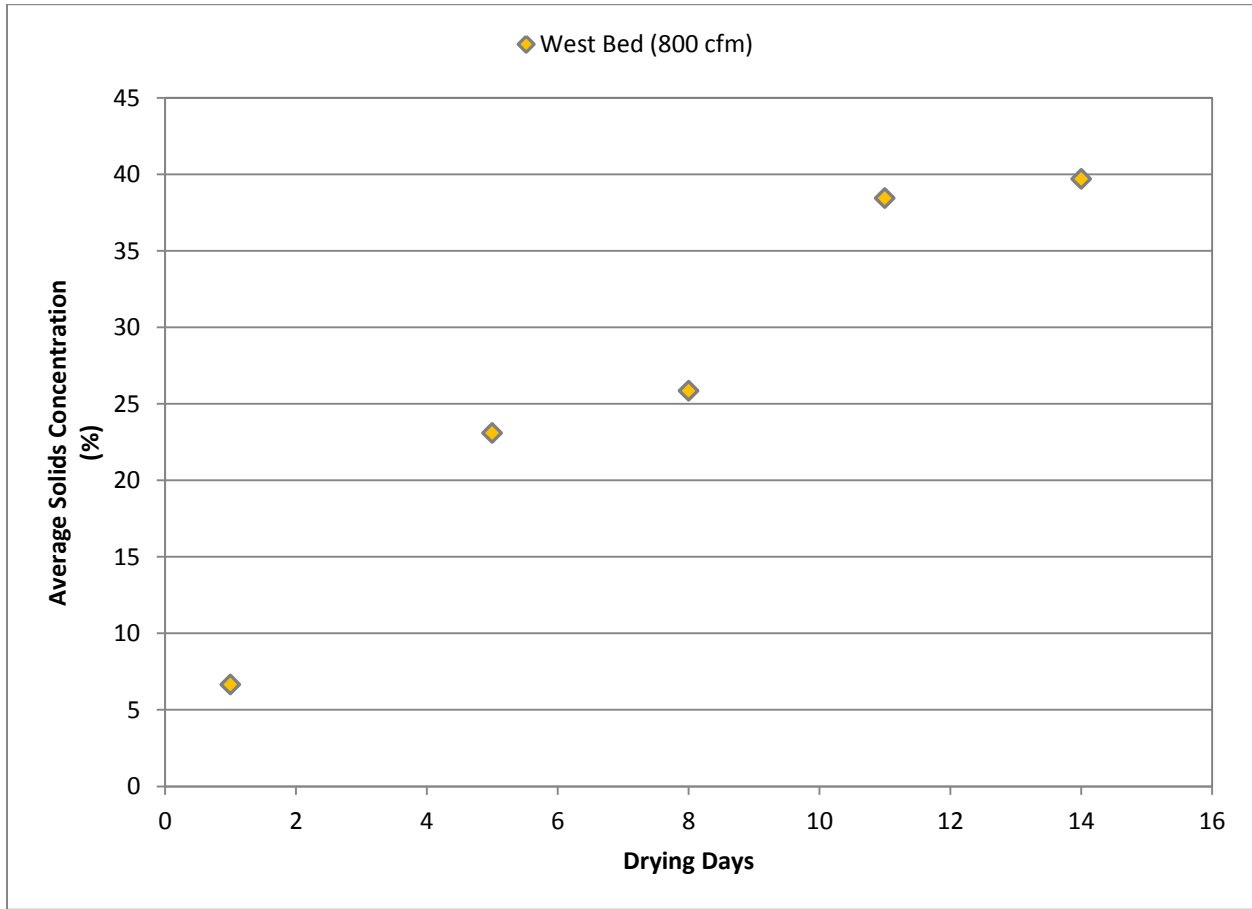


Figure 3.23 Drying performance over time during Cleveland Test 3 (1/12/2012)



Figure 3.24 Comparison of West Bed after 13 days of dewatering during Cleveland Test 1 (left photo) to West Bed after six days of dewatering during Cleveland Test 3 (right photo)

Cleveland Test 4 – January 31, 2012

The fourth test of the enhanced non-mechanical dewatering beds at Morgan WTP began on January 31, 2012. Unlike previous tests, both the East and West Beds were with the laminar-flow fan blowing 800 cfm along the long axis of the bed. However, during this test, it took the East Bed approximately three days to appear to finish draining, at which point the drained solids concentration was 7.6 percent. In comparison, the West Bed reached drained solids concentration of 7.1 percent solids after the first day, at which point it appeared to be finished draining. Parameters for Cleveland Test 4 are summarized in Table 3.11, and Figure 3.25 shows the drying performance in each bed.

As with Cleveland Test 3, significant freeze-thaw dewatering occurred during this test. Based on data logged in each bed, the East Bed was slightly warmer than the West Bed. The West Bed spent 554.1 total hours below 0°C, compared to 453.4 total hours for the East Bed. This temperature differential is primarily indicative of the time spent 0°C, since the average differential between the temperature in the West Bed and the temperature in the East Bed was less than 1°C. It is possible that the site topography caused the West Bed to receive slightly more sunlight than the East Bed since solar radiation was measured for each individual bed. If so, this may explain the slight temperature difference between the two beds.

Table 3.11
Cleveland Test 4 parameters

	East bed	West bed
Loading date	1/31/2012	1/31/2012
Initial solids concentration (%)	1.2	1.2
Calculated solids loading rate (lb/ft ²)	2.29	2.37
Drained solids concentration (%)	7.6	7.1
Measured solids concentration at target (%)	36.35	41.05
Drying days to 20+ percent solids (days)	14	14
Measured average air velocity (fps)	11.8	11.1
Average ambient temp (°F)	32.0	32.0
Average solar radiation (W/m ²)	168.7	168.7

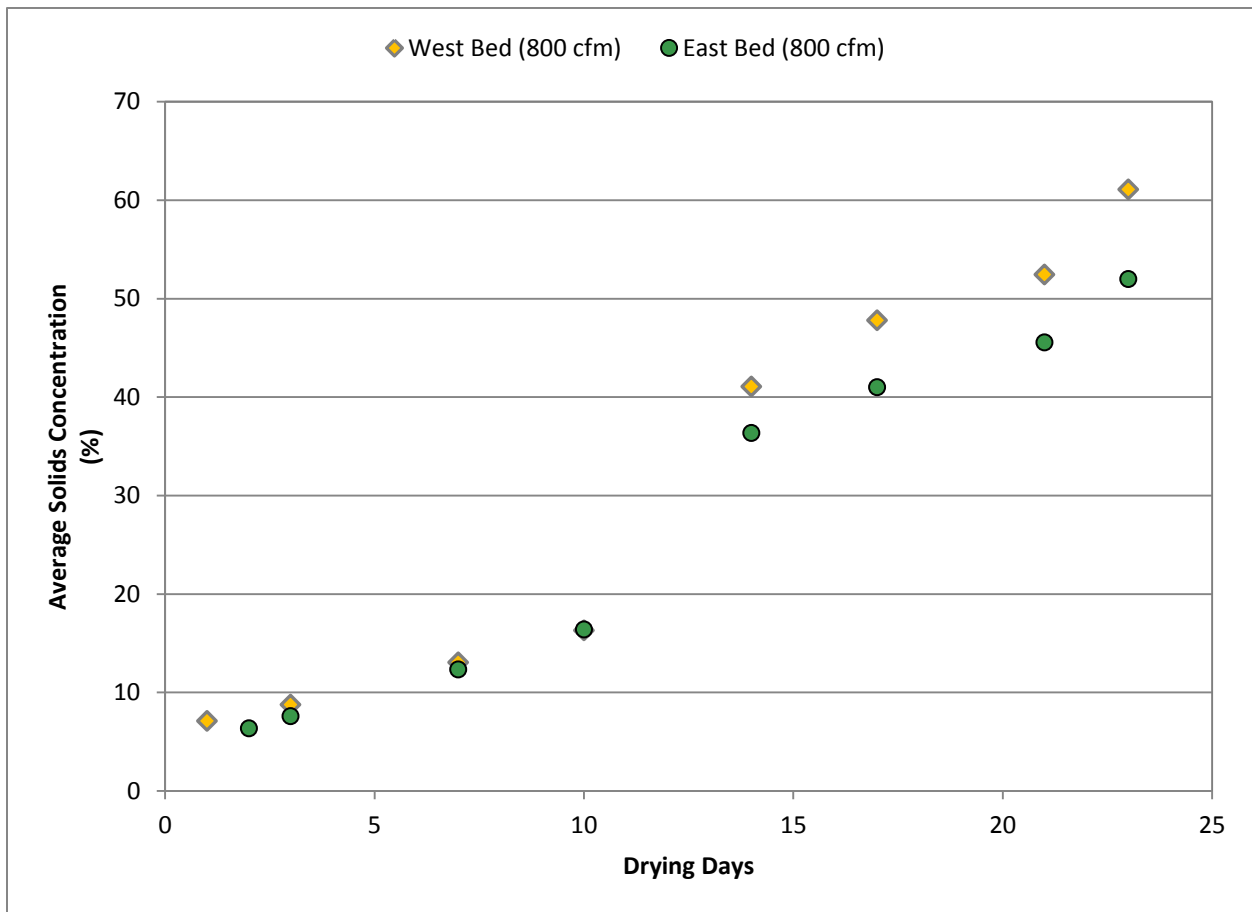


Figure 3.25 Drying performance over time during Cleveland Test 4 (1/31/2012)

Cleveland Test 5 – March 7, 2012

The fifth test of the enhanced non-mechanical dewatering beds at Morgan WTP started on March 7, 2012. As with Cleveland Test 4, both the East and West Beds were with the laminar-flow fan blowing 800 cfm along the long axis of the bed. For both of the beds during this test, the sludge had drained to less than five percent solids after one day of drying, at which point it appeared the solids were still draining. No solids measurements were recorded between drying day 1 and drying day 5, but by drying day 5 both beds had achieved a drained solids concentration in excess of 8.75 percent solids. Parameters for Cleveland Test 5 are summarized in Table 3.12, and Figure 3.26 shows the drying performance in each bed.

Table 3.12
Cleveland Test 5 parameters

	East bed	West bed
Loading date	3/7/2012	3/7/2012
Initial solids concentration (%)	1.5	1.5
Calculated solids loading rate (lb/ft ²)	3.04	2.93
Drained solids concentration (%)	9.9	8.8
Measured solids concentration at target (%)	23.3	19.65
Drying days to 20+ percent solids (days)	15	15
Measured average air velocity (fps)	12.3	11.5
Average ambient temp (°F)	56.0	56.0
Average solar radiation (W/m ²)	255.6	255.6

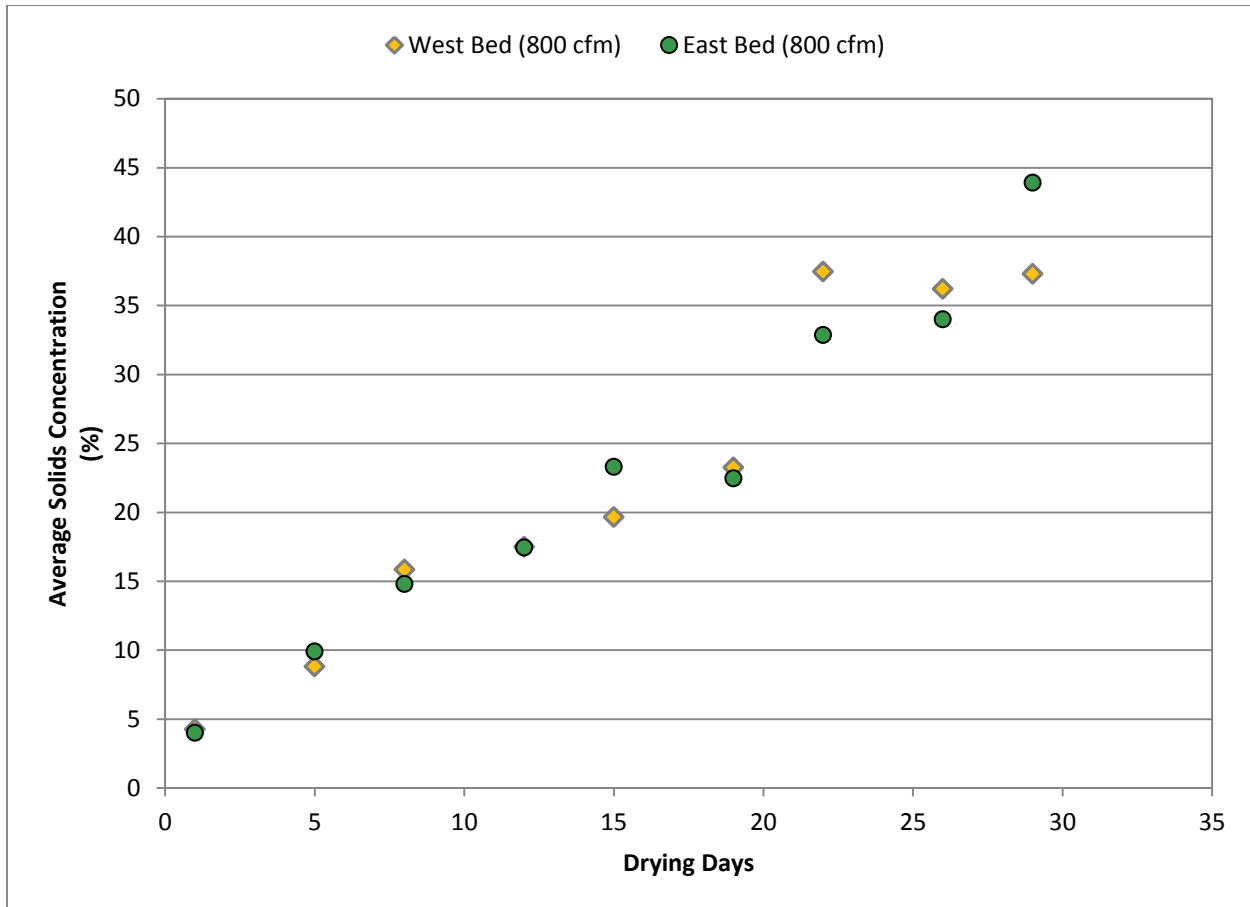


Figure 3.26 Drying performance over time during Cleveland Test 5 (3/07/2012)

Cleveland Test 6 – April 11, 2012

The sixth test of the enhanced non-mechanical dewatering beds at Morgan WTP was initiated on April 11, 2012. While both the East and West Beds were with the laminar-flow fan blowing 800 cfm along the long axis of the bed for this test, unlike previous tests the end of the West Bed was removed to allow for better distribution of air flow over the bed.

As with Cleveland Test 5, for both of the beds during this test the sludge had drained to less than 5.5 percent solids after one day of drying, at which point it appeared the solids were still draining. No solids measurements were recorded between drying day 1 and drying day 5, but by drying day 5 both beds had achieved a drained solids concentration in excess of 8.9 percent solids. Parameters for Cleveland Test 6 are summarized in Table 3.13, and Figure 3.27 shows the drying performance in each bed.

As Figure 3.27 shows, removing the end of the bed did improve performance in the field similar to the controlled environment testing. This is likely more indicative of performance at full-scale, because wall effects will be less significant as the size of the bed increases.

Table 3.13
Cleveland Test 6 parameters

	East bed	West bed
Loading date	4/11/2012	4/11/2012
Initial solids concentration (%)	1.6	1.6
Calculated solids loading rate (lb/ft ²)	3.12	2.98
Drained solids concentration (%)	9	8.95
Measured solids concentration at target (%)	19.3	21.2
Drying days to 20+ percent solids (days)	19	15
Measured average air velocity (fps)	12.2	12.4
Average ambient temp (°F)	49.2	51.0
Average solar radiation (W/m ²)	255.0	250.5

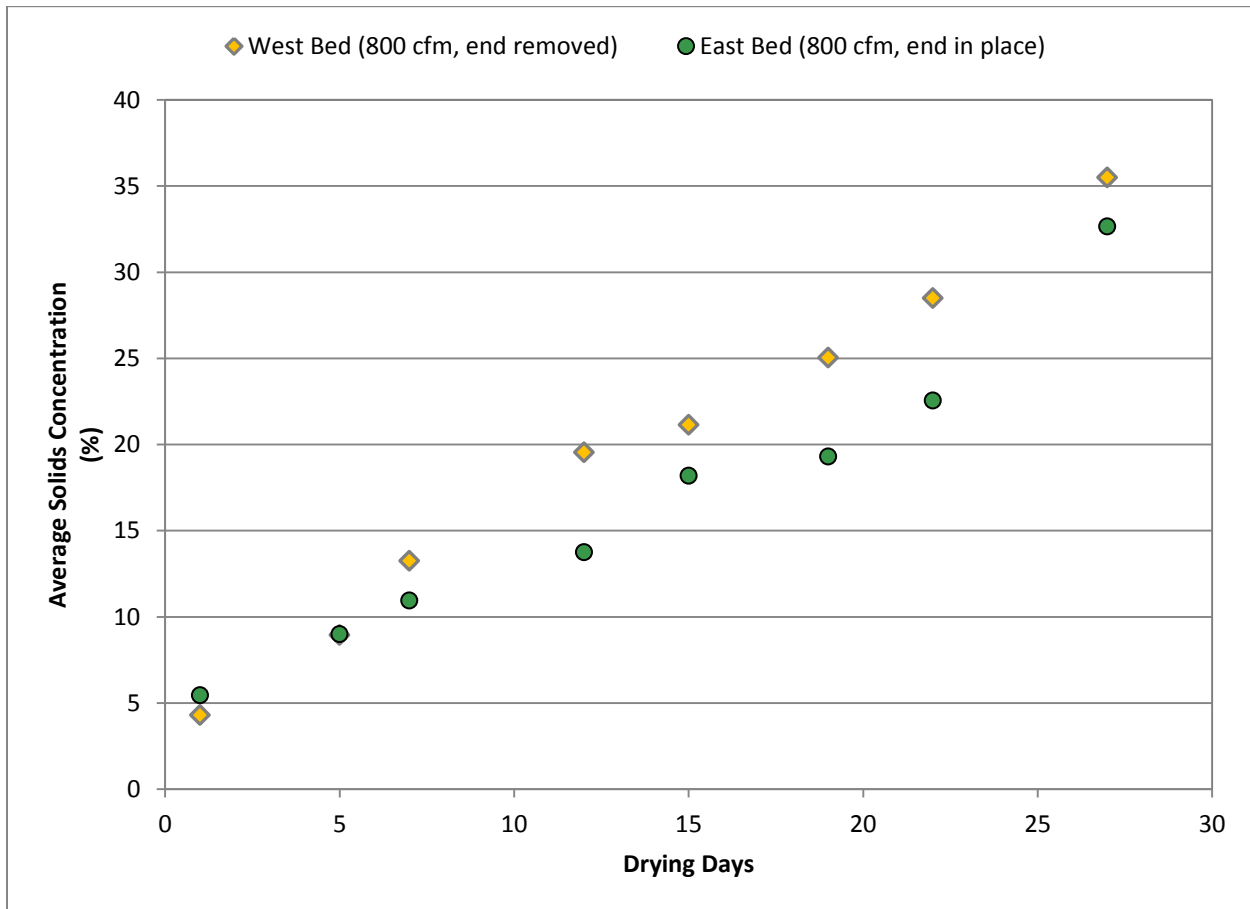


Figure 3.27 Drying performance over time during Cleveland Test 6 (4/11/2012)

Cleveland Test 7 – May 23, 2012

The seventh test of the enhanced non-mechanical dewatering beds at Morgan WTP began on April 11, 2012. As with Cleveland Test 6, both the East and West Beds were configured with the laminar-flow fan blowing 800 cfm along the long axis of the bed for this test, and the end of the West Bed was removed to allow for better distribution of air flow over the bed.

As with Cleveland Tests 5 and 6, the drainage phase took more than 24 hours for this test. For both of the beds, the sludge had drained to less than 3.5 percent solids after on day of drying, at which point it appeared the solids were still draining. The solids were re-measured on drying day 3, at which point both beds appeared to be finished draining. The drained solids concentration for this test was lower than that in Tests 5 and 6, as was the solids loading rate for the beds. Parameters for Cleveland Test 7 are summarized in Table 3.14, and Figure 3.28 shows the drying performance in each bed.

Table 3.14
Cleveland Test 7 parameters

	East bed	West bed
Loading date	5/23/2012	5/23/2012
Initial solids concentration (%)	1.3	1.3
Calculated solids loading rate (lb/ft ²)	2.5	2.4
Drained solids concentration (%)	6.7	7.2
Measured solids concentration at target (%)	23.05	23.2
Drying days to 20+ percent solids (days)	16	10
Measured average air velocity (fps)	12.2	12.8
Average ambient temp (°F)	65.4	68.9
Average solar radiation (W/m ²)	296.6	279.7

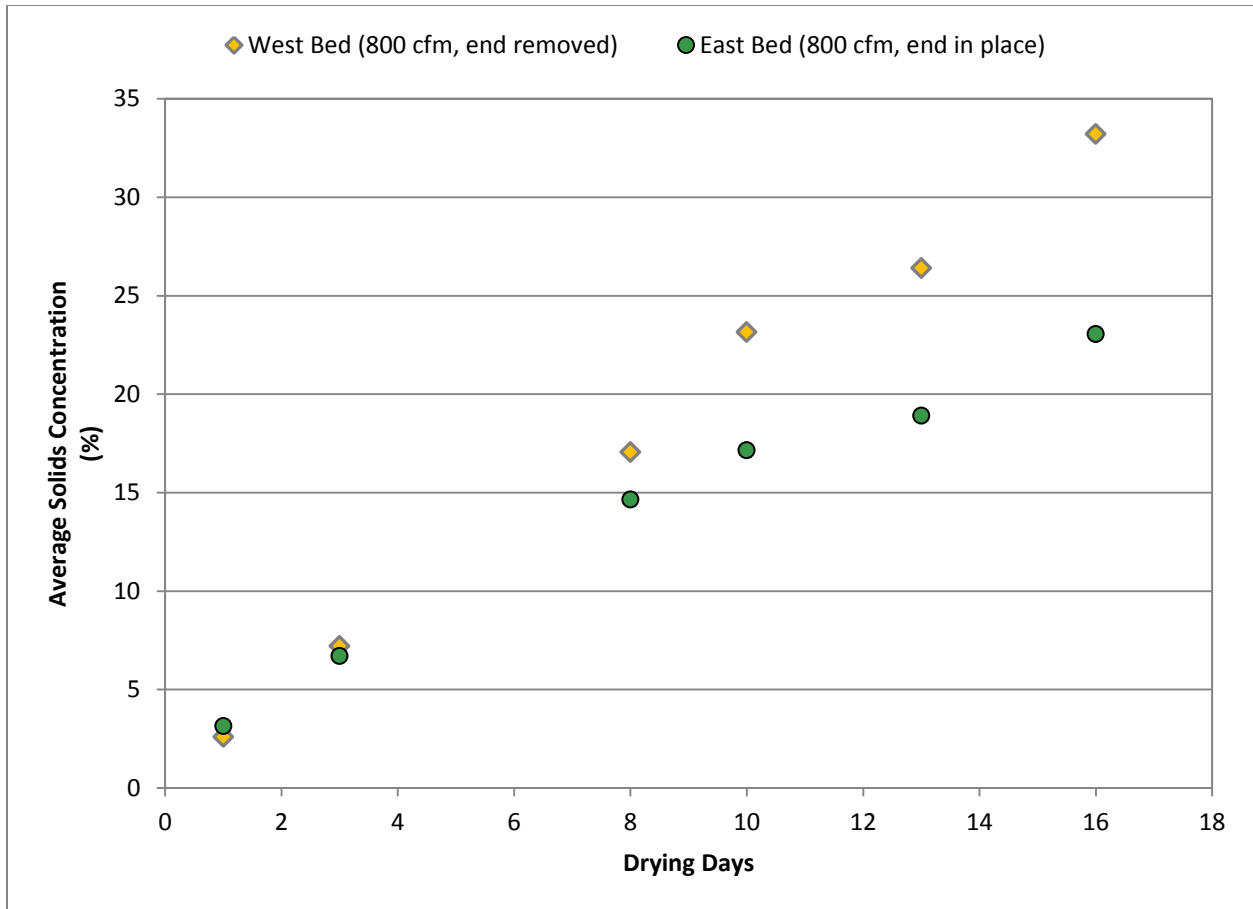


Figure 3.28 Drying performance over time during Cleveland Test 7 (5/23/2012)

Cleveland Test 8 – June 26, 2012

The final test at Morgan WTP was initiated on June 26, 2012. As with Cleveland Tests 6 and 7, both the East and West Beds were configured with the laminar-flow fan blowing 800 cfm along the long axis of the bed for this test, and the end of the West Bed was removed to allow for better distribution of air flow over the bed.

Similar to Test 7, the solids were difficult to load at the target loading rate, and were slow to drain. The East Bed was loaded at a solids loading rate of 2.51 lb/ft², but the researchers were only able to achieve 2.02 lb/ft² on the West Bed. As with Tests 5, 6, and 7, the beds weren't completely drained after 24 hours. After three days, the East Bed achieved a drained solids concentration of 7.25 percent solids, but the West Bed only drained to 6.3 percent solids due to the lower solids loading. However, both beds dried well, and achieved the target of 20 percent solids 13 days after being loaded. Parameters for Cleveland Test 8 are summarized in Table 3.15, and Figure 3.29 shows the drying performance in each bed.

Table 3.15
Cleveland Test 8 parameters

	East bed	West bed
Loading date	6/26/2012	6/26/2012
Initial solids concentration (%)	1.3	1.3
Calculated solids loading rate (lb/ft ²)	2.51	2.02
Drained solids concentration (%)	7.25	6.3
Measured solids concentration at target (%)	22.25	25.1
Drying days to 20+ percent solids (days)	13	13
Measured average air velocity (fps)	13.3	14.4
Average ambient temp (°F)	76.2	76.2
Average solar radiation (W/m ²)	301.9	301.9

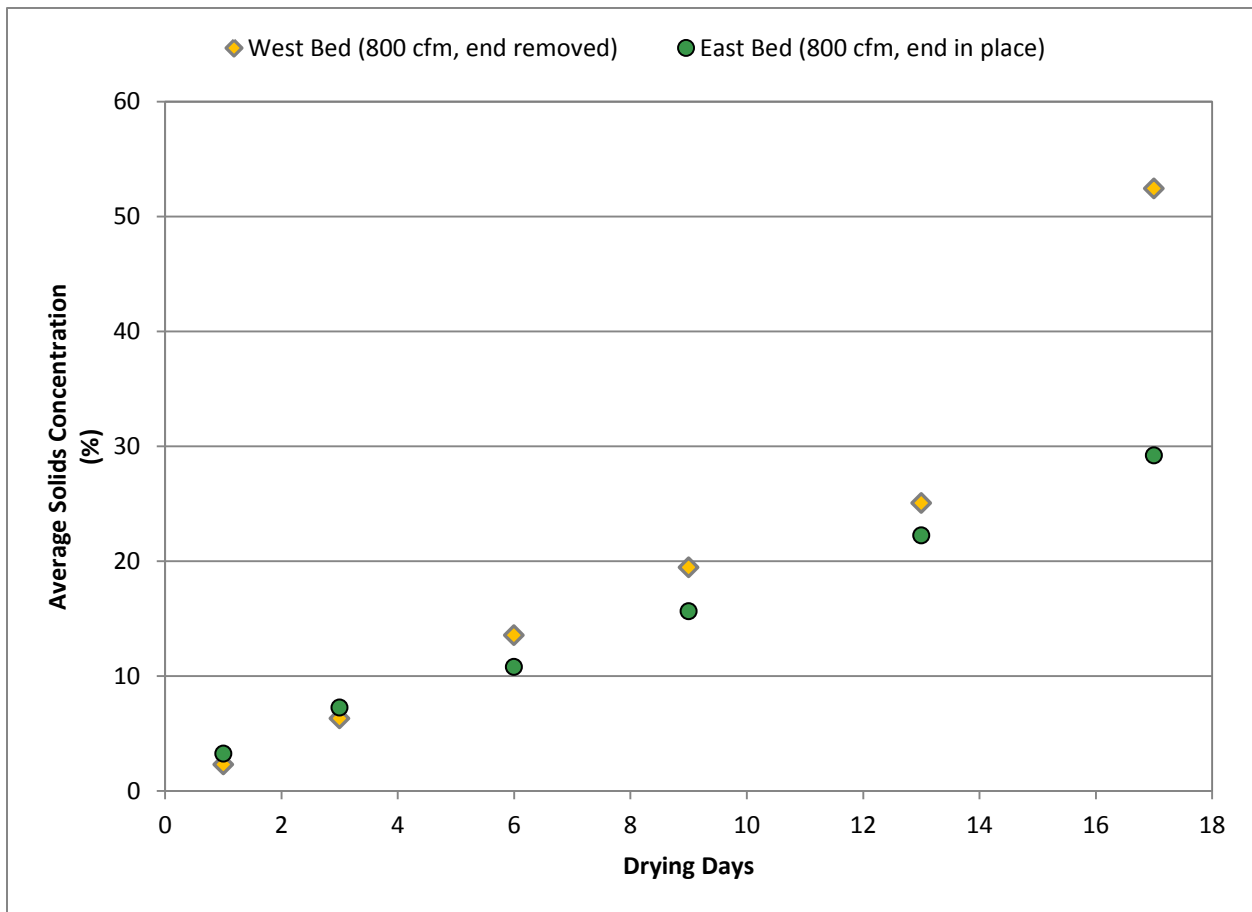


Figure 3.29 Drying performance over time during Cleveland Test 8 (6/26/2012)

Summary of Cleveland Field Pilot Studies

Theoretical Water Balance

As with the controlled-environment testing, effective evaporation rates could be calculated for each test using Equations 2.1 and 2.2. These effective evaporation rates are summarized in Table 3.16 for each test.

In addition to the effective evaporation rates, it was possible to use the temperature and humidity data recorded from each bed to calculate the vapor balance. Equation 1.1 presented the theoretical concept of this research, which was that drying is a function of the water exchange from the sludge to the air, multiplied by the air flow rate. Thus, increasing air flow rate would increase drying for a given change in water balance. The data obtained in the field was used to test this hypothesis. The theoretical balance can be calculated by Equation 3.1:

$$E = A \int_{t_1}^{t_2} \left[2.20462 \frac{\text{kg}}{\text{lb}} (W_{out} - W_{in}) Q_{eff} \times 0.0283 \frac{\text{m}^3}{\text{ft}^3} \right] \Delta dt \quad (3.1)$$

where E = evaporation (lb)
 A = bed area (ft²)
 W_{out} = vapor concentration in the air at the exhaust end of the bed (kg/m³)
 W_{in} = vapor concentration in the air at the inlet end of the bed (kg/m³)
 Q_{eff} = average effective ventilation rate (cfm/ft²)

The vapor concentration in the air is calculated by Equation 3.2:

$$W = 0.002166p / (T + 273.16) \quad (3.2)$$

where p = vapor pressure (Pa)
 T = average temperature (°C)

Equation 3.3 is used to calculate the vapor pressure:

$$p = RH \times (610.78e^{17.2694T/(T+238.3)}) \quad (3.3)$$

where RH = relative humidity (%)

Table 3.16
Summary of effective evaporation rates and Q_{eff} calculated from Cleveland test results

Test	Loading date	West bed			East bed		
		Water evaporated (lbs)	Effective evaporation rate (in./mo.)	Average effective ventilation rate (cfm/ft ²)	Water evaporated (lbs)	Effective evaporation rate (in./mo.)	Average effective ventilation rate (cfm/ft ²)
1	10/27/2011	344.9	17.9	45.6	147.9	3.31	0
2	12/14/2011	177.6	8.14	133.5	181.8	2.57	0
3	1/12/2012	575.1	35.6	393.9	N/A	N/A	N/A
4	1/31/2012	496.2	12.2	151.7	427.1	12.4	150.5
5	3/7/2012	331.3	10.6	N/A	317.5	10.2	N/A
6	4/11/2012	346.8	14.9	36.7	333.0	7.7	37.3
7	5/23/2012	413.4	18.9	36.9	476.7	11.8	34.6
8	6/26/2012	389.4	20.8	38.1	420.7	13.5	59.5

Summary of Evaporation Results

Other than Q_{eff} , the variables in Equations 3.1, 3.2, and 3.3 were all measured during testing. Q_{eff} is a conceptual variable defined based on drying performance, and is an interesting variable from a practical standpoint. It is an indicator of how efficient the air application was in drying the residuals; in other words, how efficient was the energy used in forcing the air across the bed.

The fans delivered the same volumetric flow for each test; however, due to variables in configuration and loading depths, drying efficiency varied between test. Q_{eff} was calculated for each test by comparing the measured evaporation, E , to the evaporation calculated using the vapor balance method to determine the value of Q_{eff} that would cause the two to be equal. These results are summarized, along with the effective evaporation rates, in Table 3.16. Note, Q_{eff} is not available for Test 5 due to failure of the data loggers; temperature and humidity data are not available for this test.

The ventilation fans had a capacity of 800 cfm, and were used to ventilate 18 ft² beds for these tests; therefore, the applied ventilation rate was 44.44 cfm/ft². One way to conceptualize these results is to consider 44.44 cfm/ft² to be the maximum Q_{eff} possible. This maximum Q_{eff} was exceeded for all of the winter tests (Tests 2, 3, and 4), as well as for the East Bed during Test 8. The results for Tests 2, 3, and 4 are likely indicative of freeze-thaw dewatering conditions, which are capable of exceeding the dewatering performance achievable through evaporation alone. The cause of the result for the East Bed of Test 8 is less obvious at this time. Due to the relatively low effective evaporation rate (compared to the West Bed), this result may be indicative of inaccurate temperature and/or humidity data from the data loggers. Using the results from these tests (except the winter tests and the East Bed of Test 8), the average efficiency was about 82 percent, which is quite reasonable. In other words, the applied energy via the fan was 82 percent efficient in drying the solids to an approximate 20 percent solids concentration.

Table 3.17 and Figure 3.30 compare the effective evaporation rates from the highest performing bed for each test to historical evaporation rates for the Cleveland area. The freeze-

thaw performance data have been excluded from this table because they are not indicative of normal evaporative drying rates included in evaporation records. For each test, evaporation was improved by more than 300 percent over the historical evaporation rates expected for the periods when the tests were conducted. Improvement is most pronounced during cooler months when evaporation is expected to be low.

Table 3.17
Comparison of calculated effective evaporation rates from West Bed and historical evaporation rates

Loading date	Effective evaporation rate (in./mo.)	Historical evaporation rate (in./mo.)	Improvement over historical (percent)
10/27/2011	17.9	2.6	826
12/14/2011	8.14	1.8	454
3/7/2012	10.61	2.3	456
4/11/2012	14.9	4.8	386
5/22/2012	18.9	5.4	351
6/27/2012	20.8	6.7	311

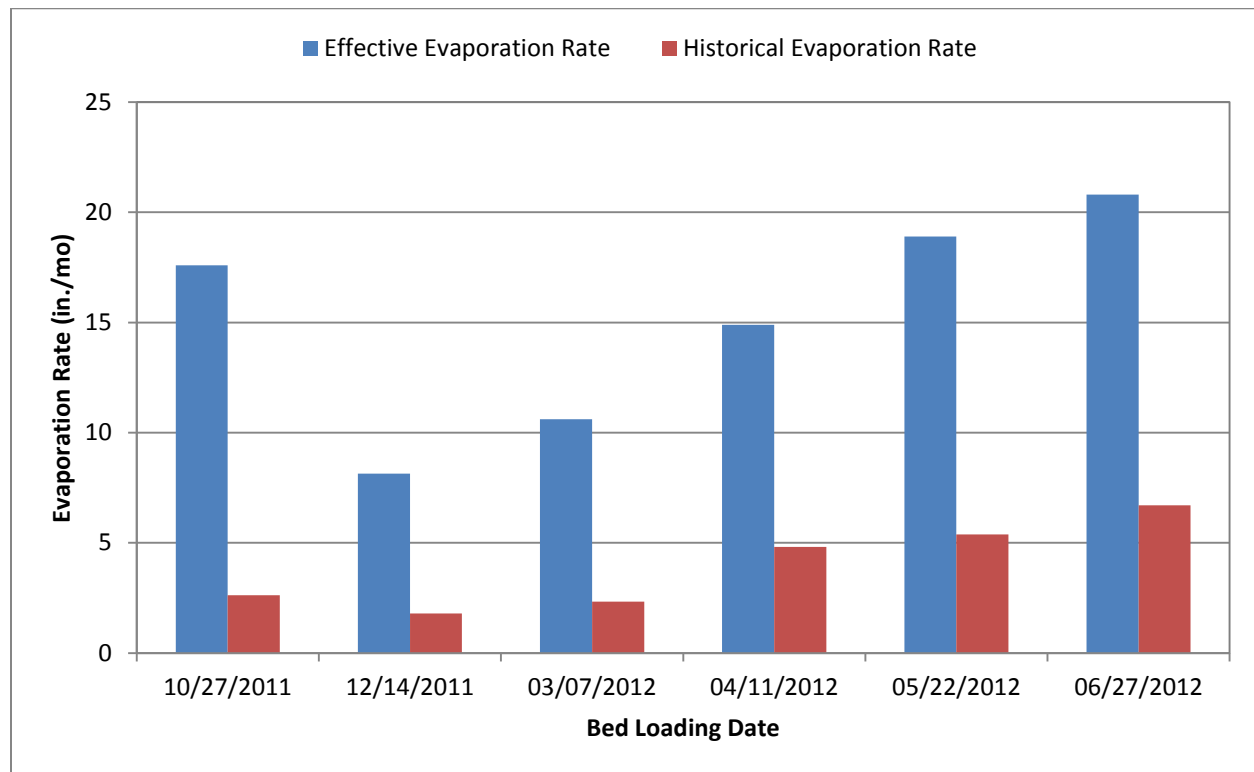


Figure 3.30 Comparison of effective evaporation rate from enhanced non-mechanical dewatering to the historical evaporation rates

If the performance from the Tests 3 and 4 were considered, improvement over historical evaporation rates would be even more pronounced. However, there are concerns that the freeze-

thaw performance observed during those tests may not be representative of normal dewatering conditions during an average Cleveland winter. The winter of 2011 to 2012 was unusually mild, with a total time of approximately 830 hours below freezing. In comparison, the average winter over the past 10 years had features approximately 1530 hour below freezing. Because freeze-thaw depends on fluctuations between below freezing and above freezing temperatures to effectively dewater the residuals, if the tests had been conducted during a colder winter with more consecutive days when temperatures did not exceed freezing in the greenhouse during the day the high dewatering rates observed during these tests may not have occurred.

Ambient Predictions

The net evaporation results were obtained over several months and represented a wide range on ambient weather conditions. It is also well established in this research that the drying results are a function of the fan flow rate. The net evaporation data that was used to compare against ambient conditions are shown in Table 3.18. Generally these are the data from Table 3.17.A control condition from October that had a zero fan velocity was included to use as a zero velocity data point and data from January 31 were included. The January 31 data were included for a cold temperature data point and the net evaporation could be calculated in the early part of the test prior to the period when it was felt that freeze-thaw was influencing the results. The ambient temperature and solar radiation data were collected from the NCDC weather station at the Cleveland Hopkins International Airport (WBAN 14820). The hourly temperature data were averaged over the period during which each bed was loaded to determine average ambient temperature. The hourly solar radiation data were similarly averaged, except the zero values from the nighttime periods were not included in the averaged data set. Therefore, the solar radiation represents the daytime average over the test period.

Table 3.18
Evaporation rate and ambient weather conditions used for regression analysis

Loading date	Bed	Calculated solids loading rate (lb/ft ²)	Drained solids conc. (percent)	Final solids conc. (percent)	Net evap. rate (in./mo.)	Average centerline velocity (fps)	Average ambient temp (°C)	Average solar radiation (W/m ²)
6/26/2012	East	2.5	7.25	22.3	20.8	13.3	24.6	301.9
5/23/2012	West	2.0	6.3	19.5	18.9	14.4	20.0	279.0
4/11/2012	West	3.0	8.95	19.6	14.9	12.4	10.6	250.5
3/7/2012	West	2.9	8.8	19.7	10.6	11.5	12.5	246.1
1/31/2012	West	2.4	7.1	41.1	10.3	11.1	0	168.7
12/14/2011	West	3.0	11.5	18.5	8.1	11.2	4.5	39.2
10/27/2011	East	3.0	8.1	19.6	3.3	0.0	6.8	136.2
10/27/2011	West	3.0	7.27	20.1	17.9	16.9	6.9	178.2

Several different attempts at trying to correlate the ambient conditions to the net evaporation were attempted. These were all based on linear multiple regression analysis using logical variable combinations. Ultimately a good and reasonable correlation was developed using the variables of ambient air temperature in Celsius, the solar radiation in W/m², and the fan velocity across the bed in fps. The fan velocity was measured during each sampling event and was measured in two locations down the bed centerline. One location was about two feet from the fan end of the bed and the other location was at the end of the bed. The readings were taken

slightly above the sludge surface. In all cases the 800 cfm fan was used, so the velocity variable serves primarily as an indicator of how well the flow was distributed across the bed. The volumetric flow rate is still an important variable as shown in Figure 3.18 but the volumetric flow was not varied in the Cleveland field tests.

The resulting regression equation is shown as Equation 3.5:

$$E = -1.36 + 0.785V_{CL} + 0.248T + 0.147S_{avg} \quad (3.4)$$

where S_{avg} = average daytime solar radiation (W/m^2)
 T = average temperature ($^{\circ}\text{C}$)
 V_{CL} = average air velocity along the centerline of the bed (fps)

The correlation coefficient, R , was 0.96 which corresponds to a variation, R^2 of 0.92. In other words 92 percent of the variation in the net evaporation can be predicted by the combination of the ambient temperature, solar radiation, and air velocity across the bed. It should also be noted that air velocity by itself can be a predictor of the net evaporation but its R^2 value by itself was only 0.68 showing that although it is the strongest variables all three parameters are needed give a strong prediction.

A significance test was also performed to verify the correlation using Equation 3.6:

$$Z = \frac{\sqrt{n-3}}{2} \times \ln \left(\frac{1+R}{1-R} \right) \quad (3.5)$$

where Z = Z-test correlation coefficient
 n = number of tests
 R = correlation coefficient

The resulting Z value is 5.0 which is greater than $Z_{0.005}$, concluding that the sample set is significant and there exists a linear relationship between net evaporation and the three variables.

Figure 3.31 illustrates the relationship between net evaporation and average bed velocity for different temperature and solar radiation values.

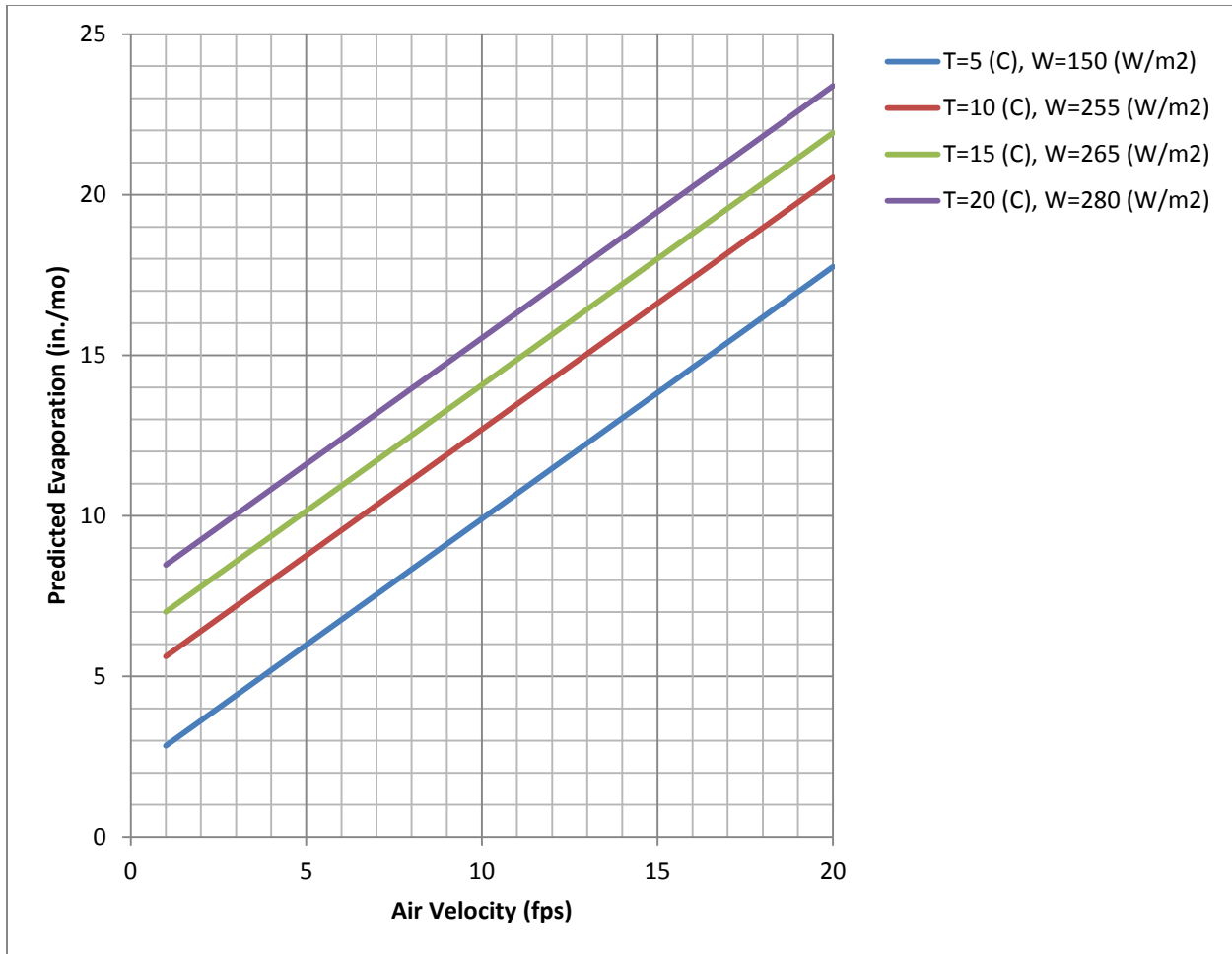


Figure 3.31 Relationship between net evaporation and average bed velocity for different temperature and solar radiation values

The relationship was quite good and covers a wide range of environmental conditions. However, it was only developed for the one site: Cleveland. While it might prove useful to predict performance at other sites, caution should be exercised until more data under varying conditions can be developed.

The controlled-environment testing suggested that, in addition to the centerline air velocity, the overall volumetric flow rate was an important variable related to evaporation. However, due to data logger failure during Test 5 there were only five usable data points for evaluating this relationship at Cleveland. Further, there was little variation in Q_{eff} for most of the usable tests, except for one data point at zero and one at 45 cfm/ft^2 . Because of these limitations, the only statistically significant multivariate regression between evaporation and Q_{eff} included temperature, but not solar radiation. This regression had a correlation coefficient of 0.99, and is shown as Equation 3.7:

$$E = 0.993 + 0.311Q_{eff} + 0.319T \quad (3.6)$$

Figure 3.32 illustrates the relationship between net evaporation and average bed velocity for different temperature and solar radiation values.

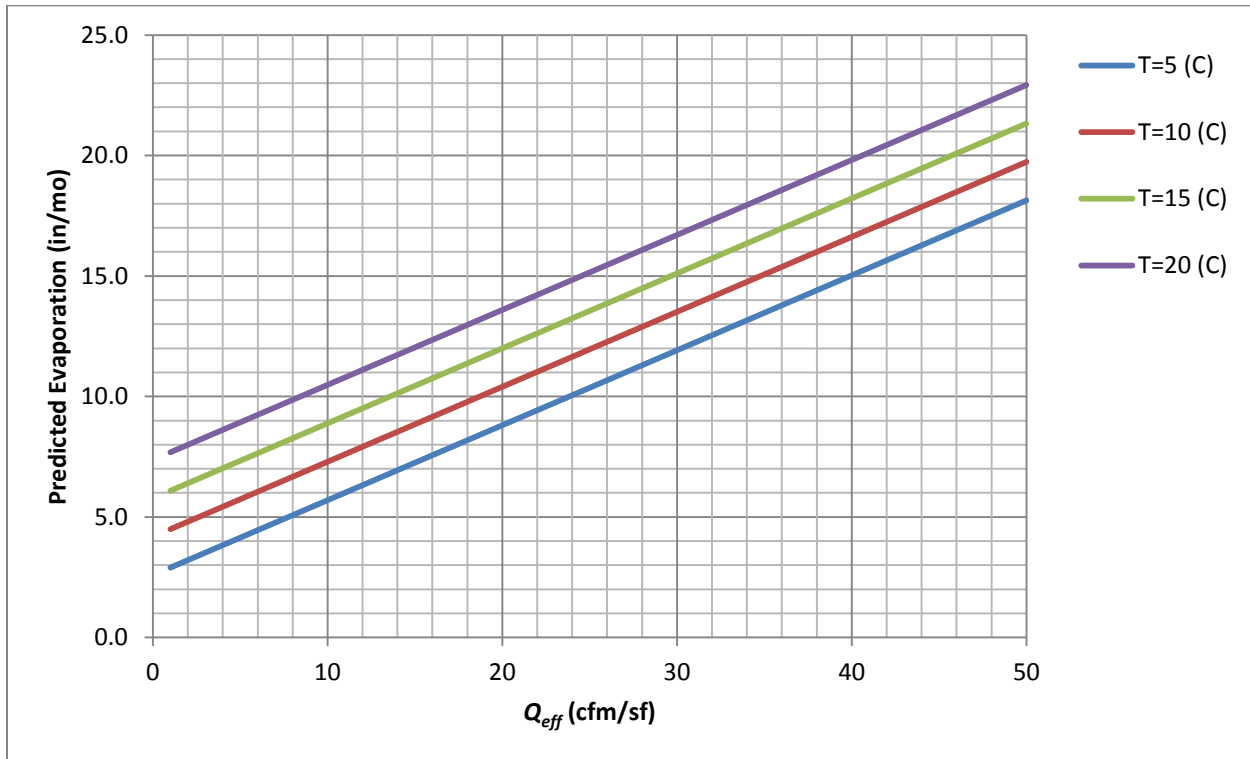


Figure 3.32 Relationship between net evaporation and Q_{eff} for different temperature values

Figure 3.32 shows that evaporation is highly dependent on the volumetric flow rate Q_{eff} ; however, that volumetric flow rate must also be effectively dispersed across the bed, which requires a balanced velocity distribution. Together, Figures 3.31 and 3.32 illustrate the importance of the ventilation, along with temperature and solar radiation, on the effective evaporation rate in the enhanced non-mechanical dewatering beds.

RALEIGH PILOT STUDIES

Field pilot studies were initiated at the E.M. Johnson WTP in January 2011, and continued through October 2012. During that time eight tests were conducted to assess whether the enhanced non-mechanical dewatering process would also be successful at drying residuals cake that had previously been dewatered via mechanical dewatering. Testing at E.M. Johnson was performed by plant staff, who loaded the test beds, turned over the solids, and took solids measurements on a bi-weekly basis. Table 3.19 summarizes the field tests conducted in Raleigh.

Table 3.19
Summary of loading dates and initial solids concentrations for Raleigh tests

Test	Loading date	Initial Solids concentration (percent)	Notes
1	1/30/2012	22.08	Full depth test
2	3/7/2012	22.78	Full depth test
3	4/10/2012	22.16	Half depth test, cake lightly tilled prior to sampling
4	5/9/2012	23.13	Half depth test, cake lightly tilled prior to sampling
5	6/8/2012	24.8	Half depth test, cake lightly tilled prior to sampling
6	7/31/2012	24.2	Full depth test, cake lightly tilled prior to sampling
7	8/27/2012	24.68	Bed loaded full, cake tilled daily
8	9/19/2012	23.13	Single windrow set inside of greenhouse

The initial solids concentration of the mechanically dewatered cake averaged 23.05 percent. For Tests 1 through 7, the test configuration consisted of a control bed located outside of the greenhouse, exposed to ambient conditions, and a test bed inside of the greenhouse that was ventilated with an 800 cfm fan. Test 8 eliminated the control outside of the greenhouse, and compared the test bed to a windrow that was 7.5-foot long by 1.17-foot high, with a base width of 3.83 feet. Both the windrow and the test bed were ventilated with 800 cfm fans, oriented to blow along the west axis. Test 9 eliminated the test bed and investigated a single windrow set with ventilation blowing directly at the end of the windrow, rather than across the cake surface.

Raleigh Test 1 – January 30, 2012

The first test of the enhanced non-mechanical dewatering process at E.M. Johnson WTP began on January 30, 2012. This first test evaluated simple drying of the cake, and did not include tilling. Cake drying in the test bed was monitored by taking two depth-composited samples every few days. Because the controlled-environment testing suggested that the test bed would dry uniformly, drying in the control bed was monitored by taking one depth-composited sample. Test results are shown in Figure 3.33.

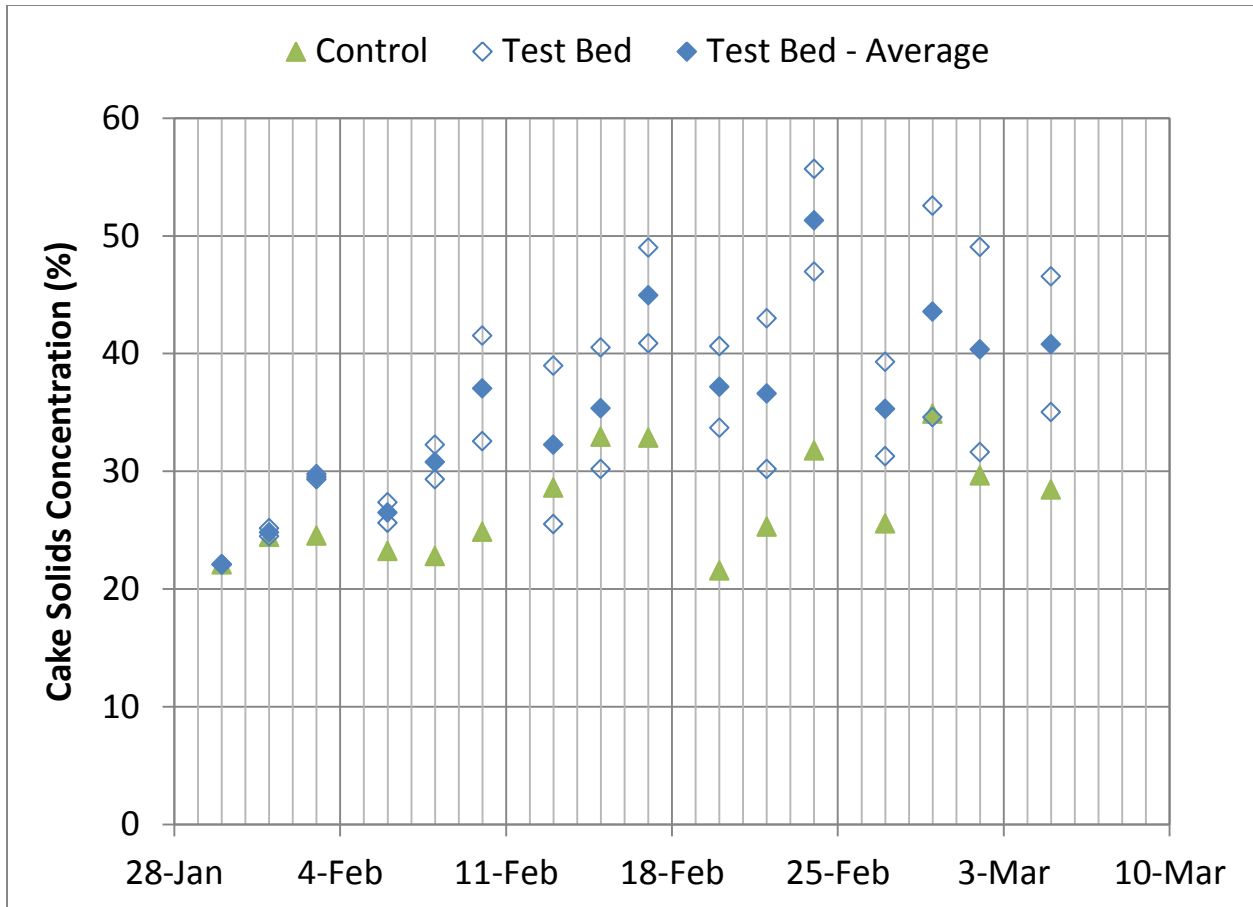


Figure 3.33 Drying performance over time during Raleigh Test 1 (1/30/2012)

While initial drying performance appeared promising during the first two sampling events, by the second week the samples in the test bed began to show significant scatter. There was not a consistent trend in solids concentration by bed location; at times the sample from the north end of the bed would have a higher solids concentration, while at other the sample from the south end of the bed would have the higher solids concentration. There was also considerable scatter in the overall trend of the average solids concentration in the test bed and in the control bed.

Overall drying performance did not meet expectations. On March 7, the run was terminated and an investigation was conducted to determine why the enhanced non-mechanical dewatering did not perform as well as expected. One factor appeared to be poor ventilation of the test bed. Unlike in Cleveland, where it was possible to attach the fans directly to the test bed, because of the porous nature of the frame used to hold the mechanically-dewatered cake, the fan was supported separate from the test bed at Raleigh. At some point during Test 1, wind shifted the greenhouse structure and moved the fan out of alignment with the test bed. The resultant air flow across the test bed is shown in Figure 3.34. The poor distribution of air shown at least partially explains the poor performance of Raleigh Test 1.

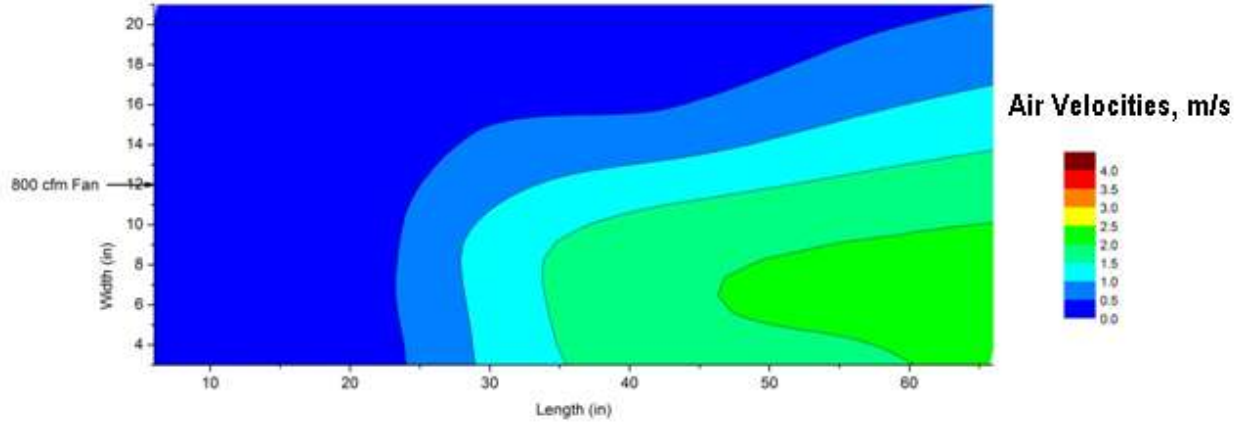


Figure 3.34 Air flow distribution across test bed at termination of Raleigh Test 1

Raleigh Test 2 – March 7, 2012

The second test of the enhanced non-mechanical dewatering process at E.M. Johnson WTP began on March 7, 2012. Prior to reloading the test bed, the fan was realigned to evenly distribute air across the bed surface. The resulting air flow distribution is shown in Figure 3.35. As with the preceding test, this test evaluated simple drying of the cake, and did not include tilling. Figure 3.36 shows the results from Raleigh Test 2.

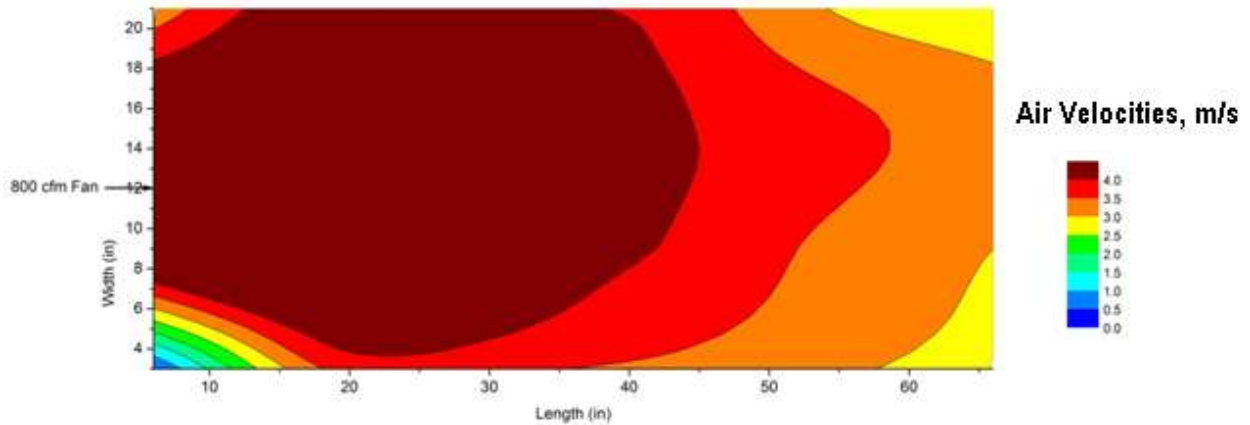


Figure 3.35 Air flow distribution across test bed at initiation of Raleigh Test 2

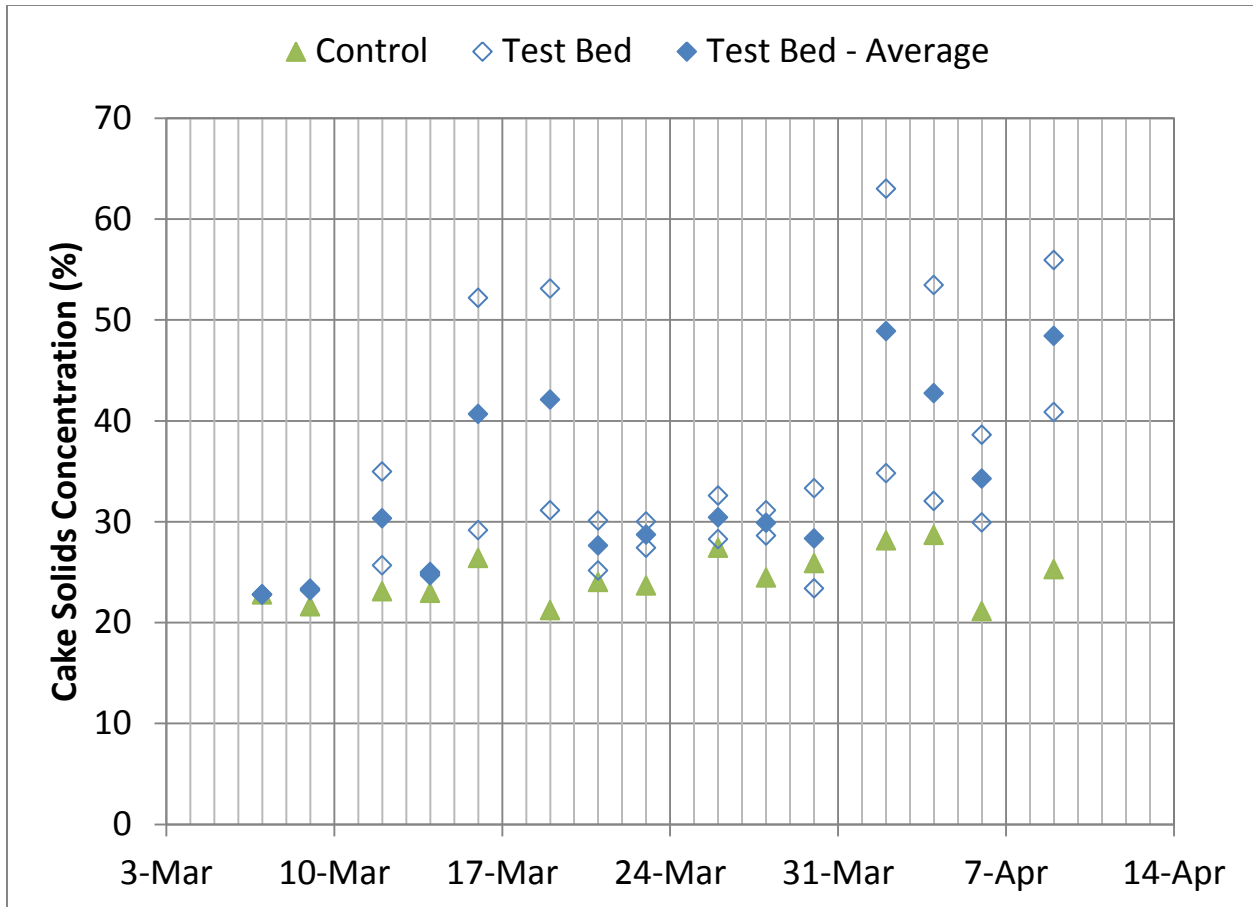


Figure 3.36 Drying performance over time during Raleigh Test 2 (3/7/2012)

As with Raleigh Test 1, during Test 2 considerable scatter was observed between samples. While the air flow across the bed was improved, the measured solids concentrations in the cake samples did not show as rapid of drying as predicted.

One potential explanation for these results is sample bias. Figure 3.37 shows the test bed at the end of Raleigh Test 1. Unlike the cake resulting from the drying tests in Cleveland, the mechanically dewatered cake in Raleigh formed large clumps or clods of residuals. Visual observation of these agglomerations suggested that they dried at different rates; clods at the top of the bed appeared to be significantly drier than those at the bottom of the bed. Although the operators attempted to collect depth-composited samples for each sample event, if there was any variance between the proportion of solids at the top of the bed to those at the bottom of the bed between sampling events, it would be difficult to observe the drying trend in the data. For example, it is possible that the samples collected between March 21, 2012 and March 30, 2012 contained a higher proportion of solids from the bottom of the bed, which would explain the relatively low solids concentration of those samples relative to samples before and after those dates.



Figure 3.37 Dried cake in the test bed at the termination of Raleigh Test 1

Raleigh Test 3 – April 10, 2012

The third test of the enhanced non-mechanical dewatering process at E.M. Johnson WTP started on April 10, 2012. Based on the results from the preceding two tests, attempts were made to homogenize the residuals in the bed. Therefore, before each sampling event, the operator manually tilled the bed by turning over the cake with a shovel. The loading depth in each bed was cut in half to assist in this tilling process. Figure 3.38 presents the results from this test.

Compared to the preceding test, the result from Test 3 showed a more consistent drying trend, although there was still scatter in the data. For this test, it took 24 days to dry the mechanically-dewatered cake from its original solids concentration of 22.2 percent to an average solids concentration of 50 percent. With a solids loading rate of 8.3 lb/ft² (assuming the initial unit weight of the cake was 70 lb/ft³), this is equivalent to a net evaporation rate of 5.0 in./mo. for the test bed. The control never reached 50 percent solids concentration.

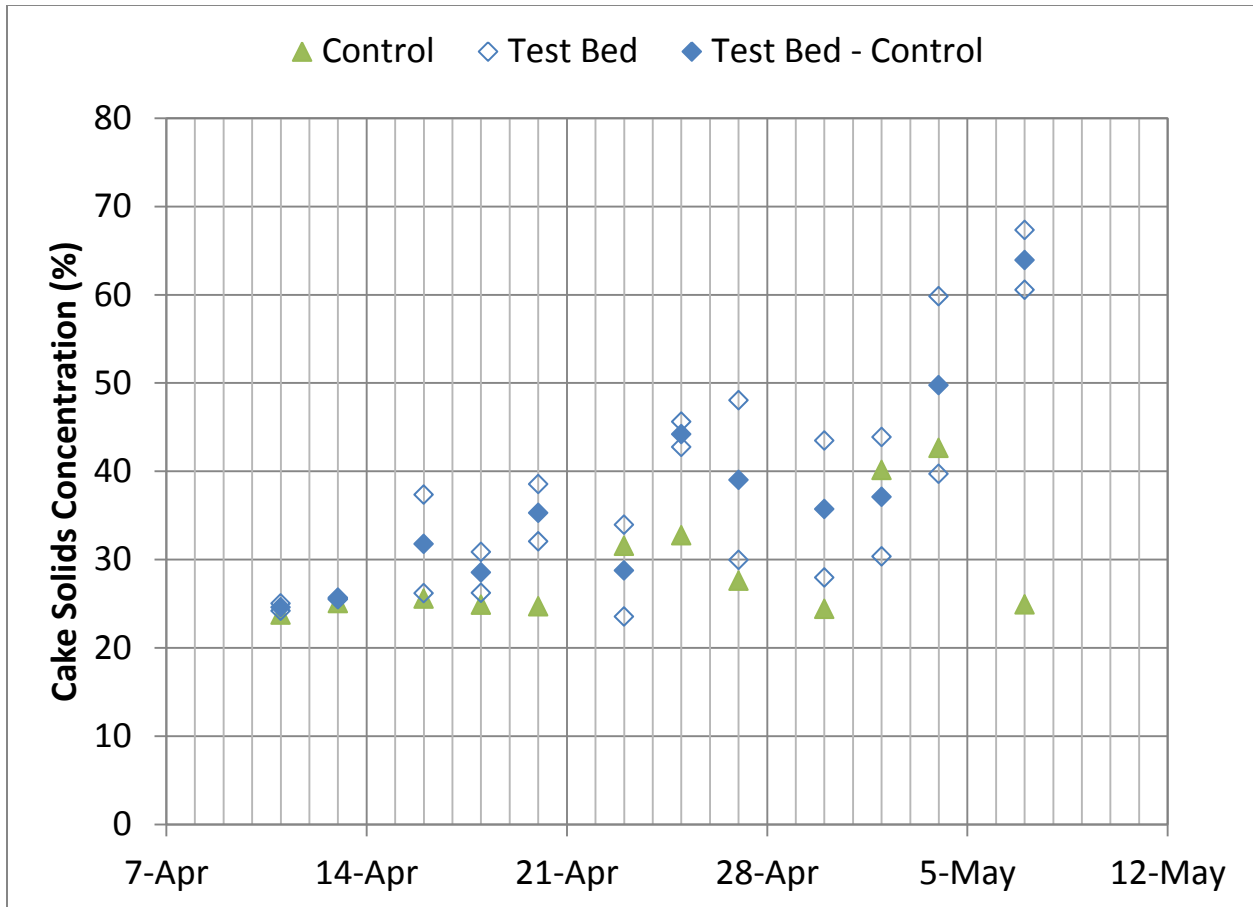


Figure 3.38 Drying performance over time during Raleigh Test 3 (4/10/2012)

Raleigh Test 4 – May 9, 2012

The fourth test of the enhanced non-mechanical dewatering process at E.M. Johnson WTP was started on May 9, 2012. As with Raleigh Test 3, the beds were loaded at half-depth and tilled prior to each sampling event. Results from this test are presented in Figure 3.39.

Compared to preceding tests, there was much less scatter in the data for Raleigh Test 5. For the initial two weeks of this test the control bed appeared to dry as well as the test bed. However, the control bed never reached 50 percent solids concentration, while the test bed was able to achieve 50 percent solids after about one month of drying. There are, however, outlier data points that make a clear differentiation difficult.

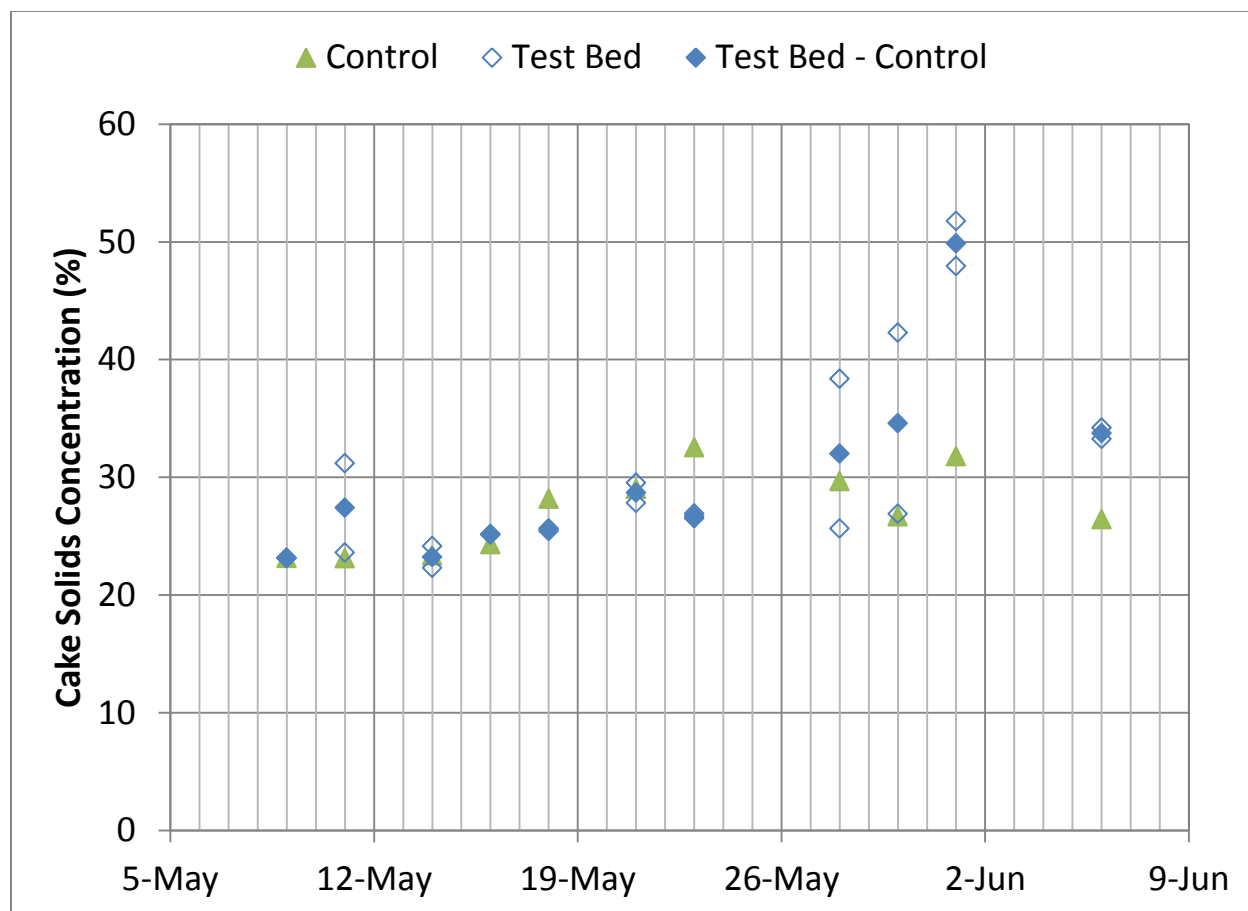


Figure 3.39 Drying performance over time during Raleigh Test 4 (5/9/2012)

Raleigh Test 5 – June 8, 2012

Following the poor performance of Raleigh Test 4, the bed was reloaded for a fifth test, which began on June 8, 2012. The conditions for this test were the same as those for Tests 3 and 4. Figure 3.40 presents the solids concentrations measured for this test.

As Figure 3.40 indicates, Raleigh Test 5 was not at all successful. Based on these results, the test was terminated and the test plan was reevaluated.

One difficulty experienced during the Raleigh testing to this point is that the sampling was being conducted by plant operators, on top of their other regular duties. Despite the best efforts of plant staff, it was difficult to monitor the test beds on top of their other duties. This was evident after further investigation following Raleigh Test 5, when it was found that the fan was once more out of alignment with the test bed. Figure 3.41 shows the resulting air flow distribution measured with the out-of-alignment fan. It is not known how long the fan was out of alignment, but based on the results from Tests 4 and 5 it is likely that the fan was knocked out of alignment as early as May 9, 2012.

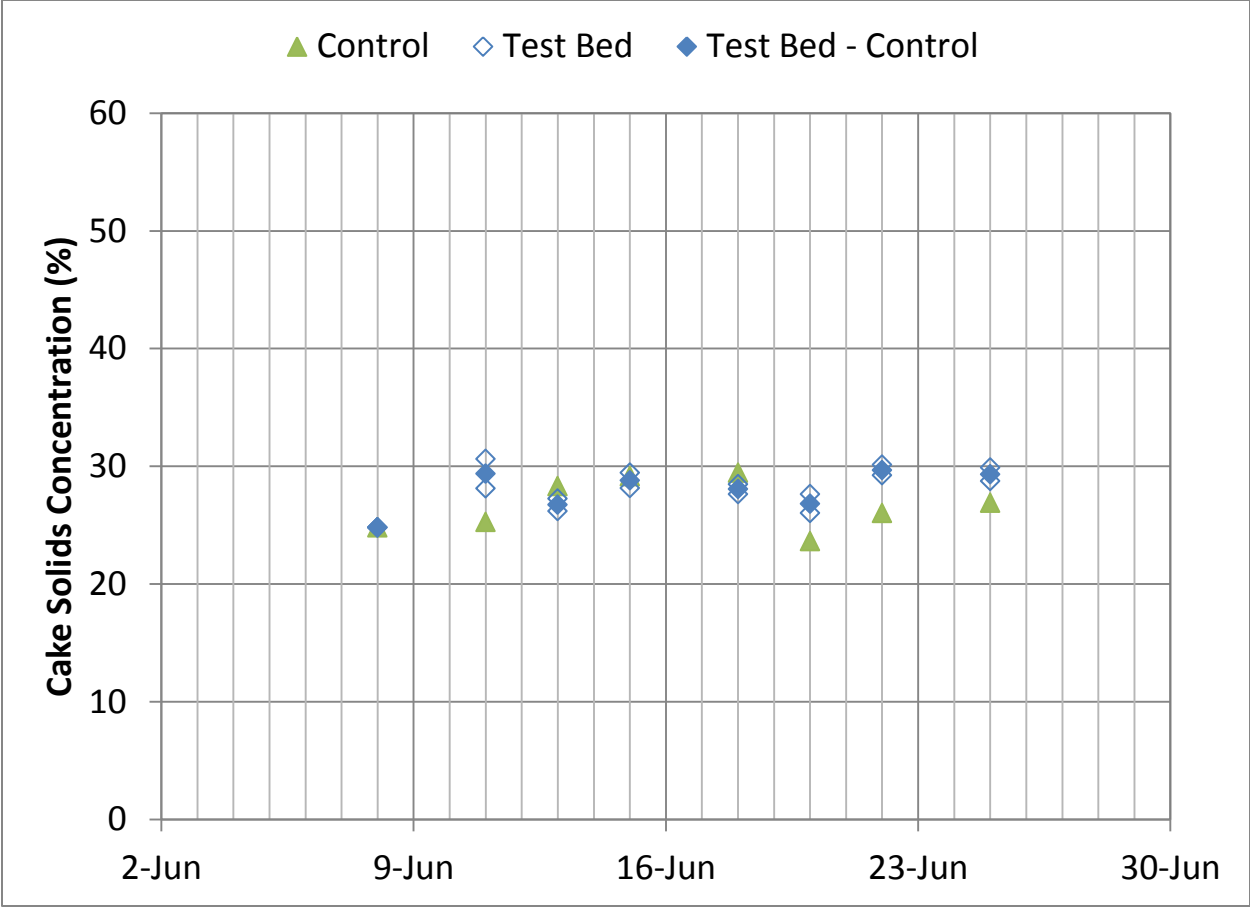


Figure 3.40 Drying performance over time during Raleigh Test 5 (5/9/2012)

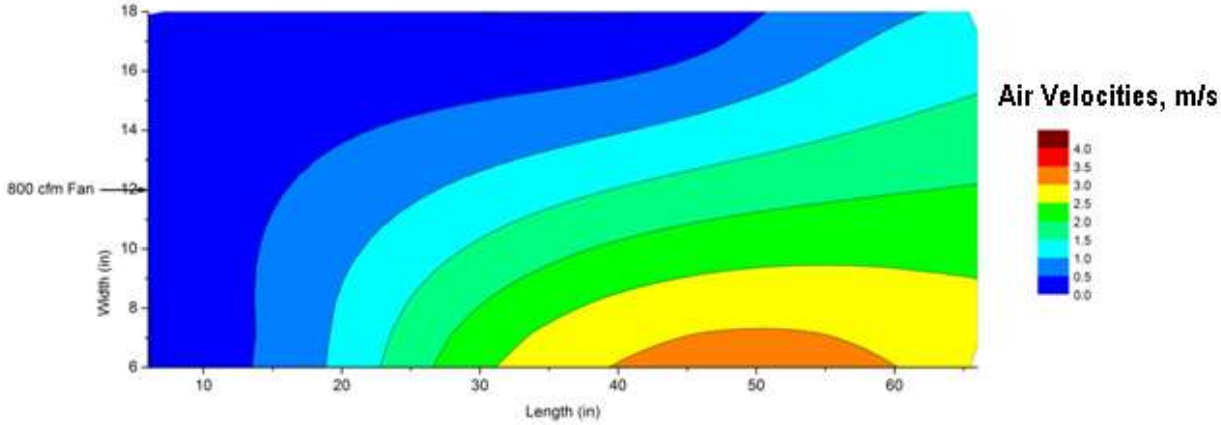


Figure 3.41 Air flow distribution across test bed following Raleigh Test 5

Raleigh Test 6 – July 31, 2012

Following Test 5, it was clear that additional effort in monitoring the test progress was needed to characterize the effectiveness of the enhanced non-mechanical dewatering process functions in drying mechanically dewatered cake. Because plant staff was already pressed for time, a graduate student from North Carolina State University was brought in to assist with the on-site monitoring work.

The sixth test of the enhanced non-mechanical dewatering process at E.M. Johnson WTP was initiated on July 31, 2012. Prior to loading the test bed, the fan was realigned for even airflow distribution across the bed. For this test, the beds were filled to a depth of 9.5 inches, which was approximately 2 inches below the top of the test frames. As with Test 3, 4, and 5, the cake was tilled prior to each sampling event. The initial solids concentration of the beds was 24.2 percent.

For this test, sample resolution was increased to four samples per bed: one at the front of the bed, one at the end of the bed, and two in the middle of the bed (one on each side). Results from each location were averaged, and are presented in Table 3.20.

Also, it should be noted that the sample collection procedure changed following the August 14 sampling event. During that sampling event, it was noted that the cake agglomerates formed by the mechanical dewatering process were difficult to break up as they dried; therefore, this made it difficult to homogenize to get a depth-composited sample. Therefore, the August 16 and 20 sampling events were modified to reduce the number of sample locations, and to increase the number of samples per location. Samples were collected from the front and end of both the test and control beds, and at each sample location three samples were collected: a sample from the top of the bed, a sample from the middle of the bed, and a sample from the bottom of the bed. There was considerable variation between the samples collected at the top of the beds and the samples from the middle and bottom of each bed, which is why the standard deviations of the August 16 and 20 sampling events are much higher. This variance in drying performance relative to depth is discussed further in the section for Raleigh Test 7.

Table 3.20
Summary of Raleigh Test 6 drying performance

Sample event	Test bed		Control bed	
	Average solids concentration (percent)	Standard deviation	Average Solids concentration (percent)	Standard deviation
8/3/2012	33.1	4.39	31.3	2.31
8/7/2012	41.5	9.86	31.3	6.06
8/9/2012	42.2	3.37	30.9	3.61
8/14/2012	43.8	8.73	33.2	4.15
8/16/2012	46.2	16.36	41.9	11.74
8/20/2012	51.1	17.12	37.0	15.56

Based on the data presented in Table 3.20, and an initial solids loading rate of 13.4 lb/ft², the average effective evaporation rate for the test bed was 4.64 in./mo., while that from the control bed was 3.08 in./mo.

Raleigh Test 7 – August 27, 2012

Following the results for Raleigh Test 6, Test 7 was initiated on August 27, 2012 with some changes from the preceding test. First, the tilling frequency was increased from once per sampling event; each day, a plant operator would manually turn over the beds to expose the solids on bottom. Secondly, three samples were taken at each sample location, based on depth. The average solids concentrations measured for each depth, over time, are shown in Figure 3.42.

The results from Test 7 are interesting in that, because the beds were turned over on a daily basis, none of the solids remained at the top of the bed or at the bottom of the bed throughout the test. Based on that, it is intuitive to assume that the results would be roughly homogeneous. However, as Figure 3.42 shows, that is clearly not the case.

For both the test bed and the control bed, the solids on top of the bed at the time of sampling were substantially dryer than the solids on the bottom of the bed. The solids on top of the test bed were, on average, 2.4 times as dry as those on the bottom of the bed, while those on top of the control bed were approximately 1.9 times as dry as those on the bottom. Since those solids are not always on top of the bed, several observations can be made. First, when exposed to the air, those solids on top of the bed must dry very rapidly. This is the case for both the enhanced non-mechanical dewatering process, and also for ambient conditions (note: unlike the Cleveland testing, in Raleigh the control bed was exposed to the wind). Second, because the solids in the middle and bottom of the bed did not likewise dry rapidly, either the layer of dry solids on top of the bed is small compared to the overall mass of the bed, or the dry solids on top of the bed re-absorb moisture as they are moved to the bottom of the bed during the tilling process.

Because of the discrepancy between the top and bottom of the beds, an average solids concentration was not calculated as it was for previous testing. Instead, the solids concentration of the beds was estimated using the measured depth of the bed. After 10 days, the depth of the test bed decreased from 9.5 to 5.5 inches, while the depth of the control bed decreased from 9.5 to 7.0 inches. Based on an initial solids concentration of 24.7 percent, the final concentrations of the test bed and control bed were 42.6 percent and 33.5 percent, respectively. These data correspond to an effective evaporation rate of 13.5 in./mo. in the test bed, compared to the rate of the control bed at 8.4 in./mo.

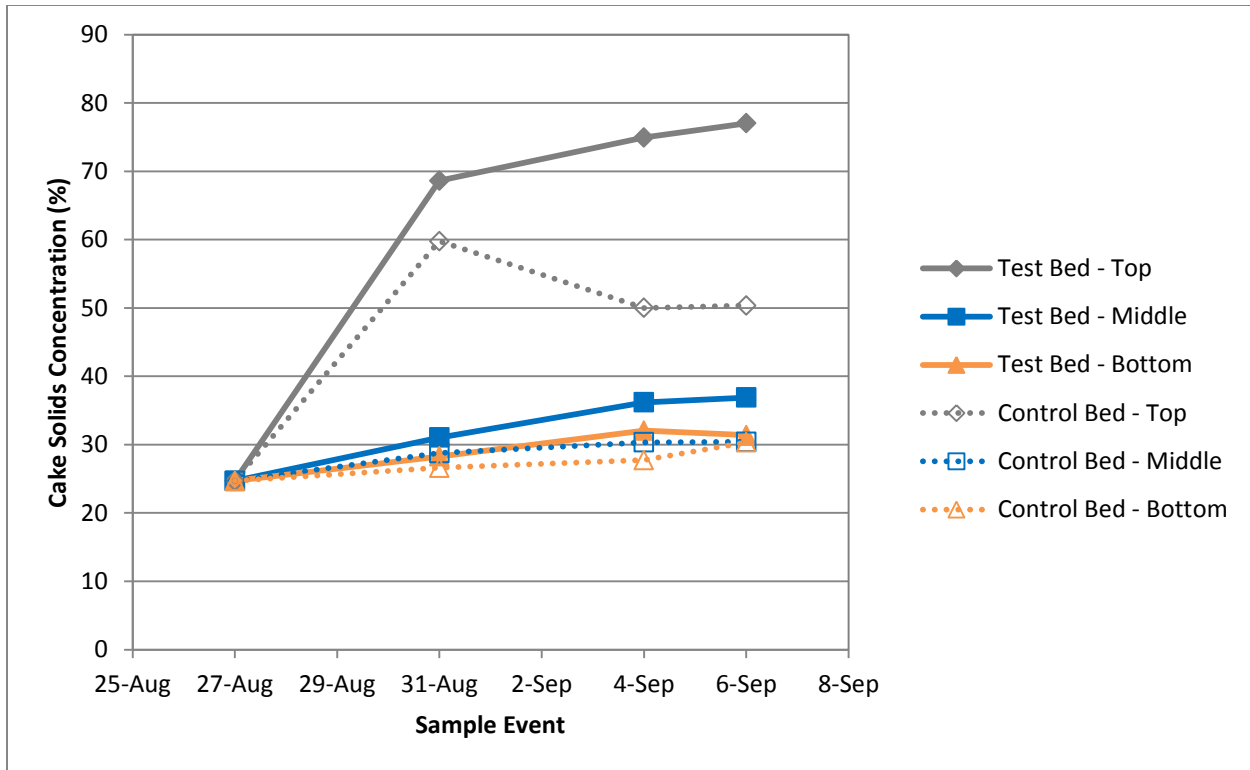


Figure 3.42 Drying performance over time, by depth, during Raleigh Test 7

Raleigh Test 8 – September 19, 2012

The results of Raleigh Test 7 suggested that the cake solids concentration would be difficult to measure for subsequent testing due to the difficulty in differentiating the overall depth of dry solids on top of the beds to the moister solids in the middle and on the bottom of the beds. In light of this, the approach for further testing was re-evaluated.

The frames used for containing the test and control beds were originally conceived of to standardize the mass of solids between the test and the control; without the use of the frames, it would be difficult to ensure that the control bed did not contain more solids than the test bed, or vice versa. The frames were permeable to allow for evaporation through the sides, but it was thought that the frames might be artificially retaining moisture. Further, in full-scale applications, the solids would not be in frames but would instead be windrowed to allow for ease in tilling.

With that in mind, the control and test beds were eliminated for Raleigh Test 8 and replaced by a single large windrow in the middle of the greenhouse, as shown in Figure 3.43. Two 800 cfm fans were aligned to blow down the long axis of the windrow, and produced the air flow distribution shown in Figure 3.44.

As with the preceding tests, solids measurements from Test 8 indicated a substantial difference in solids concentration between the top of the windrow and the bottom of the windrow. Therefore, the volume of the windrow was used, together with the initial solids concentration, to assess the average cake solids concentration of the windrow. Those data are shown in Figure 3.45.



Figure 3.43 Windrow configuration for Raleigh Test 8

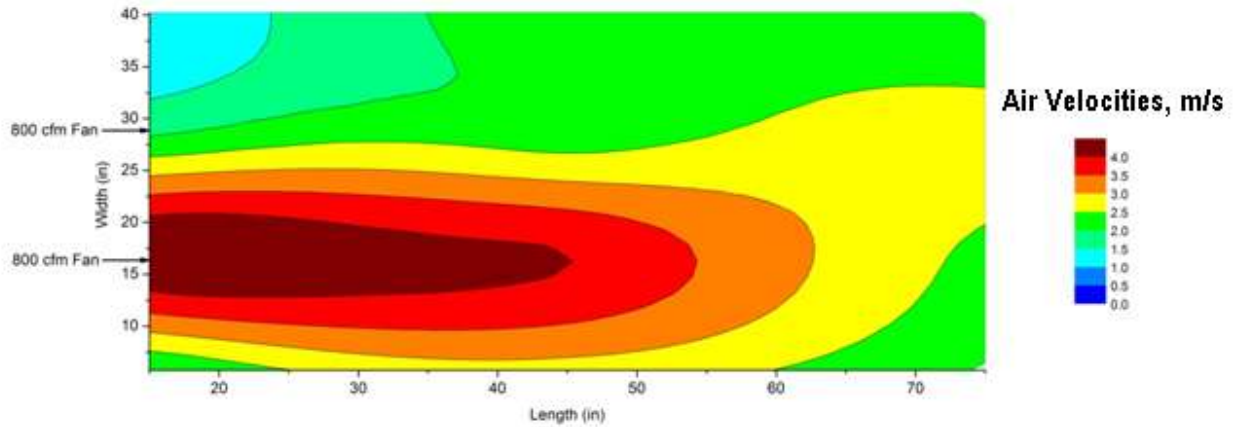


Figure 3.44 Air flow distribution over windrow for Raleigh Test 8

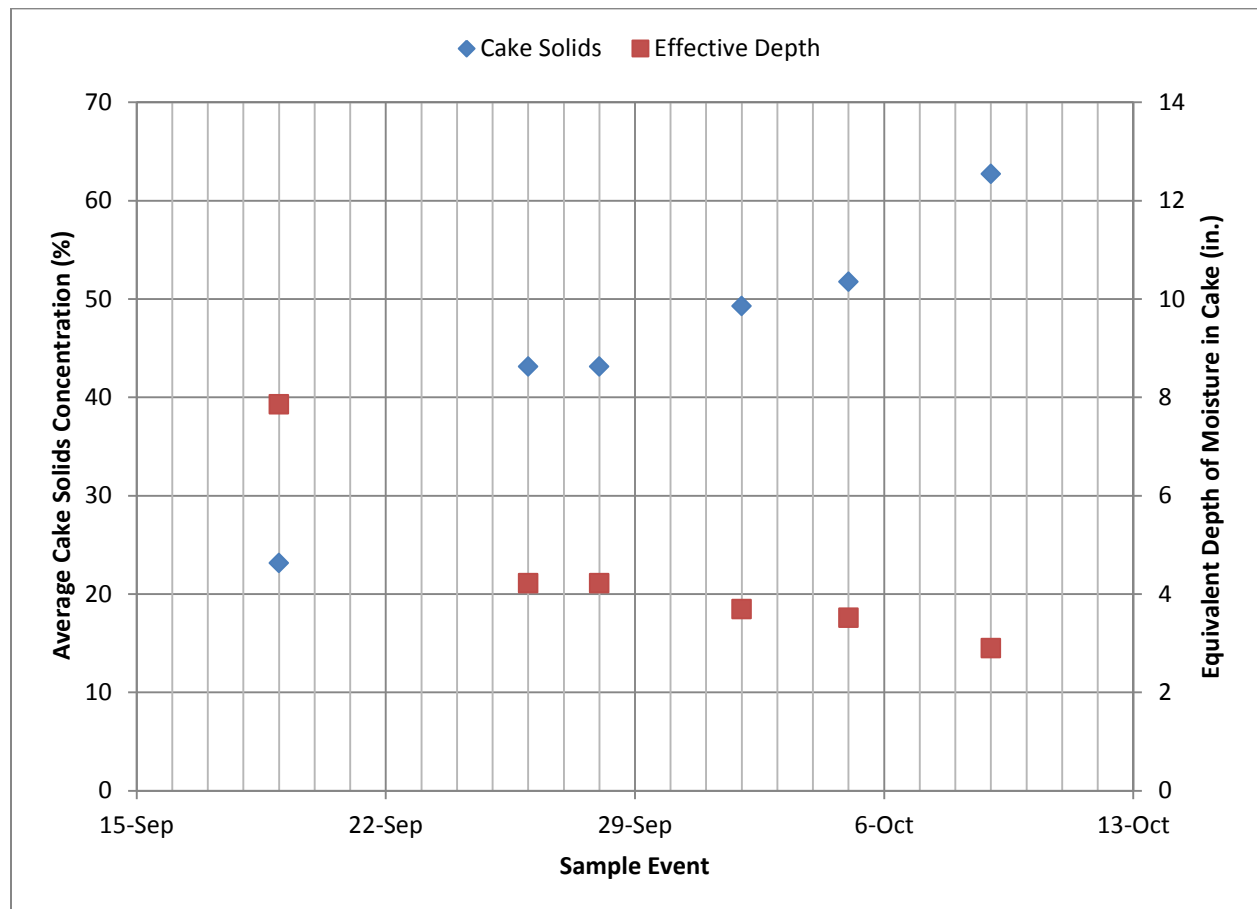


Figure 3.45 Drying performance over time during Raleigh Test 8

The drying data shown in Figure 3.45 indicate that the majority of evaporation occurred during the initial week of drying. During this time, the effective evaporation rate was 15.6 in./mo. and the solids concentration increased by 86 percent. As the cake became drying,

evaporation began to slow. The windrow reached 50 percent solids after 13 days of drying, over which time the average effective evaporation rate was 9.6 in./mo.

Summary of Raleigh Field Pilot Studies

Field testing at Raleigh indicated that the drying of mechanically-dewatered residuals is fundamentally different than the drying of thickened residuals. When thickened residuals are dried using the enhanced non-mechanical dewatering process, and freeze-thaw does not occur, the residuals dry as part of a cohesive whole. Although desiccation cracking does divide the residuals, as shown in Figure 3.46, the cake remains physically connected so that moisture from the center of the cake can move via capillary action to the surface of the cake, where it can be evaporated.

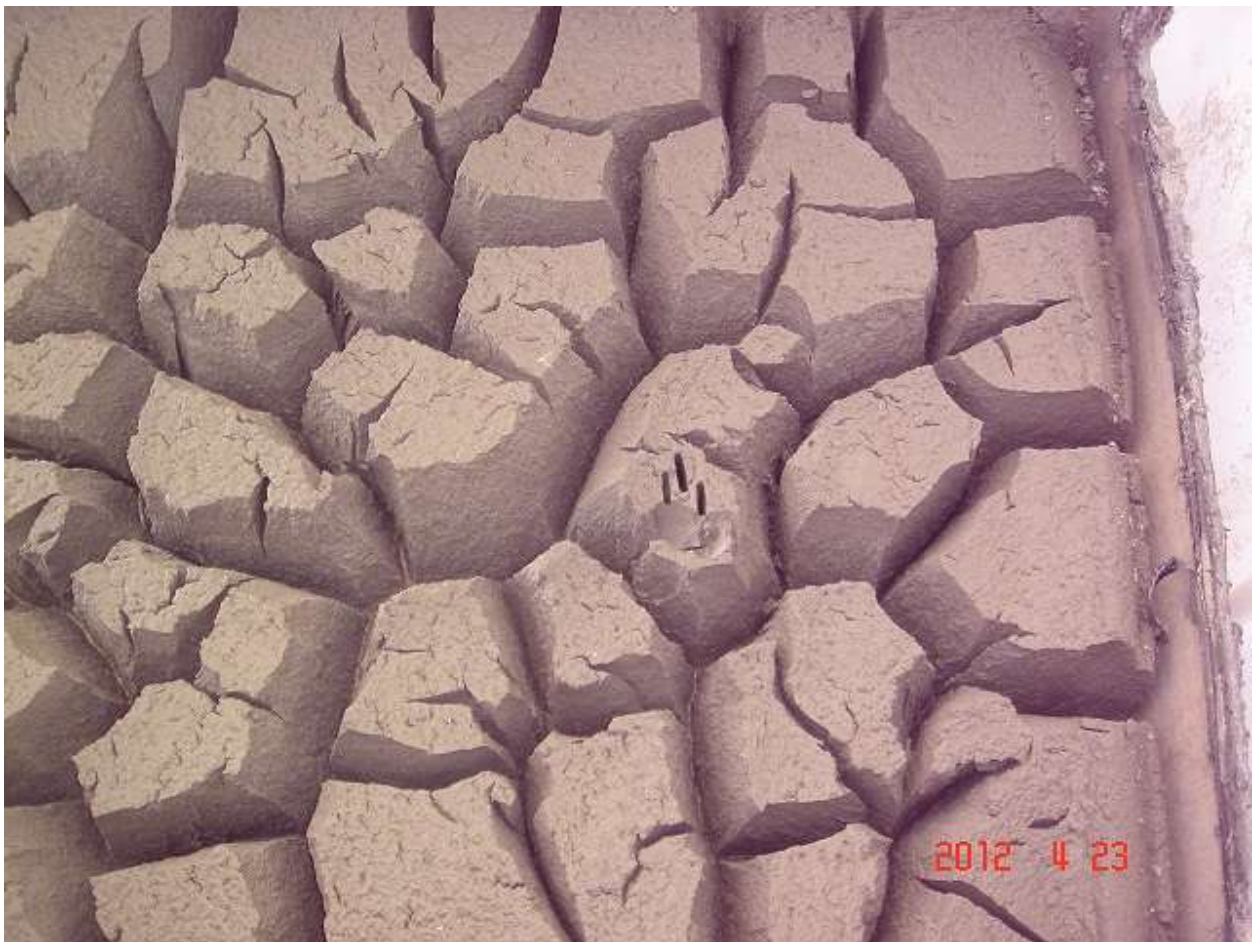


Figure 3.46 Example of desiccation cracking during drying of thickened sludge

Mechanically-dewatered residuals, at least the Raleigh belt press solids, have already been divided into small agglomerations of dewatered cake. While this cake contains much less moisture than the thickened sludge, it is interspersed with void spaces between the thickened sludge, as shown in Figure 3.47. These void spaces appear to impede the transport of moisture through the dewatered cake by preventing the movement of water from the bottom of the cake

layer to the surface. Little evaporation occurs in the void spaces themselves because the lack of air flow means the void spaces quickly become saturated with water vapor. While the solids at the exposed cake surface can dry rapidly, the evaporation of water for the lower layers is impeded. This process has been noted in soil evaporation studies, where tillage primarily affects soil moisture content at the soil surface; although the near surface soil may dry, evaporation from lower soil layers does not occur (Schwartz et al., 2010).



Figure 3.47 Example of the structure of mechanically-dewatered cake during drying

While this testing illuminated an important difference in the process of drying mechanically-dewatered residuals compared to the drying of thickened residuals, additional testing may be needed to assess the effectiveness of the enhanced non-mechanical dewatering process in drying mechanically-dewatered residuals. Raleigh Tests 1 through 6 indicating a high level of variability in measured solids concentrations, most likely associated with the gradient in solids concentration from the surface to the bottom of the bed. However, each of those test, excepting Test 5, indicated that it is possible to dry the previously dewatered cake to solids concentrations of 50 percent or more within a month of drying.

For Raleigh Tests 7 and 8, we able to obtain more consistent results that allow the comparison of the effective evaporation rates for the test and control beds, and for the windrow configuration. During Raleigh Test 7, the enhanced non-mechanical dewatering bed had an effective evaporation rate of 13.5 in./mo., which was a 60 percent improvement over the effective evaporation rate of the control bed at 8.4 in./mo. During Raleigh Test 8, which evaluated the effectiveness of dewatering a windrow of residuals rather than the controlled volume of the test bed, the effective evaporation rate to get the bed to 50 percent solids concentration was 9.6 in./mo.

CHAPTER 4 CASE STUDIES

COSTING

Total capital cost for the enhanced non-mechanical dewatering process has three primary components: the drying beds, the enclosing structure, and the fans for ventilation. Of these three, the first two are most significant; the fans are relatively inexpensive, provided that power is available at the dewatering site.

Drying Beds

The design of the drying beds is very similar to traditional non-mechanical dewatering beds. Vandermeijden and Cornwell (1998) describe the design of such beds in detail, so the details of designing such beds will only be touched on briefly in this report.

Drying beds are essentially shallow, flat basins used to store residuals as they dry. Beds designed to dewater thickened sludge should have permeable bottoms that allow free water released from the sludge to percolate through during the drainage phase. The most common configuration for such beds includes an underdrain system of perforated or slotted pipe, covered with support gravel and sand. In order to minimize sand loss when the dewatered residuals are removed from the beds, it is recommended that the beds include concrete runners oriented along the longitudinal axis of the bed to support the treads of the removal equipment (e.g. front-end loader, skid-steer loader, etc.) and to guide the loader bucket across the top of the sand. A liner system under the beds may be required by local regulators to prevent drainage water from entering groundwater supplies. Beds designed for the drying of mechanically-dewatered cake may be designed with solid bottoms due to the lack of free water drainage from the residuals.

Drying bed installations typically include multiple beds so that residuals can be actively loaded as the previously loaded residuals are drying. Bed walls generally range from 2 to 3 feet high above the sand surface, depending on design loading depth for the residuals, and may be constructed of cast-in-place concrete, concrete block, or earthen berms. Because the beds must be able to retain the residuals during loading, they are typically set with the free surface of the residuals at or below the surrounding grade. Therefore, access ramps are required to allow equipment to enter the beds for cleaning.

Installations designed for dewatering thickened sludge should feed residuals to the bed using either a distribution box or series of nozzle pipe outlets. Depending on the size of the bed, multiple application points may be required to allow for uniform loading of the residuals. Piping to the application points is typically ductile iron, and should be designed to maintain a sufficient volume to avoid residuals settling (typically ≥ 2.5 fps for coagulation sludges).

Enclosing Structure

The enhanced non-mechanical dewatering process benefits from the inclusion of an enclosing “greenhouse” structure for multiple reasons.

Commercially-available enclosures tend to fall into one of three categories: greenhouses, hoop houses, and stretched-fabric structures. Greenhouses (Figures 4.1 and 4.2) generally

feature a steel frame supporting glass, acrylic, or polycarbonate panels. Due to the weight of the panels, greenhouses typically feature a more substantial supporting framework than the other types of structures and may be limited in the distance that can be spanned between support columns. Hoop houses (Figure 4.3) and stretched-fabric structures (Figure 4.4) differ primarily in the configuration of the supporting framework. Hoop house frames generally consist of a series of arches connected longitudinally to form the structure. Stretched-fabric structures, by comparison, typically include vertical side walls that may be topped with either a structural arch or peaked roof structure. The typical covering for both hoop houses and stretched-fabric structures is a coated polyethylene fabric, although other fabric materials are available. Fabrics can have different levels of opacity; while a transparent fabric will maximize solar radiation transmission to the drying beds, a small amount of opacity will serve to diffuse the incoming solar radiation across the bed, which may provide for more uniform drying. Hoop houses and stretched-fabric structures can generally span greater distances than traditional greenhouse structures, including spans in excess of 150 feet. Depending on the size of the drying bed, it would be possible to span the longitudinal axis of the bed, which would allow a single hoop house or stretched-fabric structure to span multiple beds.

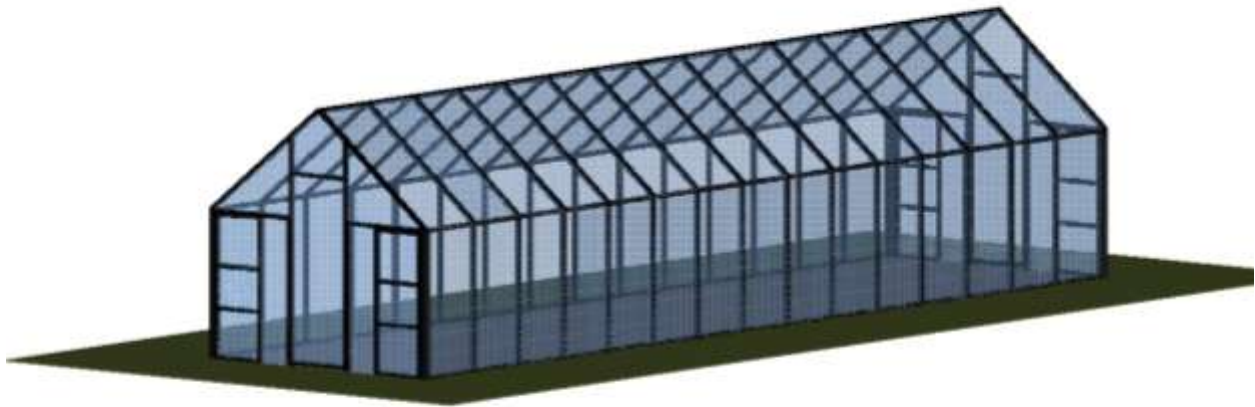


Figure 4.1 Sketch of traditional greenhouse structure, individual installation

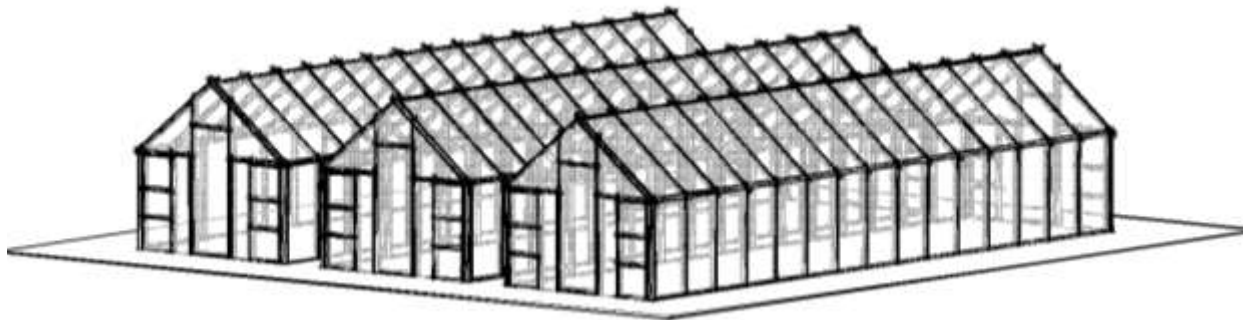


Figure 4.2 Sketch of traditional greenhouse structure, multiple installation

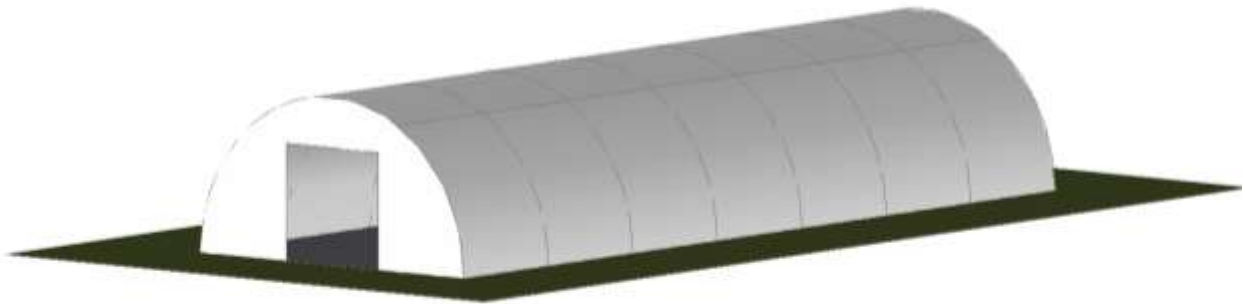


Figure 4.3 Sketch of a hoop house structure

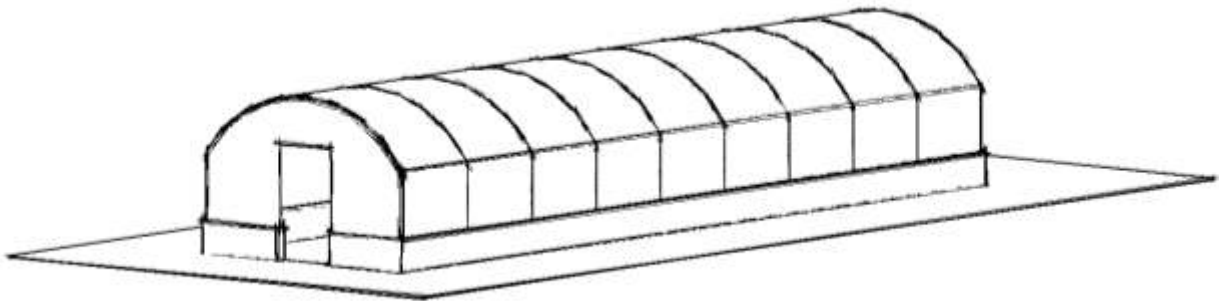


Figure 4.4 Sketch of a stretched-fabric structure

Ventilation Fans

Based on the pilot-scale results, successful ventilation of the beds requires even air flow distribution at a high rate of velocity. High-velocity fans, strategically located around the perimeter of the bed, can meet these requirements. High velocity fans can be purchased in a number of sizes ranging from 24 in. diameter to 54 in. and covering flows from 5,600 cfm to 42,500cfm. The flow patterns must be assessed to obtain a good velocity distribution throughout the bed, especially at the end. The preliminary work in this research showed both the importance of the total volumetric air flow in cfm per square foot of bed area, as well as the velocity achieved across the bed. The data of Figures 3.18, 3.31, and 3.32 suggest that the air flow should be in the 8 to 30 cfm/ft² of bed area range and that the longitudinal velocity should be around 8 to 12 fps. An optimization model could be developed for a specific application to evaluate the trade-off between fan airflow used versus the area required for drying. As shown below, the fan capital cost is minor compared to the sand bed overall cost, but fan operating cost can be significant. It may be that a reasonable approach is to put fans in at the higher flow range but only run them as needed for the different seasons and sludge production.

Example Installation Costs

Capital and operating costs were developed for a generic enhanced non-mechanical dewatering installation consisting of six 50-foot by 150-foot drying beds, which is roughly equivalent to one acre of drying area. Figures 4.5 through 4.7 show the configuration of this generic installation.

Capital costs were developed for the generic installation shown in Figures 4.5 through 4.7, and are presented in Table 4.1. Costs for the sand drying beds were developed based on a quantity take-off of the units and typical unit costs for concrete, sand, piping, etc. Costs for the fans and the stretched-fabric structure to enclose the beds were based on manufacturer quotes.

The costs presented in Table 4.1 provide a rough estimate of the relative contribution of each factor to the overall cost of the installation; the fans and electrical work required comprise about 10 percent of the direct construction cost of the installation, with the remaining cost divided fairly evenly between the sand drying beds themselves and the enclosing structure. Indirect construction costs, including mobilization, bonding, contingency, and engineer design, will increase total cost by approximately 50 percent. The overall construction cost per unit of drying area is approximately \$67 per square foot.

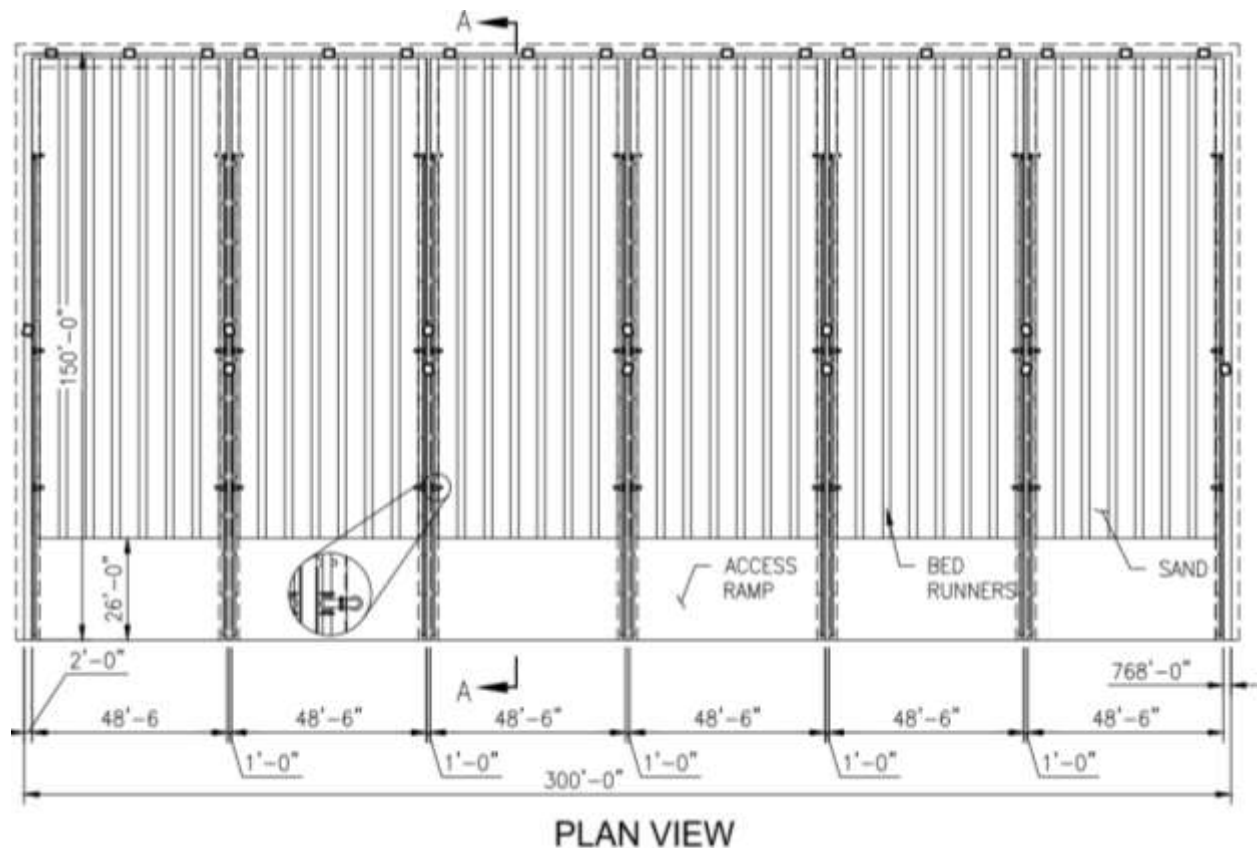


Figure 4.5 Plan view of generic six-bed enhanced non-mechanical dewatering installation

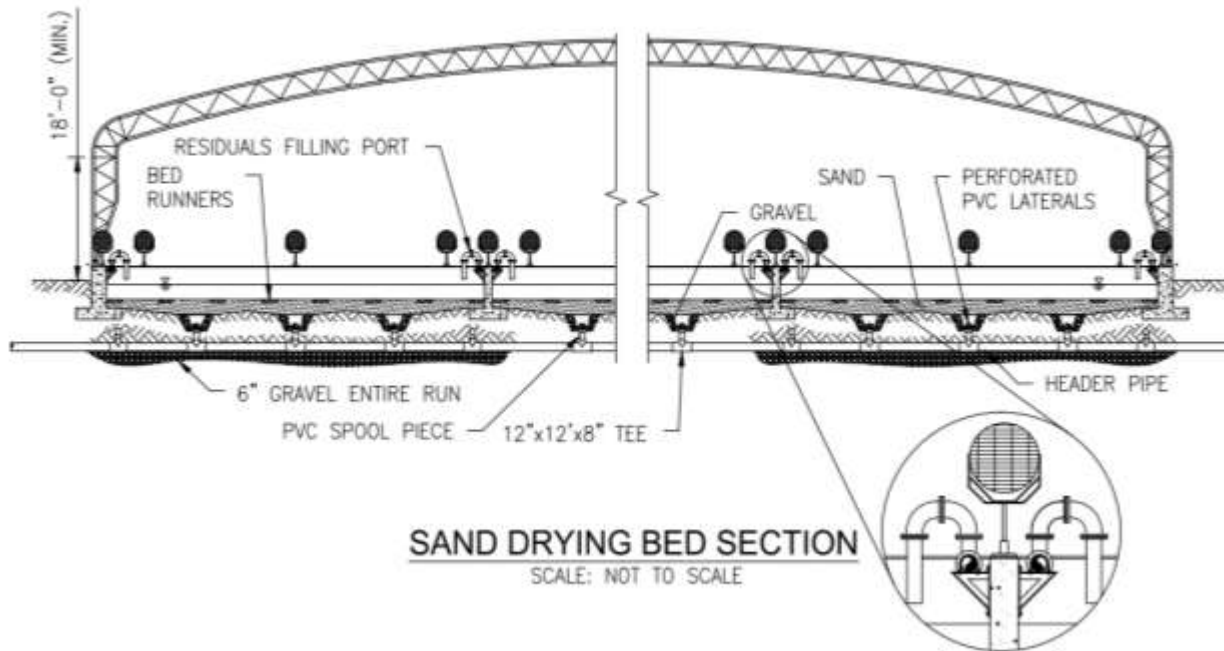


Figure 4.6 Section view along lateral bed axis of generic six-bed enhanced non-mechanical dewatering installation

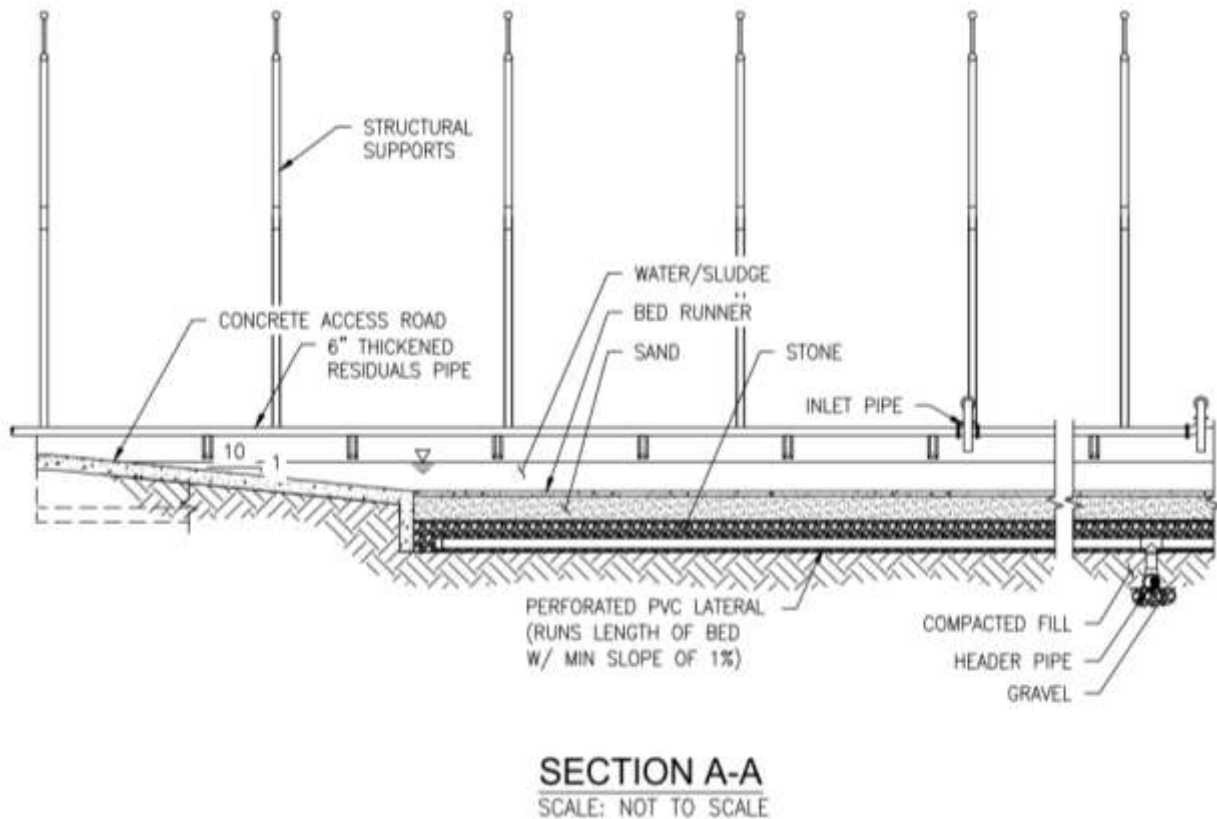


Figure 4.7 Section view along longitudinal bed axis of generic six-bed enhanced non-mechanical dewatering installation

Table 4.1
Capital costs for generic six-bed enhanced non-mechanical dewatering installation

Item	Cost
Sand Drying Beds	\$ 1,052,000
Fans	156,000
Electrical/Controls	53,000
Structures	945,000
subtotal	\$ 2,050,000
Mobilization/Bonding (20%)	\$ 410,000
Contingency (25% [†])	\$ 276,000
subtotal	\$ 2,736,000
Engineering (10%)	\$ 274,000
Total	\$ 3,010,000
Total per ft² of drying area	\$ 66.89

[†]Contingency for structures included in structure cost

The cost savings of constructing enhanced non-mechanical dewatering beds is highly site-specific, and will depend on the current method of managing residuals at a given water treatment plant and the fee structure for disposing of those residuals. If the plant currently does not use residuals treatment technologies and disposes of sludge either via direct discharge to water bodies, via the municipal sewer system, or via liquid haul, it will be possible to compare the capital cost of constructing new enhanced non-mechanical dewatering beds to the capital cost of other dewatering methods. However, it is difficult to compare the cost savings to the existing residual management method because the method of disposal will not be the same after going to a dewatering technology (i.e. haul and disposal costs vs. discharge costs).

Plants that currently dewater residuals will be able to calculate the cost savings of enhanced non-mechanical dewater of residuals based on their current disposal costs. Cost savings will depend on three factors: annual solids production (in terms of dry-tons), the cost of transporting and disposing of the residuals (in terms of wet-tons), and the amount of drying that can be achieved from the enhanced non-mechanical dewatering process. Figure 4.8 presents the potential cost savings from drying mechanically-dewatered residuals from 20 percent solids concentration to 50 percent solids concentration.

As Figure 4.8 shows, using the enhanced non-mechanical dewatering process to further dry residuals that have been previously mechanically dewatered can result in significant cost savings, particularly as annual solids production increases and as the cost of residuals transport and disposal increases. While these savings must be compared to the overall cost of adding the enhanced non-mechanical dewatering process to the existing residuals management schema, for some utilities the cost-benefit ratio should be favorable.

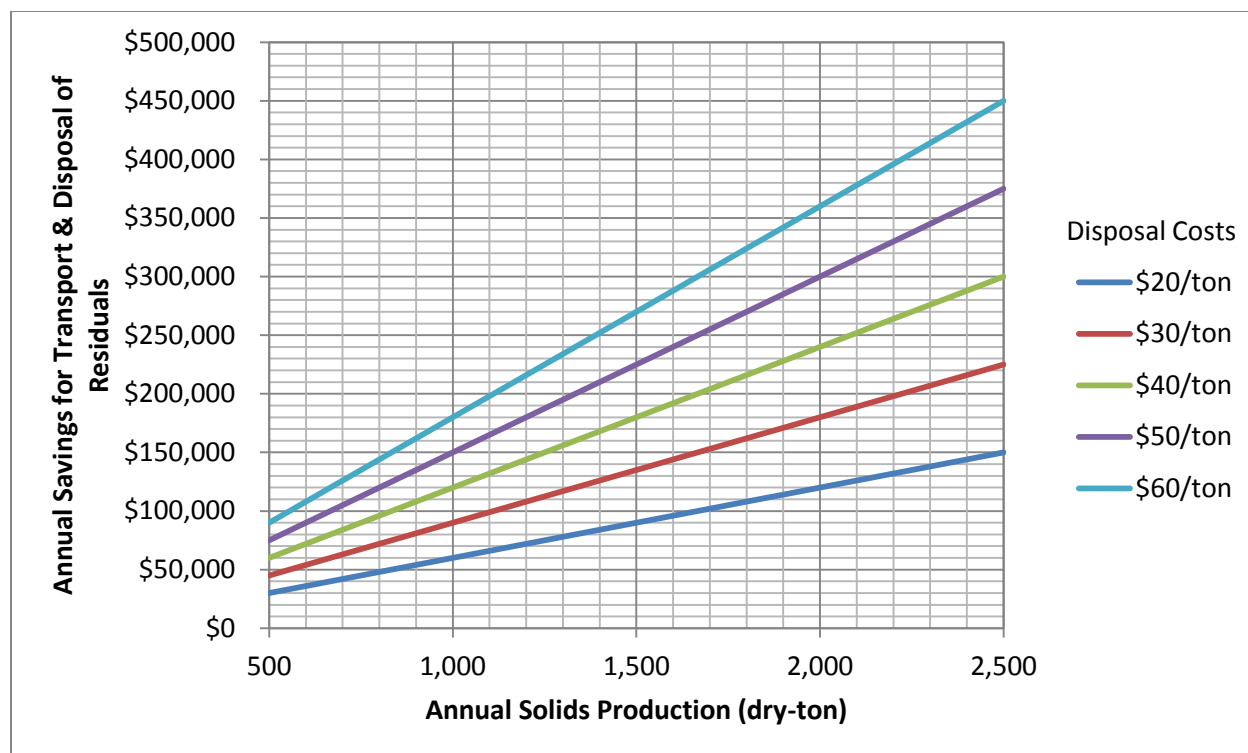


Figure 4.8 Annual cost savings from drying mechanically dewatered residuals from 20 percent solids concentration to 50 percent solids concentration

CLEVELAND CASE STUDY

The Morgan WTP in Cleveland currently discharges all of the residuals generated at the plant to the municipal sewer system. In 2008, alternatives methods of residuals management, including mechanical dewatering and traditional non-mechanical dewatering beds, were analyzed for this plant (EE&T, 2008). Solids production data from this study was used, together with the data from the Cleveland field testing, to update the alternatives analysis with an enhanced non-mechanical dewatering bed option.

The total surface area required for the enhanced non-mechanical dewatering beds was estimated using a numerical model based on the sand drying bed performance modeling concepts presented in Vandermeijden and Cornwell (1998). In brief, the model uses the plant's daily solids production to determine the number of sand beds that would be filled each day, based on user-defined drying bed geometry and solids loading rates. For this modeling effort, 50-foot by 145-foot drying beds were used with an assumed loading rate of 2.5 lb/ft². Each bed is considered to be loaded to a depth equivalent to the target drained solids concentration, which in this case was assumed to be 7.6 percent (the average drained solids concentration from the Cleveland field testing). The model then uses daily evaporation rates to determine the water lost from each bed, until the target solids concentration of 20 percent is reached. At that point, the bed is made available again for loading for fresh solids. The model includes time for bed loading, draining, and cleaning.

This model had previously been used to estimate the total area of traditional non-mechanical dewatering bed area required to treat the residuals from Morgan WTP, using

historical evaporation data presented in Table 3.17. The model was re-ran using the effective evaporation rates presented in Table 3.17 to determine the total area of enhanced non-mechanical dewatering beds required to treat the same solids production. Figure 4.9 compares the total area required by the traditional dewatering beds to that required by the non-mechanical dewatering beds, over time. Using enhanced non-mechanical dewatering beds rather than traditional beds reduces the required bed area by approximately 70 percent, from ~12 acres down to less than 4 acres.

This reduction in drying bed area is significant, because one of the challenges in implementing non-mechanical dewatering at Morgan WTP has been lack of available space near the plant. Quite simply, there are not 12 acres available on-site for traditional non-mechanical dewatering beds and surrounding properties are already developed, limiting expansion possibilities. So while the traditional non-mechanical dewatering at Morgan WTP was economically attractive (see Tables 4.2 and 4.3, below), there was not enough room on-site to build them. However, there are approximately 6 acres available on-site in an area occupied by an abandoned clear well, which could be used for siting enhanced non-mechanical dewatering beds at Morgan WTP. Figure 4.10 shows a potential layout for the enhanced non-mechanical dewatering beds on top of the former clear well structure.

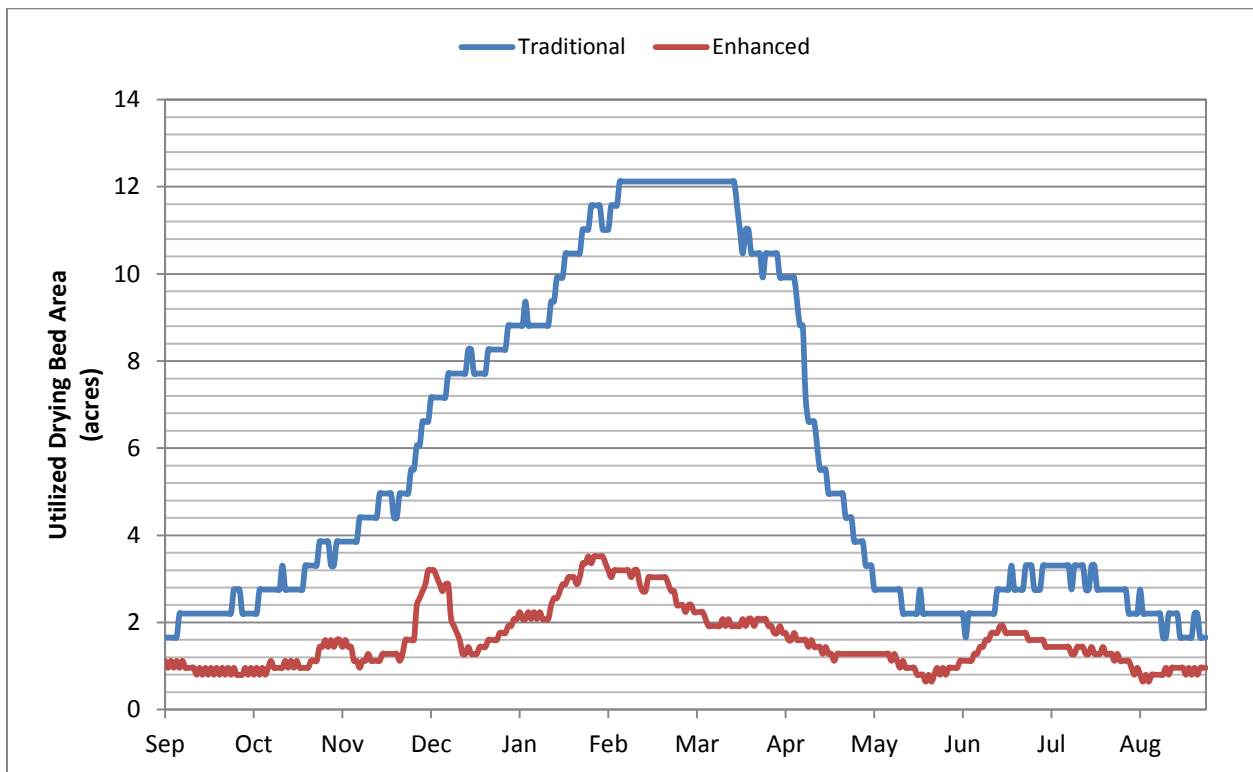


Figure 4.9 Comparison of total drying bed area required for traditional and enhanced non-mechanical dewatering beds for Morgan WTP

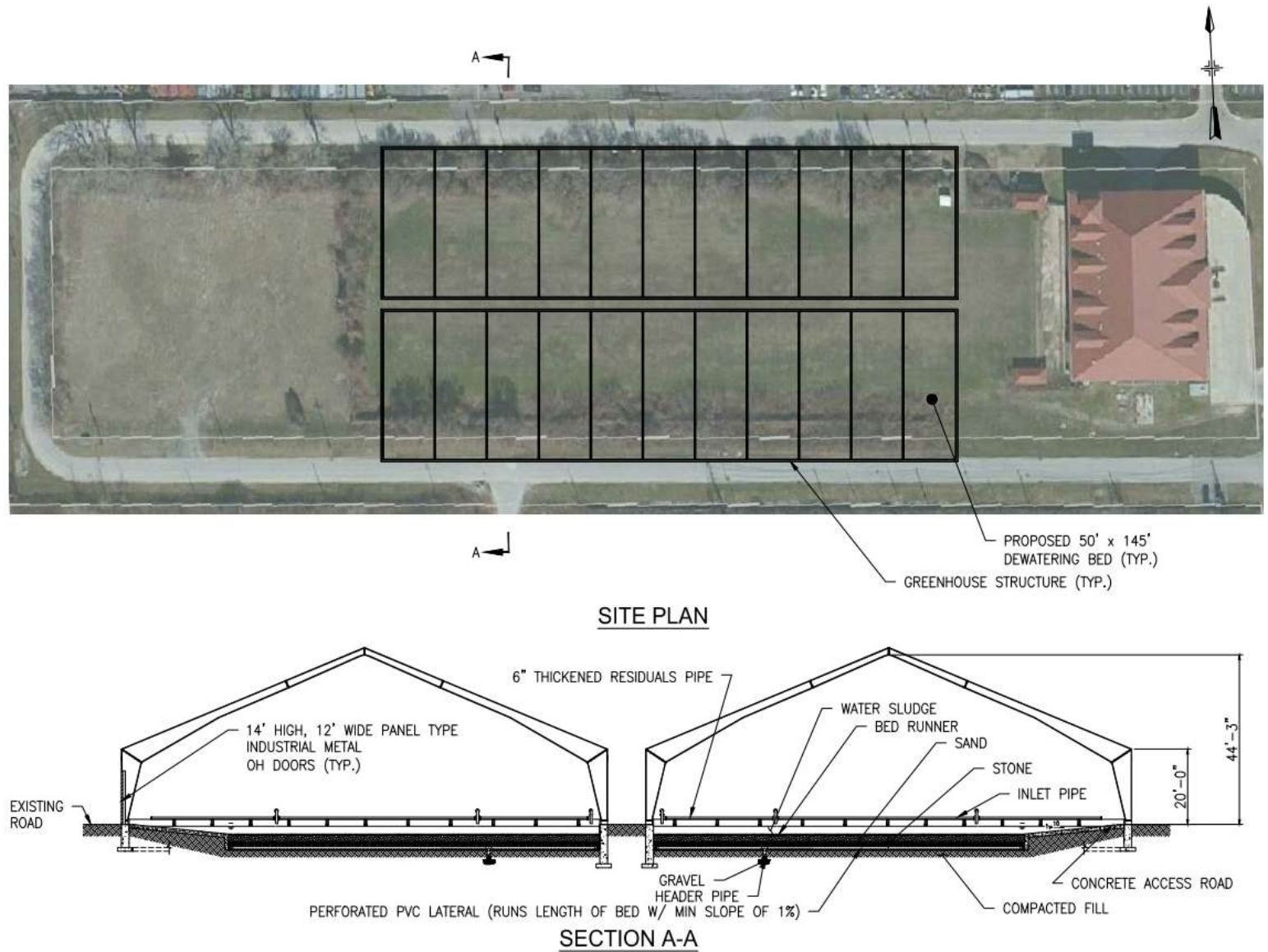


Figure 4.10 Potential layout for enhanced non-mechanical dewatering beds at Morgan WTP

As shown in Figure 4.10, the enhanced non-mechanical bed layout would take advantage of the existing ring road around the abandoned clear well for accessing/cleaning the beds. The beds would be arranged in two banks of 11 beds each, and each bank would be enclosed in a 149-foot by 550-foot stretched-fabric structure. Bed configuration would be similar to that shown in Figures 4.5 through 4.7.

Capital and annual operations and maintenance (O&M) costs were developed for the enhanced non-mechanical dewatering option and compared to the costs that were previously estimated for the mechanical dewatering and traditional non-mechanical dewatering options, which were updated from the 2008 report to 2013 dollars. These costs are presented in Table 4.2. Annual O&M costs for the enhanced drying bed option were assumed to remain the same as was estimated for the traditional non-mechanical dewatering option, aside from the power cost associated with operating the fans. Power costs for the enhanced non-mechanical dewatering option were developed by calculating the total number of hours each bed would be operated annually, based on the modeled bed utilization shown in Figure 4.9. Out of the total 192,720 bed-hours available annually (22 beds by 8,760 hours/year), only 91,956 bed-hours were needed. These hours of operation were then multiplied by the total horsepower for the fans installed in each bed, and converted to kWh. A common value of \$0.1225/kWh was used to be consistent with the cost assumptions made in the previous study. Further, as can be seen in Figure 4.8 there are actually several months that the fans are not needed at all as the area available exceeds that required by traditional drying. In this analysis the power cost was not reduced by the time when fans could be turned off.

A primary objective of the project was to research if non-mechanical dewatering could be made feasible for large water plants where sufficient land is often not available. In the case of the Morgan Plant, the enhanced non-mechanical dewatering would fit in the land available and would therefore be a feasible option. An added benefit as it turns out is that the enhanced beds were actually less expensive than the traditional bed. Although the enhanced drying requires a greenhouse type structure, the less are required offset the structure costs. Annual O&M costs are also slightly higher for the enhanced non-mechanical option due to the power consumption of the fans. However, the overall total annualized cost of the enhanced non-mechanical dewatering option is approximately 77 percent that of the traditional non-mechanical dewatering option, and approximately half that of the centrifuge dewatering option.

In addition to the residuals management options presented in Table 4.2, Morgan WTP could continue to dispose of residuals to the municipal sewer system as is currently practiced. However, the projected sewer fees for 2013 exceed \$1.5 million, and sewer rates are projected to continue to increase by 10 percent annually over the next five years. After that, it is assumed that sewer costs will increase by five percent annually for the following 15 years. For comparison, annual O&M costs for the three dewatering options are assumed to inflate at four percent annually. The present value of all four residuals management over the next 20 years is presented in Table 4.3

Table 4.2
Comparison of capital costs for dewatering options at Morgan WTP

	Centrifuge (dollars)	Traditional non- mechanical dewatering (dollars)	Enhanced non- mechanical dewatering (dollars)
Capital cost (2008 dollars)	16,828,173	13,555,565	N/A
Capital cost (2013 dollars)	19,402,953	15,629,623	9,742,005
Annualized capital cost	1,691,638	1,362,662	819,535
Annual O&M costs	473,395	111,155	320,382
Total annualized cost	2,165,033	1,473,817	1,139,917

Table 4.3
Comparison of present value costs (20 years, 6% interest) for residuals management options at Morgan WTP

	Sewer discharge (dollars)	Centrifuge (dollars)	Traditional non- mechanical dewatering (dollars)	Enhanced non- mechanical dewatering (dollars)
Capital Cost (2013 dollars)	0	19,402,953	15,629,623	9,742,005
Present worth of annual costs (interest = 6%)	36,937,714	8,266,365	1,940,974	5,594,471
Total present worth	36,937,714	27,669,318	17,570,597	14,994,471

RALEIGH CASE STUDY

The E.M. Johnson WTP currently uses three belt filter presses to dewater residual solids generated at the plant. After dewatering, the solids are stockpiled on-site, and then are periodically removed via a contract hauler for land application on surrounding rural properties. The cost of the transport is based on a sliding scale, as shown in Table 4.4. In addition to the costs shown in Table 4.5, there is an additional \$7.00/ton fee for managing and spreading the residuals.

Table 4.4
Sliding cost scale for transport of residuals from E.M. Johnson WTP

Cost per ton (dollars)	Transport distance
8.00	1 to 35 miles
10.50	36 to 55 miles
13.50	56 to 70 miles
15.50	71 to 90 miles
18.50	91 to 110 miles
21.50	111 to 130 miles

Table 4.5
Residual solids removal costs at E.M. Johnson WTP for FY2010

Month	Total tonnage removed	Total monthly cost (dollars)	Cost per ton removed (dollars)
Jan	1,726.63	27,704.32	16.05
Feb	1,320.77	29,717.33	22.50
Mar	1,640.76	33,500.08	20.42
Apr	1,368.26	30,576.57	22.35
May	1,156.32	24,961.51	21.59
Jun	1,006.56	22,233.53	22.09
Jul	1,135.10	26,296.68	23.17
Aug	1,155.10	27,487.12	23.80
Sept	834.80	19,545.40	23.41
Oct	1,203.81	28,248.78	23.47
Nov	907.90	21,512.96	23.70
Dec	672.90	14,429.70	21.44
Total	14,128.91	\$306,213.98	N/A

Because the transport fee changes based on the distance each load is transported, the cost per ton changes from month to month. Table 4.4 presents the total tonnage of residuals removed from the E.M. Johnson WTP in 2010, along with the cost of residuals transport and spreading by month and the equivalent cost per ton for transport and spreading of the residuals. As Table 4.5 shows, the total cost of residuals disposal in 2010, was \$306,213.98.

The average solids concentration of the cake produced by the belt filter presses in 2010 was 21.8 percent. The field testing conducted at E.M. Johnson WTP indicated that it should be possible to further dry the residuals to at least 50 percent solids concentration with the enhanced non-mechanical dewatering process. Table 4.6 illustrates the potential cost savings associated with further drying the mechanically-dewatered residuals to a 50 percent solids concentration.

Table 4.6 shows that reducing the solids concentration of the residuals from the average of 21.79 percent coming off of the belt filter presses to a solids concentration of 50 percent would reduce the total tonnage removed from the site by almost 8,000 tons per year, which would result in a cost savings of \$172,765.98.

In order to determine infrastructure costs, it is necessary to determine how much area will be needed for the enhanced non-mechanical dewatering beds. The total area required will depend on the solids loading rate used, which is a function of the loading depth, and the total number of bed turnovers required each year.

The estimated unit weight for the 21.8 percent solids concentration cake coming off of the belt filter presses is 70 lb/ft³. Therefore, solids loading rate (in lb/ft² wet solids) can be determined by specifying the depth of the residuals in the dewatering beds. The field testing varied the bed depth between 6 inches to 12 inches of residuals, while the windrow that was tested had an effective depth of 7.45 inches (calculated by assuming the total volume of the windrow was distributed evenly over the windrow footprint). These correspond to loading rates of 35, 43.4, and 70 lb/ft² wet solids, respectively.

Table 4.6
Comparison of residual solids removal costs at 21.8 and 50.0 percent solids concentration

Month	Total tonnage removed @ 21.79%	Total tonnage removed @ 50.0%	Cost per ton for transport and Spreading (dollars)	Total monthly cost @ 21.79% (dollars)	Total monthly cost @ 50.0% (dollars)
Jan	1,726.63	752.47	16.05	27,704.32	12,073.54
Feb	1,320.77	575.59	22.50	29,717.33	12,950.81
Mar	1,640.76	715.04	20.42	33,500.08	14,599.33
Apr	1,368.26	596.29	22.35	30,576.57	13,325.27
May	1,156.32	503.92	21.59	24,961.51	10,878.23
Jun	1,006.56	438.66	22.09	22,233.53	9,689.37
Jul	1,135.10	494.68	23.17	26,296.68	11,460.09
Aug	1,155.10	503.39	23.80	27,487.12	11,978.89
Sept	834.80	363.81	23.41	19,545.40	8,517.89
Oct	1,203.81	524.62	23.47	28,248.78	12,310.82
Nov	907.90	395.66	23.70	21,512.96	9,375.35
Dec	672.90	293.25	21.44	14,429.70	6,288.46
Total	14,128.91	6,157.38	N/A	\$306,213.98	\$133,448.05

Prior to installation of the belt filter presses at E.M. Johnson WTP, the plant relied on 18 non-mechanical dewatering beds for residuals management, which were divided into two banks of 9. These 30-foot by 130-foot beds still are still in-place, but are not currently used other than for general storage. One bed was converted to house four elevated thickened sludge storage tanks, and four beds were paved with concrete to provide an area for stockpiling dewatered cake before it is removed from the site. Because this existing infrastructure was available, it was assumed that one bank of nine beds could be converted to enhanced drying beds, as shown in Figure 4.11. To keep costs low, the side with the existing drying pad was selected. Other than the stretched-fabric structure to enclose the beds, and the fans, the only capital costs needed for this option are those for paving the remaining five beds.

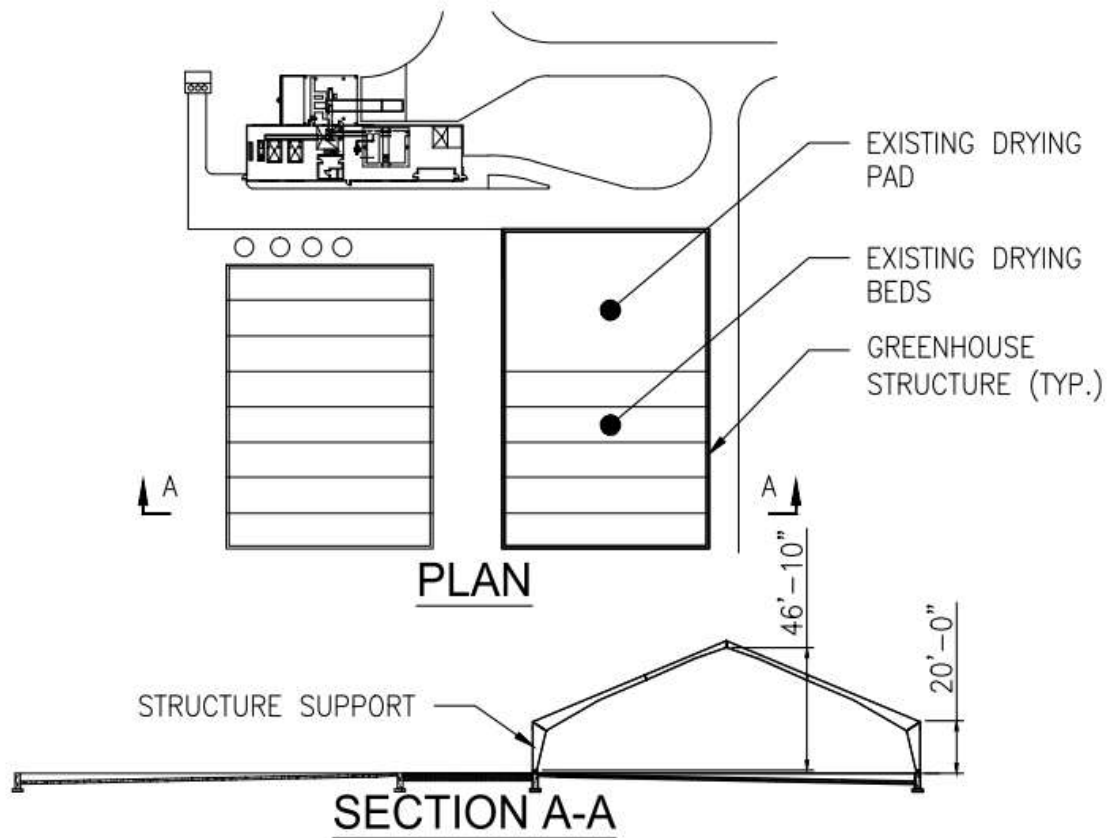


Figure 4.11 Sketch of potential enhanced non-mechanical dewatering bed layout at E.M. Johnson WTP

The nine beds give a total area of 35,100 ft² that could be used to dry the mechanically-dewatered cake. Based on the annual solids production and the loading rates discussed previously, the total area required for drying can be calculated. The annual yield of the beds can then be calculated by dividing the total area required for drying by the available bed area, as shown in Table 4.7.

Table 4.7
Comparison of required annual yield based on loading depth for E.M. Johnson WTP

Month	Total tonnage removed @ 21.79%	Total Area Required (ft ²)		
		Loading depth = 6 inches	Loading depth = 7.45 inches	Loading depth = 12 inches
Jan	1,726.63	98,665	79,710	49,332
Feb	1,320.77	75,473	60,974	37,736
Mar	1,640.76	93,758	75,746	46,879
Apr	1,368.26	78,186	63,166	39,093
May	1,156.32	66,075	53,382	33,038
Jun	1,006.56	57,518	46,468	28,759
Jul	1,135.10	64,863	52,402	32,431
Aug	1,155.10	66,006	53,325	33,003
Sept	834.80	47,703	38,539	23,851
Oct	1,203.81	68,789	55,574	34,395
Nov	907.90	51,880	41,913	25,940
Dec	672.90	38,451	31,065	19,226
Total	14,128.91	807,366	652,265	403,683
Available Area (ft²)				35,100
No. of Bed Turnovers Per Year		23.0	18.6	11.5

The majority of the field testing at E.M. Johnson WTP indicated that it will require approximately one month to dry the mechanically dewatered cake to a final solids concentration of 50 percent. Therefore, it appears that the only feasible loading depth for the enhanced non-mechanical dewatering beds is 12 inches, which will require that the beds be turned over approximately once per month to maintain sufficient free area to accommodate the residuals that are generated.

Since there is a loading depth that seems feasible, the cost of installing the enhanced non-mechanical dewatering beds at E.M. Johnson was calculated. Capital costs for upgrading the existing sand drying beds, as shown in Figure 4.11, are presented in Table 4.8.

As seen in Table 4.8, the total estimated capital cost for the enhanced non-mechanical dewatering beds at E.M. Johnson WTP is \$1,225,125. Amortized over 20 years at six percent interest, this gives an annualized capital cost of \$90,147.

In addition to the annualized capital cost, the primary cost of the enhanced non-mechanical dewatering beds is the cost of power to operate the fans. The number of fans shown in Table 4.8 is based on the number of 42,500 cfm fans required to give an effective volumetric air flow rate of 30 cfm/ft² over the beds. Each fan has a 5 horsepower motor installed, and based on the field results it was assumed that each fan would need to operate approximately 90 percent of the time throughout the year effectively dry the solids. Based on these assumptions, the total annual power usage would be 705,778 kWh, which at the City's rate of \$0.075/kWh would result in a power cost of \$52,933 to operate the fans.

Table 4.8
Capital costs for converting existing sand drying beds to enhanced non-mechanical dewatering beds at E.M. Johnson WTP

Item	Quantity	Units	Unit price	Total cost
Asphalt	682.5	TN	\$ 130	\$ 88,725
Fans	24	EA	5,200	124,800
Structure	1	LS	724,116	670,116
			Subtotal	\$ 883,641
			Mob/Bond	20%
			Contingency	25%
			Subtotal	\$ 1,113,750
			Engineering	10%
			Total	\$ 1,222,125

Based on this analysis, the total estimated annual cost for installing and operating enhanced non-mechanical dewatering beds at E.M. Johnson WTP is \$143,080. However, the total estimated cost savings from the enhanced non-mechanical dewatering beds is only \$172,766. While the use of the enhanced non-mechanical dewatering process at E.M. Johnson would result in net cost savings, it appears that the payback period would be more than 10 years based on the analysis described above. It may be possible to further increase savings and decrease cost by optimizing fan operation and/or drying the residuals to higher solids concentrations during periods of the year that are amenable to dewatering, but additional research would be needed to investigate these options.

AQUA CASE STUDY

As part of this work, two water treatment plants owned and operated by Aqua America were evaluated. The first plant, the Mentor On-the-Lake WTP operated by Aqua Ohio, currently uses two traditional sludge dewatering lagoons for collecting and drying the residuals generated by the plant. However, at this facility, plant staff have been able to substantially improve the performance of these lagoons by manually tilling the residuals with mechanical equipment to improve drying. The case study for this plant will focus on the effectiveness of those efforts. The second facility, the Shenango WTP operated by Aqua Pennsylvania, currently uses a belt filter press that only dewateres residuals to around 14 percent solids concentration. The cost-effectiveness of replacing the belt filter press with an enhanced non-mechanical dewatering bed at this facility will be evaluated.

Mentor On-the-Lake WTP

Mentor On-the-Lake WTP is a conventional coagulation-filtration water treatment facility that uses alum for coagulation. The plant has a capacity of 18 mgd, and in 2011 its production averaged 7 mgd. The residuals generated at this plant (clarifier blowdown and spent filter backwash water), are discharged to one of two 2 MG unlined earthen lagoons for storage

and drying. Once the residuals have sufficiently dried, they are removed by Solids, Inc. (Newcastle, PA) who hauls the dewatered solids to their soil amendment operation where they are beneficial reused. The removal operation takes approximately one week, and occurs once per year.

Staff at Mentor On-the-Lake WTP have examined different methods in the past of reducing costs for residuals disposal. Prior to 2009, plant staff had experimented with renting a backhoe to turn over the residuals in the lagoon to increase drying. This showed promise, but they were limited in the amount of time they could keep the rental on-site to assist with drying.

Based on the results with the rental equipment, Aqua Ohio purchased a long-reach track hoe specifically to be used for tilling sludge at Mentor On-the-Lake WTP. Plant mechanics fabricated a 10-foot attachment, shown in Figure 4.12, to extend the reach of the track hoe's 50-foot arm, which allows the track hoe to reach all areas inside of the 100-foot wide lagoons. Figure 4.13 shows the method used to till the residuals.



Figure 4.12 Extension arm fabricated by Mentor On-the-Lake WTP mechanics to till over sludge lagoon residuals



Photo Courtesy of Aqua Ohio

Figure 4.13 Residuals being tilled in the Mentor On-the-Lake WTP Sludge Lagoons

The impact of tilling the residuals at Mentor On-the-Lake has been significant. After tilling and drying, the residuals in the sludge lagoons reach approximately 50 percent solids concentration. Data were not available regarding the solids concentrations in the lagoons prior to tilling, but plant staff estimated that the solids averaged 25 percent solids before tilling was implemented.

In 2011, 1,417 tons of solids were removed from the Mentor On-the-Lake WTP at a cost of \$48,586 for transport and disposal. If the solids had been removed at a solids concentration of 25 percent, which the lagoons had averaged prior to the tilling operations, the cost for transport and disposal of the residuals would have been \$97,172 if removed at the same cost per wet ton. Therefore, the tilling operations reduced the cost for transport and disposal of the residuals by approximately \$48,586.

However, it should be recognized that there are additional costs associated with the tilling operations. Approximately eight to ten extra hours of staff time per week is required to till the residuals; the cost of this overtime in 2011 was \$15,000. Power costs for the supernatant decant pump was \$4,000 in 2011, although these costs would apply regardless of whether the residuals were tilled.

Based on the above info, the cost of residuals management at Mentor On-the-Lake WTP in 2011 was \$67,586. \$15,000 of this cost was directly associated with the tilling activities. However, if tilling had not been implemented at Mentor On-the-Lake WTP in 2011, the cost of residuals management is estimated to have been increased by \$48,000 due to the increase in transport and disposal fees. Therefore, simply by tilling the residuals in the sludge drying lagoons, the Mentor On-the-Lake WTP is estimated to have reduced annual residuals management costs by more than 33 percent, saving over \$33,000.

Shenango WTP

Shenango WTP is a coagulation-filtration water treatment facility that uses a high-rate ballasted clarification process for its primary clarification step. The plant has a maximum capacity of 16 mgd, and with daily production averaging between 9 to 10 mgd. Ballasted clarifier blowdown and spent filter backwash water are sent to an upflow clarifier that has been modified for residuals clarification. Underflow from this basin is sent to two gravity thickeners, and the thickened sludge is then dewatered by two belt filter presses. The dewatered cake is stored in roll-off containers, which are regularly removed from site by a contracted hauler. The end use of the cake is for daily cover at a nearby landfill.

The existing residuals management practice at Shenango WTP is limited by the existing belt filter presses, which produced a dewatered cake that averages between 14 to 15 percent solids concentration. In October 2010, Aqua Pennsylvania contracted with a belt filter press' manufacturer's representative to conduct a field review of the filter presses and to make recommendations to optimize performance. The representative tested a few different equipment adjustments and conducted bench testing of different polymer types and doses, and concluded that the current performance of the presses could not be improved.

The relatively poor performance of the belt filter presses significantly increases disposal costs at Shenango WTP. Table 4.9 presents the average solids hauled, by month, from Shenango WTP from 2001 to 2008, along with the equivalent mass of dry solids. In 2011, the most recent year for which hauling costs were available, Shenango WTP paid \$99,890 to dispose 3,278 tons of wet solids, which is equivalent to \$30.47 per wet-ton. Table 4.9 also presents the equivalent cost of disposing of the average solids production from 2001 to 2008, at the 2011 hauling rates.

Table 4.9
Average solids production at Shenango WTP (2001 through 2008) and disposal cost

Month	Tonnage hauled (wet-tons)	Tonnage hauled (dry-tons)	Hauling and disposal cost (dollars)
January	247	37.1	7,539
February	213	32.0	6,504
March	221	33.2	6,748
April	247	37.1	7,531
May	249	37.3	7,579
June	248	37.3	7,572
July	316	47.4	9,635
August	284	42.7	8,665
September	260	39.0	7,928
October	294	44.0	8,947
November	209	31.3	6,367
December	255	38.3	7,782
Total	3,045	457	92,796

Of the \$92,796 it would cost to dispose of the annual average solids production at Shenango WTP, more than \$78,000 of that cost simply to haul and dispose of water. While water treatment plant residuals will always contain some bound water that is extremely difficult

to remove, the poor performance of the existing belt-filter presses at Shenango leaves room for potential cost savings through enhanced non-mechanical dewatering.

Two scenarios were evaluated for Shenango WTP. The first scenario investigated replacing the existing belt filter presses with enhanced non-mechanical dewatering beds, while the second looked at using the enhanced non-mechanical dewatering beds to further dry the mechanically dewatered residuals, as in Raleigh.

Scenario 1 – Replacement with Enhanced Non-Mechanical Dewatering Beds

This scenario used the regression equations (Equations 3.5 and 3.7) developed from the Cleveland data to estimate effective evaporation for enhanced non-mechanical dewatering at Shenango. The weather monitoring stations closest to Shenango, PA did not report solar radiation data, so temperature was used to estimate the effective evaporation rates using Equation 3.7. For all months, an effective volumetric flow rate of 35 cfm/ft² was used. Effective evaporation rates, by month, for the enhanced non-mechanical dewatering process at Shenango WTP are shown in Table 4.10.

Table 4.10
Calculated effective evaporation rates for Shenango, PA

Month	Average temperature (°C)	Q_{eff} (cfm/ft ²)	Effective evaporation rate (in./mo.)
January	-3.93219	35	11.32
February	-3.85842	35	11.35
March	2.232812	35	13.29
April	8.704545	35	15.35
May	13.87586	35	17.00
June	18.76347	35	18.56
July	21.02395	35	19.28
August	20.24009	35	19.03
September	16.72896	35	17.91
October	10.00081	35	15.77
November	5.257576	35	14.26
December	-1.2311	35	12.19

These effective evaporation rates were used, together with the average monthly solids production, to model the enhanced non-mechanical dewatering process at Shenango WTP, using the same procedure as discussed previously for modeling in Cleveland. This model indicated that seven 30-foot by 75-foot dewatering beds would be needed to dry the residuals produced at Shenango WTP, for a total drying area of 15,750 ft².

However, unlike the Morgan WTP, Shenango WTP already dewateres its residuals to some extent, so the cost savings associated with moving to an enhanced non-mechanical dewatering process as the primary dewatering process will be primarily associated with the reduction in transport and disposal costs associated with the higher solids concentration achievable with the enhanced non-mechanical dewatering process. The modeling work performed for Shenango WTP assumes the solids will be removed after reaching 20 percent solids, so the savings that can be achieved will be associated with the difference in cost between

disposing of residuals with a 15 percent solids concentration, as is presently achieved at Shenango WTP, and the cost of disposing of residuals with a 20 percent solids concentration. These costs are presented in Table 4.11. Further cost savings would be achieved through the reduction in belt filter press O&M, although the extent of the reduction in those costs is not known at this time.

Table 4.11
Potential cost savings from increasing dewatered cake solids concentration from 15 percent to 20 percent at Shenango WTP

Month	Tonnage hauled at 15% solids concentration (wet-tons)	Tonnage hauled at 20% solids concentration (wet-tons)	Hauling at disposal cost at 15% solids concentration (dollars)	Hauling disposal cost at 20% solids concentration (dollars)
January	247	186	7,539	5,654
February	213	160	6,504	4,878
March	221	166	6,748	5,061
April	247	185	7,531	5,648
May	249	187	7,579	5,684
June	248	186	7,572	5,679
July	316	237	9,635	7,226
August	284	213	8,665	6,499
September	260	195	7,928	5,946
October	294	220	8,947	6,710
November	209	157	6,367	4,775
December	255	192	7,782	5,836
Total	3,045	2,284	92,796	69,597

Based on the costs presented in Table 4.11, Shenango will only be able to reduce annual transportation and disposal costs by approximately \$23,000 per year, if the existing belt filter presses were replaced with enhanced non-mechanical dewatering beds. To reach breakeven, the annualized capital cost of the beds would need to be less than \$1.50/ft², which is not feasible for a new installation. Based on this analysis, it does not appear that replacing the belt filter presses with enhanced non-mechanical dewatering beds is a feasible option for Shenango WTP.

Scenario 2 – Additional Drying with Enhanced Non-Mechanical Dewatering Beds

While replacing the belt filter presses with enhanced non-mechanical dewatering beds does not appear to be a feasible option at Shenango WTP, it may be possible to achieve cost savings by drying the mechanically-dewatered residuals with enhanced non-mechanical dewatering beds, as was investigated at Raleigh. The Raleigh data showed that it should be possible to dry the mechanically-dewatered residuals to at least 50 percent solids concentration, which could save significantly more than was possible in Scenario 1. Table 4.12 presents the potential cost savings that could be achieved. As Table 4.12 shows, this scenario presents potential annual savings of approximately \$65,000 based on reduced hauling and disposal costs.

Table 4.12
Potential cost savings from increasing dewatered cake solids concentration from 15 percent to 50 percent at Shenango WTP

Month	Tonnage hauled at 15% solids concentration (wet-tons)	Tonnage hauled at 50% solids concentration (wet-tons)	Hauling at disposal cost at 15% solids concentration (dollars)	Hauling disposal cost at 20% solids concentration (dollars)
January	247	74	7,539	2,262
February	213	64	6,504	1,951
March	221	66	6,748	2,024
April	247	74	7,531	2,259
May	249	75	7,579	2,274
June	248	75	7,572	2,272
July	316	95	9,635	2,890
August	284	85	8,665	2,599
September	260	78	7,928	2,378
October	294	88	8,947	2,684
November	209	63	6,367	1,910
December	255	77	7,782	2,335
Total	3,045	914	92,796	27,839

The Shenango WTP has some unique advantages that would simplify the implementation of enhanced dewatering of mechanically-dewatered residual solids. Previous improvements at the plant converted an old up flow clarifier to a residuals clarifier, which essentially stores solids before they are discharged to the two 40-foot diameter thickeners on-site. However, this clarification area is not necessary, because the gravity thickeners are adequately sized to receive residuals directly from the ballasted clarification process (and would likely benefit from the more continuous inflow that would come from that process). Therefore, it would be possible to take the residuals clarifier out of service and reuse that area for enhanced non-mechanical dewatering.

As Figure 4.14 shows, the residuals clarifier is almost directly south of the belt filter press building, so it is possible to construct a screw conveyor between the two structures to transport mechanically-dewatered cake directly from the belt filter presses to the enhanced non-mechanical dewatering area. The only other steps needed to convert the residuals clarifier to an enhanced non-mechanical dewater bed would be to demolish and remove the existing clarification equipment, cut an access doorway sufficient for a front loader to enter the structure to turn over and remove dewatered cake, and to add the fans. Estimated costs for these modifications are presented in Table 4.13.

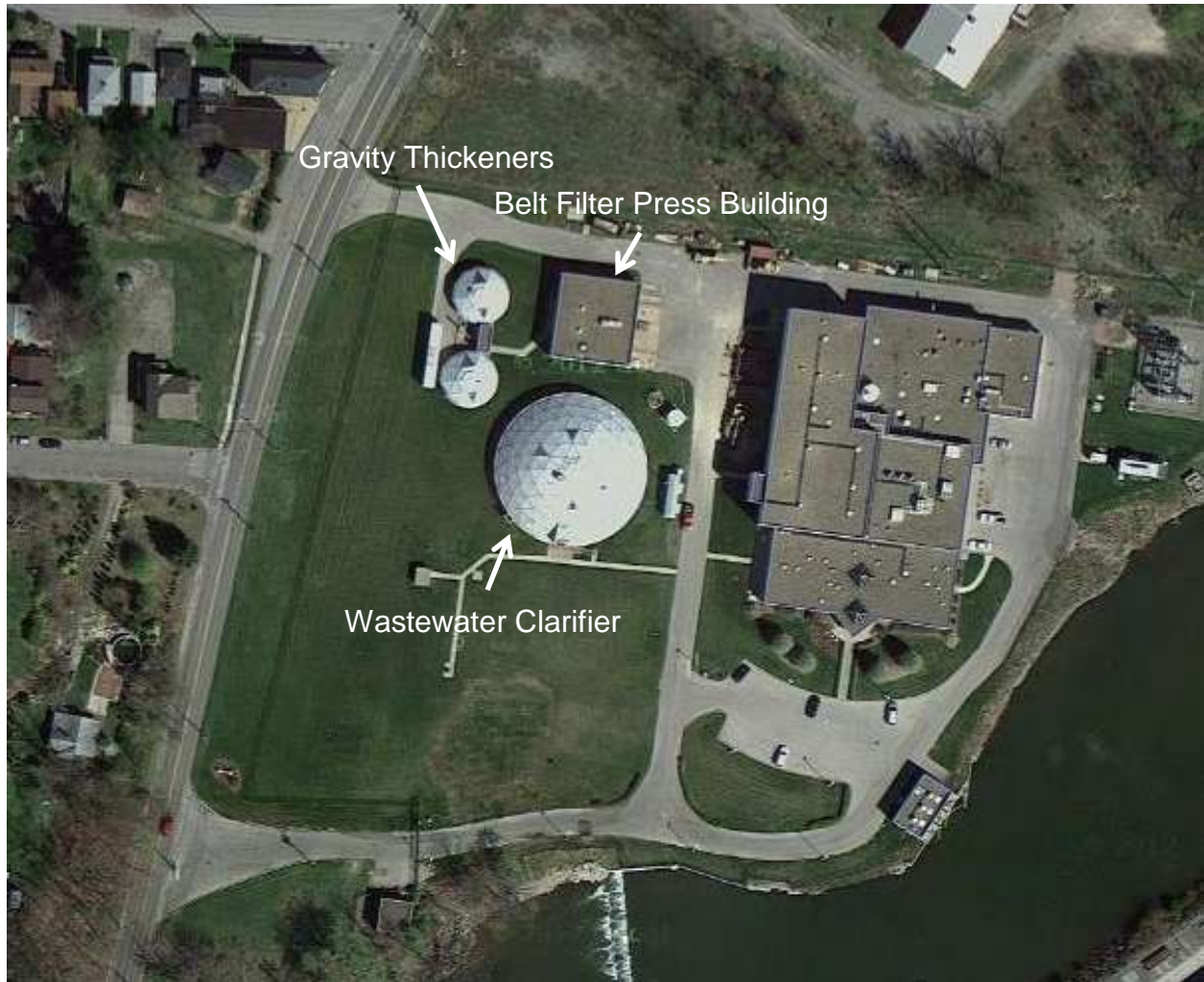


Figure 4.14 Aerial view of Shenango WTP site

Table 4.13
Capital costs for converting existing residuals clarifier to enhanced non-mechanical dewatering beds at Shenango WTP

Item	Qty	Units	Unit price	Total cost
Piping modifications	1	LS	\$ 50,000	\$ 50,000
Demolition of clarifier internals	1	LS	75,000	75,000
Entrance doorway construction	1	LS	50,000	50,000
Screw conveyor	100	LF	600	60,000
Fans	4	EA	5,200	20,800
			Subtotal	\$ 255,800
			Mob/Bond 20%	\$ 51,160
			Contingency 25%	\$ 63,950
			subtotal	\$ 370,910
			Engineering 10%	\$ 37,090
			Total	\$ 408,000

For the cost estimate shown in Figure 4.13, it was assumed only half of the residuals clarifier area would be used for dewatering. This provides over 4,750 ft² of drying area. Table 4.14 summarizes the total drying area required to spread out the monthly residuals production at Shenango WTP to either 6 inches or 7.5 inches, as was previously used in Raleigh.

Table 4.14
Comparison of required annual yield based on loading depth for Shenango WTP

Month	Tonnage hauled (wet-tons)	Total area required (ft ²)	
		Loading depth = 6 inches	Loading depth = 7.5 inches
January	247	2,121	1,697
February	213	1,829	1,464
March	221	1,898	1,518
April	247	2,118	1,695
May	249	2,132	1,705
June	248	2,130	1,704
July	316	2,710	2,168
August	284	2,437	1,950
September	260	2,230	1,784
October	294	2,517	2,013
November	209	1,791	1,433
December	255	2,189	1,751

Based on the data shown in Table 4.14, it would be necessary to turn over the drying area less than six times a year to accommodate the annual solids production. Raleigh data indicated that mechanically-dewatered cake could be dried from a solids concentration of 20 percent to 50 percent in less than a month, on average. This suggests that it should be possible to dry the mechanically-dewatered cake at Shenango WTP from 15 percent solids concentration to 50 percent solids concentration in two months, if not to a higher concentration.

Assuming the installed fans run every day, 24 hours per day, the power consumption from the four 5-Hp fans would be approximately 32,674 kWh annually. At an average power cost of \$0.1225/kWh, the annual power costs would be approximately \$4,000. Considering the \$65,000 cost savings that could be achieved by drying the residuals to 50 percent solids concentration and the estimated capital cost of \$408,000 to convert the wastewater clarifier to an enhanced non-mechanical dewatering building, the payback period for these improvements will be less than seven years.

Based on this analysis, it appears that converting the existing residuals clarifier to a non-mechanical dewatering area to dry the mechanically-dewatered cake from 15 percent solids concentration to 50 percent solids concentration would be beneficial, and reduce overall costs at Shenango WTP.

CHAPTER 5 SUMMARY

In this study, an enhanced non-mechanical dewatering process, which uses forced-air ventilation and enclosures to increase the rate of evaporation from water treatment plant residuals, was investigated. Testing was conducted under controlled-environment conditions at EE&T's pilot testing facility in Newport News, and under field conditions in Cleveland, OH and Raleigh, NC. The controlled-environment testing and field testing in Cleveland investigated the use of the enhanced non-mechanical dewatering process to dewater thickened sludge, while the Raleigh field testing investigated the use of the enhanced non-mechanical dewatering process to further dewater mechanically-dewatered residuals.

The results from the pilot testing were used to develop case studies showing the costs and benefits of using the enhanced non-mechanical dewatering process at three different water treatment plants. The major findings from the pilot testing and case studies are summarized in this chapter.

CONTROLLED-ENVIRONMENT TESTING

Controlled-environment testing indicated the importance of both volumetric flow rates and velocities in drying water treatment plant residuals. It was demonstrated that evaporation correlated strongly with overall volumetric flow rate, which is implicit in the vapor-balance calculations that predict evaporation rates; increasing the amount of air flowing over the bed increases the amount of air into which moisture can evaporate. Figure 5.1 clearly illustrates the linear relationship between applied volumetric air flow and evaporation, although other factors such as air flow evaporation (which controls velocity distribution over the bed) also play a factor.

Figure 5.1 suggests that air flow velocity over the bed, which is related to the fan configuration, also plays a role in evaporation. When comparing beds that received the same volumetric flow rates that were applied at different velocities, it is clear that evaporation is function of the velocity of the air moving over the residuals strongly effects evaporation. Comparison of velocity rates to solids concentration measurements indicated that areas receiving the highest velocities over their surface experienced the most evaporation, while areas receiving lower velocities dried to a lesser extent. Areas that did not receive air flow due to wall effects dried much more slowly than the portions of the beds that were ventilated. This clearly indicates that a balanced distribution of air flow and air velocities over the residuals is important to achieving good drying throughout the bed.

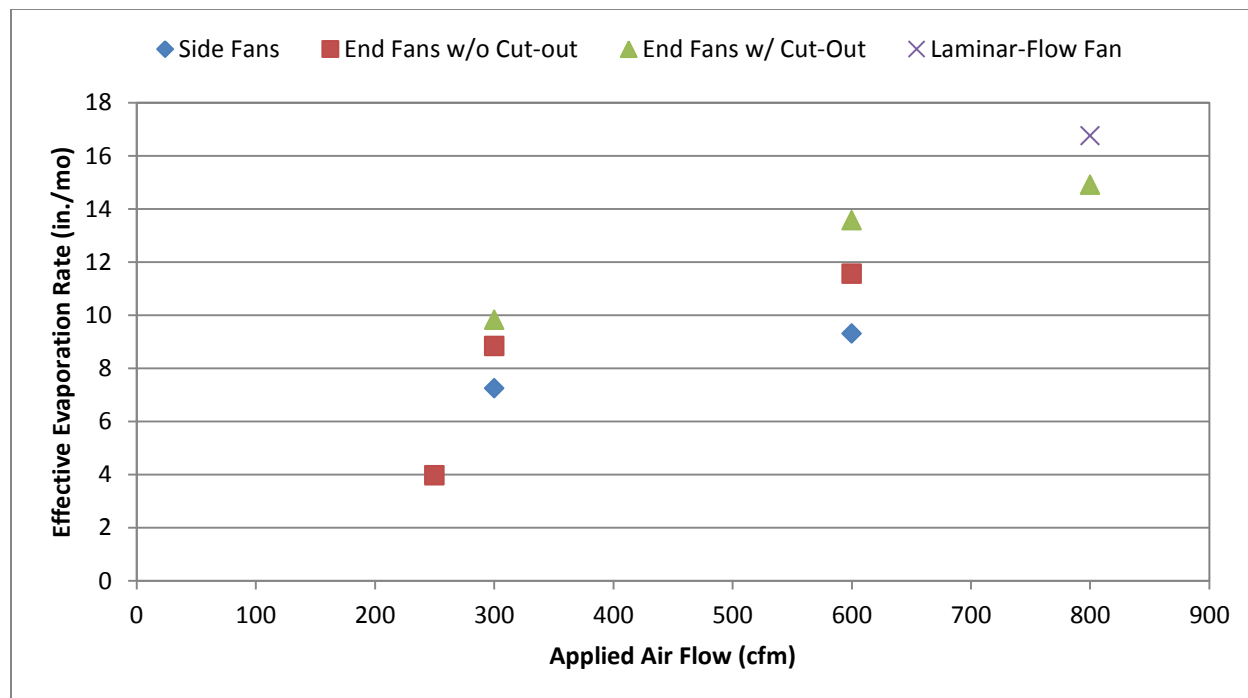


Figure 5.1 Effective evaporation rate as a function of applied air flow

CLEVELAND FIELD TESTING AND CASE STUDY

Pilot-scale field testing was conducted at the Morgan WTP in Cleveland, OH from October 2011 through July 2012. Effective evaporation rates achieved in the pilot test units were significantly higher than historical evaporation rates for the Cleveland area with an observed 300 percent to 800 percent improvement in evaporation, depending on the season. In addition to evaporation, freeze-thaw dewatering was observed in the enhanced non-mechanical dewatering test beds during December, January, and February. While evaporation isn't the mechanism by which freeze-thaw induces dewatering, the dewatering performance during the periods when freeze-thaw occurred would be equivalent to relatively high evaporation rates. However, freeze-thaw data were not used for modeling performance of the enhanced non-mechanical dewatering process because conditions required for freeze-thaw dewatering may not occur every year.

Two regressions were developed using the Cleveland data. The first linked effective evaporation from the bed to applied volumetric air flow rate (Q_{eff}) and the ambient temperature (T), and is shown in Figure 5.2.

This correlation follows the same trend observed in Figure 5.1, and also accounts for temperature variations observed during the test. It should be noted that this relationship is based on limited data from one testing location, so additional testing is needed before it should be extrapolated to other locations.

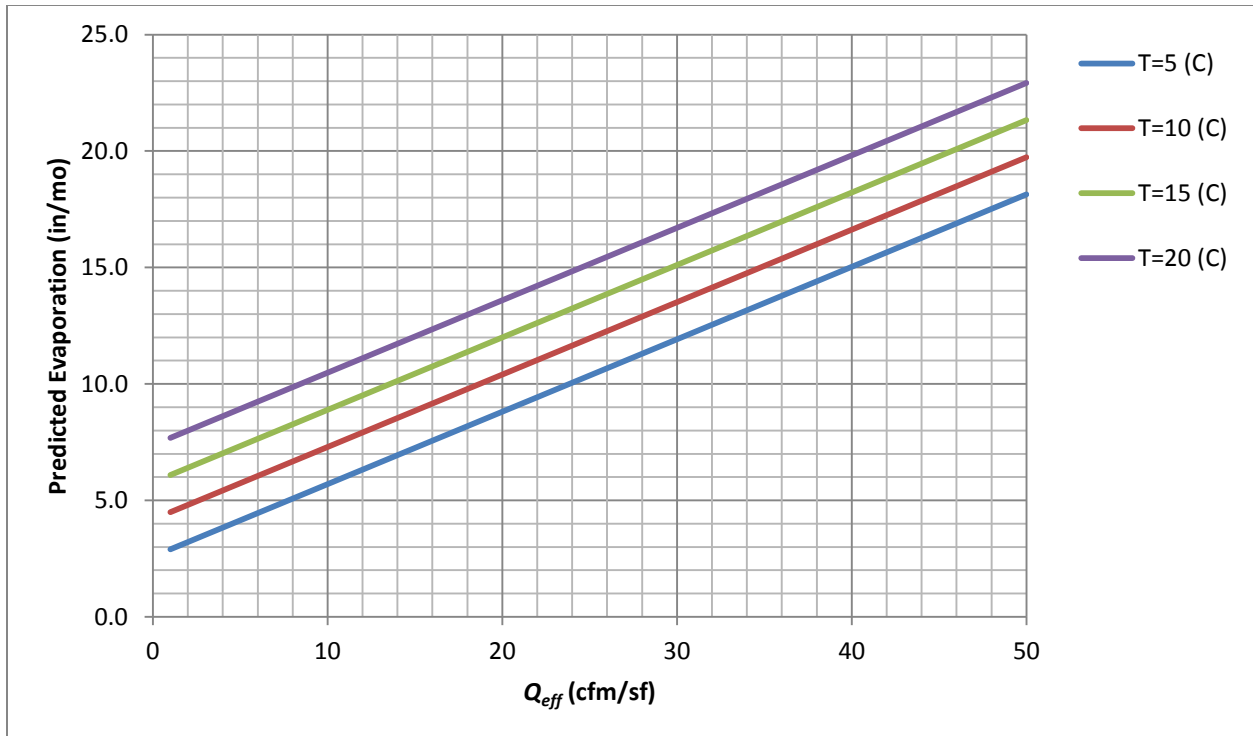


Figure 5.2 Relationship between net evaporation and applied volumetric flow rate for different temperature values

A second correlation to effective evaporation rate was developed using the average air velocity over the centerline of the bed, and is shown in Figure 5.3. This correlation also pulls ambient temperature (T , °C) and ambient solar radiation (R , watts/m²) as controlling factors for evaporation. However, the same caveats apply as with the relationship shown in Figure 5.2; this correlation is based on limited data from one testing location, so additional testing is needed before it should be extrapolated to other locations.

Data from the field testing was used to model area requirements for enhanced non-mechanical dewatering beds at Morgan WTP. These model results were compared to previous modeling efforts used to size traditional mechanical dewatering beds for the same facility. It was demonstrated that the enhanced non-mechanical dewatering process would be able to reduce the area required for dewatering by more than two-thirds compared to traditional non-mechanical dewatering beds.

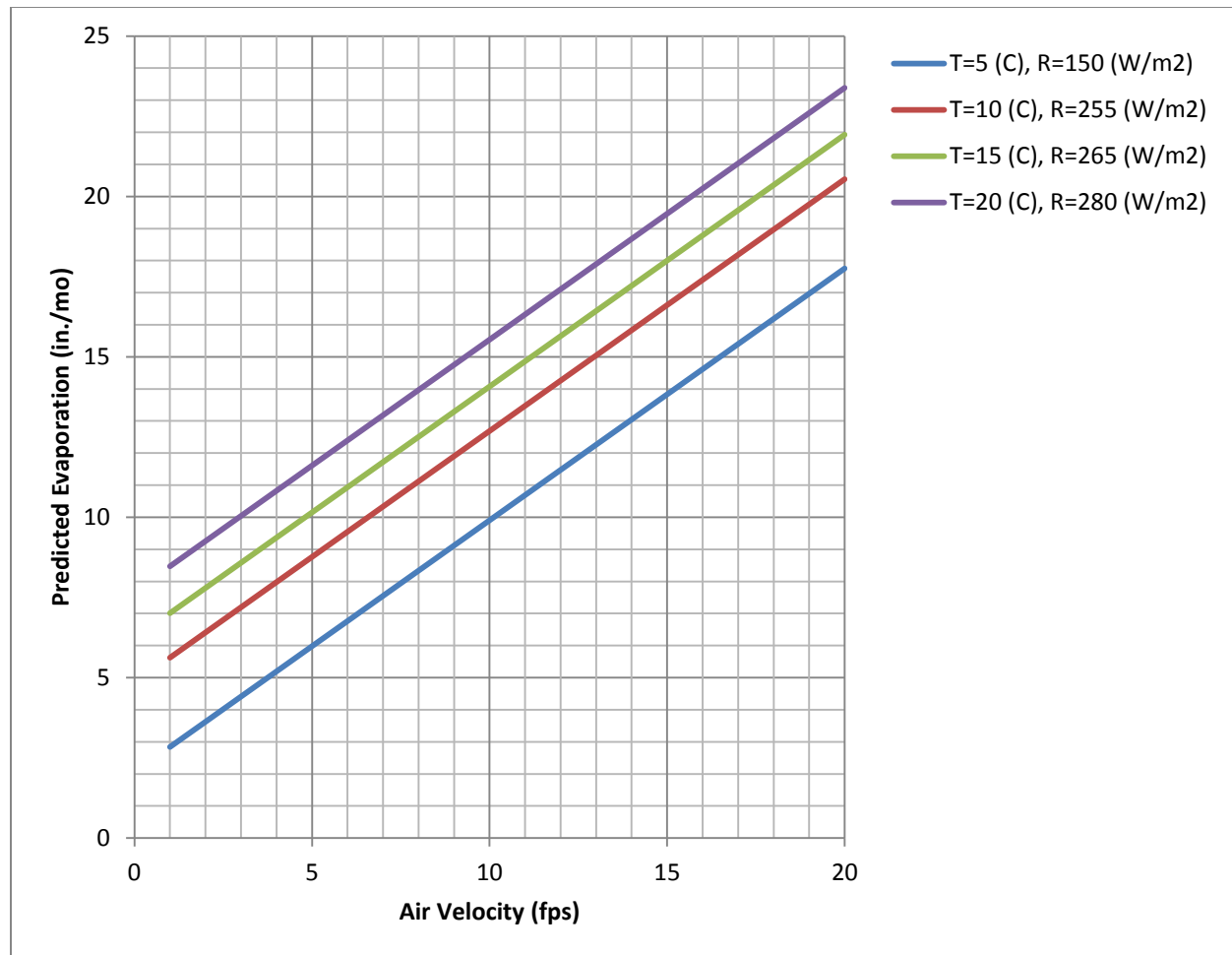


Figure 5.3 Relationship between net evaporation and average bed centerline velocity for different temperature and solar radiation values

A layout was developed for the enhanced non-mechanical dewatering beds at Morgan WTP, and the cost for those facilities was compared to costs for traditional non-mechanical dewatering beds, centrifuge dewater, and sewer disposal that had been developed for a previous study. The 20-year present value cost for the enhanced non-mechanical dewatering beds was 15 percent less than the next least expensive option (traditional non-mechanical dewatering beds) and approximately 60 percent less expensive than the current residuals management process (sewer disposal) at Morgan WTP.

This case study clearly shows that the enhanced non-mechanical dewatering process can be cost-effective and relatively low-footprint for large water treatment plants.

RALEIGH FIELD TESTING AND CASE STUDY

Pilot-scale field testing was conducted at the E.M. Johnson WTP in Raleigh, NC from January 2012 through October 2012. This field testing investigated the drying of residuals that had been previously dewatered by the belt filter presses. It became apparent over the course of testing that drying of mechanically-dewatered residuals is fundamentally different than drying of

thickened residuals, as had been investigated in the controlled-environment testing and in Cleveland. During the drying of thickened residuals, the cake remains physically connected so that moisture from the center and bottom of the cake layer can move the surface of the cake via capillary action. Because evaporation can only happen at the air: liquid interface, this capillary action serves to create more uniform drying across the depth of the cake layer.

Mechanically dewatered residuals, at least those produced by the belt filter presses at E.M. Johnson WTP, are not part of a cohesive whole but instead consist of small agglomerations of dewatered cake, interspersed with void spaces. When piled into a drying bed or windrow, the cake on the surface of the layer dries rapidly, but the center and bottom of the cake layer dries very little. Tilling may help enhance drying by exposing previously covered cake to the surface, but even with daily tilling it was noted that the center and bottom of the cake was significantly moister than the surface layer of cake.

Because of this phenomenon, there was a high level of variability in measured solids concentrations during early testing. The latter testing, which was better characterized, indicated that the enhanced non-mechanical process may increase the effective evaporation rate from previously mechanically-dewatered residuals by up to 60 percent. This testing also indicated that the enhanced non-mechanical dewatering process is capable of drying mechanically-dewatered residuals to a 50 percent solids concentration in less than 30 days, although data is limited and represents just one particular location.

The case study performed for this facility investigated converting the existing, unused dewatering beds to enhanced non-mechanical dewatering beds by paving the existing beds, adding a stretched fabric structure, and adding fans. The study found that a net cost savings would be possible, but the payback period for the necessary improvements would exceed 10 years, primarily due to the relatively low disposal costs (on a \$ per wet-ton basis) that E.M. Johnson WTP now pays.

AQUA CASE STUDY

Case studies were performed for two facilities operated by Aqua America. The first facility, the Mentor On-the-Lake WTP operated by Aqua Ohio, uses sludge lagoons for the non-mechanical dewatering of its residuals. However, plant staff have been able to reduce the volume of residuals removed from the site in half by manually tilling the residuals using a track hoe as they dry. This tilling has roughly doubled the final solids concentration that can be achieved in the lagoons from approximately 25 percent solids concentration to approximately 50 percent solids concentration. By making a small expenditure in overtime hours for staff to till the residuals, the plant has been able to reduce annual residuals management costs by more than 33 percent.

The other facility investigated was the Shenango WTP operated by Aqua Pennsylvania. This facility currently uses two belt filter presses to dewater its residuals, but because these presses are only able to achieve a dewatered solids concentration of approximately 15 percent, the overall hauling and disposal costs are relatively high. An option to replace the presses with enhanced non-mechanical dewatering beds was investigated, but because no capital costs were required to produce the 15 percent cake using existing equipment, the cost savings from producing 20 percent cake were not large enough to justify the construction of a new dewatering process.

However, although enhanced non-mechanical dewatering for the thickened sludge did not appear to be cost effective, using the enhanced non-mechanical dewatering process to further dewater the mechanically-dewatered cake produced by the belt filter presses appears promising. If an existing residuals clarifier is converted to an enhanced non-mechanical dewatering bed, it would provide sufficient area to allow residuals to dry for more than two months before they needed to be removed, at which time they should be able to dry to at least 50 percent solids concentration. The payback period for the capital costs to convert the residuals clarifier would be less than seven years.

AREAS FOR FUTURE RESEARCH

This work identified several areas where future research would be beneficial. First and foremost, research into optimizing the air flow over the beds is needed. This research found that drying is a function of both total volumetric air flow over the bed and air flow velocity over the bed. While the two are related, the relationship is complex due to the changing surface of the cake and the different air spray patterns of different fans. When registers were used to more evenly distribute air flow during this work, it was found that they reduced the velocity of the air to the extent that it was detrimental to drying. Research into methods to maintain high velocities across the beds without concentrating air flow, perhaps through computational fluid dynamics modeling, would be beneficial. It is also not known if multiple fans on beds in close proximity to each other would interfere with one another.

Another area that needs additional research is the drying of mechanically-dewatered cake. Although testing at Raleigh indicated that it is possible to dry mechanically-dewatered cake to 50+ percent solids, there was a wide range of scatter in the data because the uneven drying of the cake makes direct measurement of its solids concentration difficult. Future research should focus on characterizing the solids concentration of the cake using the overall volume reduction achieved in the cake pile rather than through direct solids concentration measurements.

One factor that should be considered by future researchers is whether it is beneficial to turn off the ventilation fans at times to optimize energy use. As Figure 5.4 shows, the major advantage that the enhanced non-mechanical dewatering process offers over the traditional non-mechanical dewatering process is a reduction in bed area required during low evaporation times of the year. In the case of the Morgan WTP, presented in Figure 5.4, it appears that the area required for traditional non-mechanical dewatering from May through September is less than the total area that would need to be provided for the enhanced non-mechanical dewatering process. It may be beneficial to turn off the fans during these months to more fully utilize available bed space and to reduce energy costs. Likewise, due to lower temperatures and higher relative humidity at night, evaporation has a strong diurnal pattern and is lower at night than during the daytime hours. In light of this, it may be beneficial to turn off the fans at night when evaporation relative to the energy input to the beds is lower.

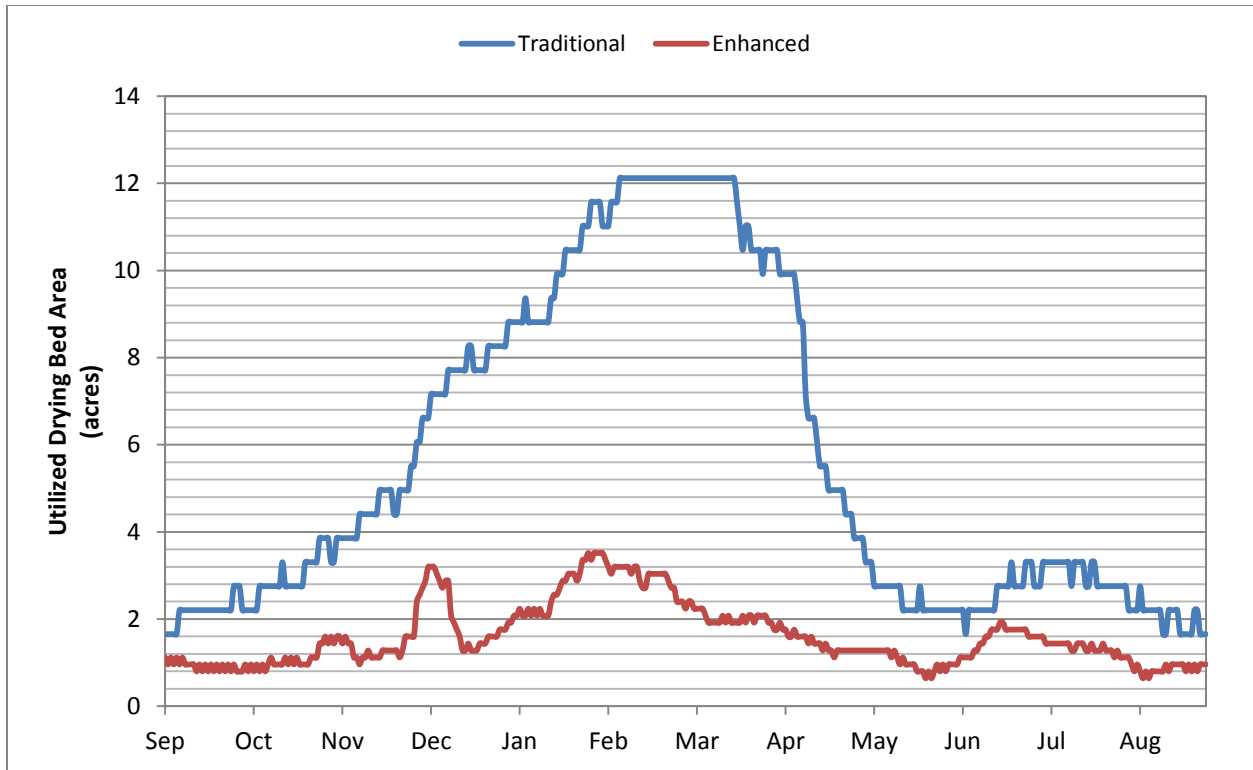


Figure 5.4 Comparison of total drying bed area required for traditional and enhanced non-mechanical dewatering beds for Morgan WTP

Finally, additional test data at other locations is needed to verify the regression equations developed linking effective evaporation to air flow/velocity, ambient temperature, and ambient solar radiation. While the regressions developed for this work appear to have a high level of correlation, they are based on relatively few data and would benefit from additional data.

REFERENCES

- Allen, R.G., L.S. Pereira, D. Raes, and M. Smith. 1998. *Crop evapotranspiration – Guidelines for computing crop water requirements*. FAO Irrigation and drainage paper 56. Rome.
- EE&T. 2008. *Analysis of Alternatives for Residuals Management at the Morgan WTP*. Report for Cleveland Division of Water.
- Mathioudakis, V.L., A.G. Kapagiannidis, E. Athanasoulia, V.I. Diamantis, P. Melidis, and A. Aivasidis. 2009. Extended Dewatering of Sewage Sludge in Solar Drying Plants. *Desalination*, 248:733-739.
- Ruiz, T. and C. Wisniewski. 2008. Correlation between dewatering and hydro-textural characteristics of sewage sludge during drying. *Separation and Purification Technology*, 61:204-210.
- Sartori, E. 2005. A Critical Review of Equations Employed for the Calculation of the Evaporation Rate from Free Water Surfaces. *Solar Energy*, 68(1):77-89.
- Schwartz, R., R.L. Baumhardt, and S.R. Evett. 2010. Tillage effects on soil water redistribution and bare soil evaporation throughout a season. *Soil & Tillage Research*, 110:221-229.
- Seginer, I. and M. Bux. 2005. Prediction of evaporation rate in a solar dryer for sewage sludge. *Agricultural Engineering International: the CIGR Ejournal*. Manuscript EE 05 009. Vol. VII.
- Seginer, I. and M. Bux. 2006. Modeling Solar Drying Rate of Wastewater Sludge. *Drying Technology*, 24:1353-1362.
- Slim, R., A. Zoughaib, and D. Clodic. 2008. Modeling of a solar and heat pump sludge drying system. *International Journal of Refrigeration*, 31:1156-1168.
- Vandermeijden, C. and D.A. Cornwell. 1998. *Nonmechanical Dewatering of Water Plant Residuals*. Denver, Colo.: AwwaRF and AWWA.
- Vaxelaire, J., J. M. Bongiovanni, P. Mousques, and J.R. Puiggali. 2000. Thermal Drying of Residual Sludge. *Water Research*, 34(17):4318-4323.
- Zhao, L. W.M. Gu, P.J., He, and L.M. Shao. 2010. Effect of air-flow rate and turning frequency on bio-drying of dewatered sludge. *Water Research*, 44:6144-6152.

ABBREVIATIONS

A	bed area
<i>c</i>	control variables
°C	degrees Celsius
cfm	cubic feet per minute
D_E	equivalent depth
$D_{E,d}$	equivalent depth of the drained solids
$D_{E,t}$	equivalent depth at time <i>t</i>
<i>e</i>	outdoor environment factors
<i>E</i>	average evaporation rate
EA	each
°F	degrees Fahrenheit
fpm	feet per minute
fps	feet per second
ft ²	square foot
ft ³	cubic foot
Hp	horsepower
<i>i</i>	interest rate
in.	inches
kWh	kilowatt hour
lb	pound
LS	lump sum
m	meters
m ²	square meters
MG	million gallons
mm	millimeters
mo.	month
<i>n</i>	number of tests
<i>p</i>	vapor pressure
Q_{eff}	Average effective ventilation rate

Q_v	Volumetric flow rate
Q_v	Ventilation air rate
R	correlation coefficient
R_A	Solar radiation
RH	relative humidity
s	second
s	state of the sludge
S_{avg}	average daytime solar radiation
SLR	solids loading rate
SS	solids concentration
T	average temperature
T_A	Air temperature
T_t	number of drying days to time t
T_d	number of drying days to reach the drained solids concentration
TIL	Use of sludge tilling
TN	ton
TSS	total suspended solids
TTF	time to filter
V_{CL}	average air velocity along the centerline of the bed
W	vapor concentration in the air
W	watts
WTP	water treatment plant
Z	Z-test correlation coefficient
ρ	Density of air
ω	Humidity ratio
ω_{in}	Air humidity